Photovoltaic Water Pump System

Harsono Hadi

Course of Intelligent Mechanical Systems Engineering,

KOCHI UNIVERSITY OF TECHNOLOGY

A Dissertation Submitted to the Faculty of
Kochi University of Technology in Partial Fulfillment of
The Requirement for the Degree of

Doctor (Philosophy)

August 2003

Photovoltaic Water Pump System

by

Harsono Hadi

A Dissertation Submitted to the Faculty of
Kochi University of Technology in Partial Fulfillment of
The Requirement for the Degree of

Doctor (Philosophy)

Approved by :

Shinobu TOKUDA (Director)

Tadashi NARUSAWA

Akira YOKOGAWA

Shuoyu WANG

Kazuhiro KUSUKAWA

Table of Contents

List of Figures

List of Tables

Chapter 1

Introduction

1.1 Background

To cover the energy requirement, the researches are being made for conventional or renewable energy. One of the renewable energy is solar energy, which can be the main source or alternative energy source in the power generator. Excellence of using the renewable energy is clean energy and friendly to the environment. Beneficially solar radiation is equally distributed in the any place on the earth, its density isn't large, irradiation fluctuate sharply with the fickle weather, and the solar energy cannot be stored, which cause no conflict on the earth and on each one in peace. In fine details, the irradiance intensity is influenced by the factors: geographic (longitude, latitude) of the location. The location around the equator has good irradiation throughout the year, but the location around the pole particularly in winter season has little irradiation. Based on these reason, the equipment of solar energy in the tropic area is more effective than other places (subtropics and pole). The survey, the observation and measurement must be made to sure the irradiance intensity of a location. Although in the tropic area, the topography of the location and the weather also affect the irradiation. For example, the location at the mountain is often rain or cloudy. As a result, the total irradiation in one day is low. Based on the converting energy, the solar energy is classified into: direct (thermic)[29] and indirect (photonic)[14]. In the thermic system, the solar energy is used direct to heat the object. For example: solar drying, thermal pump and desalination, etc. In the photonic system, the solar energy works as the photonic energy. In this thesis, the author researches for

the photonic system especially the photovoltaic pump system. The photovoltaic system has main component, which is named the solar generator. The solar generator consists of some photovoltaic modules. To obtain big power capacity, a photovoltaic module has some solar cells those are connected in series and parallel and the modules are also installed in series and parallel. In order to avoid dust, water, rain, heat and humidity, the solar cell is encapsulated with the frame of the flat glasses. The electric energy produced by the solar generator is direct current (dc). In addition to the irradiance intensity and temperature, the power output of the solar generator also depends on the solar cell efficiency.

The application of the photovoltaic system has advantages and weakness.

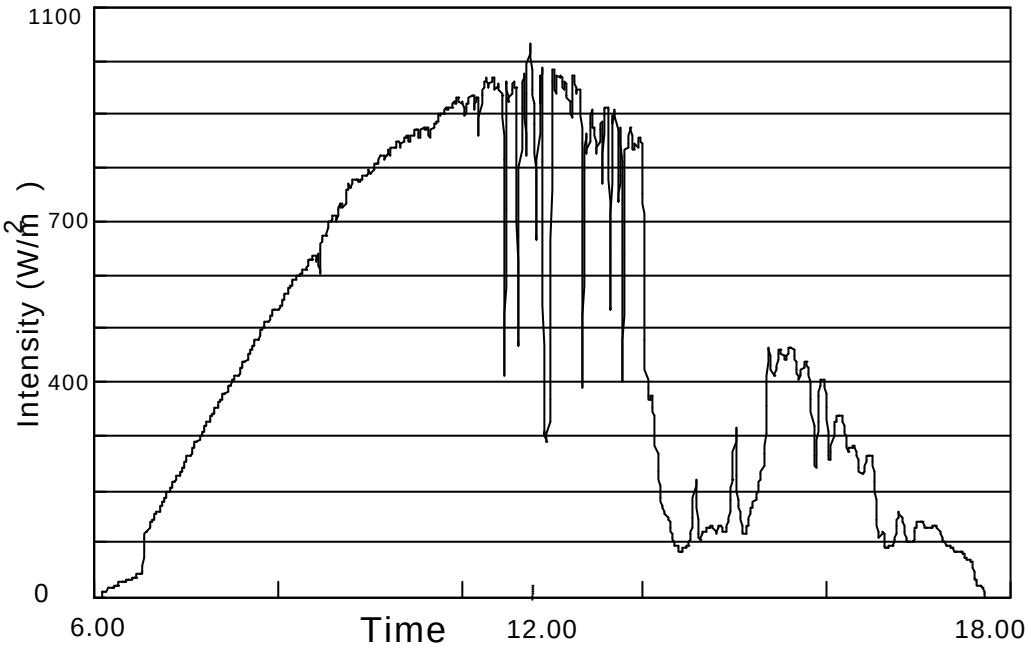

Figure 1.1: Intensity of the sun radiation in one day

Weakness

- Sun radiation

  The irradiance intensity of the sun radiation in one day always changes and fluctuates. The Figure 1.1 is an example of the irradiation of not good weather. The irradiation starts around 6 o'clock and increase at the maximum value (approximate 900 W/m^2) at 12 AM. After 11 AM the irradiation fluctuates,

because the sky is cloudy and rainy later. After that the irradiance intensity is gradually decrease. Around 18 PM the irradiation is zero. The sun radiation is main source for the photovoltaic system, so the performance of the photovoltaic system depends on the irradiance intensity.

- Efficiency

  The efficiency of solar cell is relative low 15% [4] for the mono-crystal silicon and 12% for the poly-crystal silicon. As a result, to get big capacity of the solar generator, large area of the solar cell and places are necessary. The new material and process are researched to replace the silicon, which is main material for the solar cell, but still too expensive and low efficient.

- Price

  In current time, the silicon is main material for the solar cell. In the world, the material silicon is not so much and always bounded with other material. Purifying silicon from other material is needed high process and expensive cost. From the reasons, the price of the photovoltaic module is expensive (1 watt peak ≈ 4,- US$)[32].

Opportunity

- Renewable and clean energy

  Different from the fossil or nuclear energy, the conversion process from the photonic energy into the electrical energy produces no waste materials, which are harmful to the environment. Because this conversion is friendly to the environment, the solar energy is clean energy. The electric energy from solar generator is classified into the renewable energy, because the main energy source is taken from the nature or the sun radiation.

- Space and rural area

  In the rural area and the space, to get the energy source is not easy. Only solar energy is possible to use as the energy source. With the solar photovoltaic system, the electric power can be obtained and the operation of the photovoltaic system is

possible without the operator, the photovoltaic system is suitable for the rural area and the space.

- Low maintenance

  The solar generator produces the electric energy from the solar energy, which exists by nature and the fuel is not necessary for the operating of photovoltaic system. The lifetime of the photovoltaic module is estimated around 10-15 years. In rural area and space, the equipment in the photovoltaic system is designed and set without the operator or run automatically. Because of this, the maintenance and operational cost of the photovoltaic system is low.

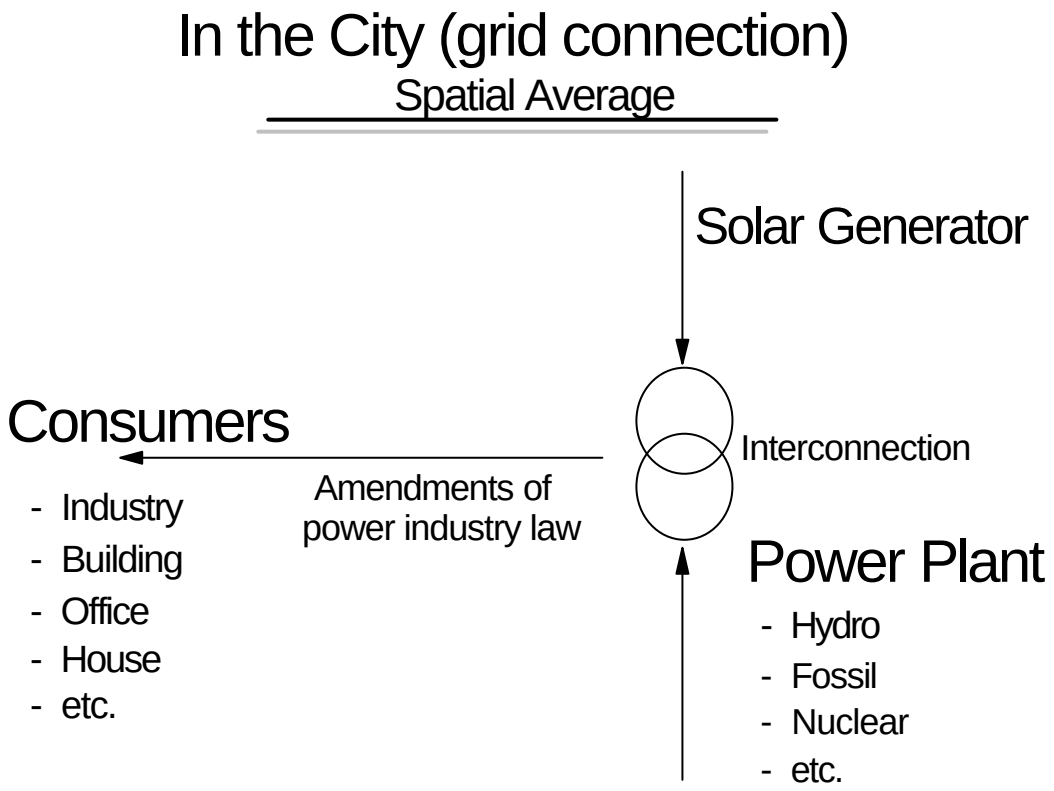

Figure 1.2: Interconnection between the solar generator and other generators

1.1.1 In the City

In the modern community, the electric energy is basic demand. In the big city and country, electric energy is supplied by multi power plants with the source energy: fossil, hydro, nuclear, and thermal generator, etc. The solar generator can also be used as the power generator. With the reasons expensive price, low efficiency of the photovoltaic module and the fluctuation of the output, the solar generator is only as alternative generator. However since the recent amendments of power industry law, electric power produced from even a small house solar generator can be sold through the utility lines. These generators are connected together. The power supply can be smoothened by the interconnection over the vast area and power plants. The schema is shown in the Figure 1.2, the power utility in the city is no problem any more and enough. The solar generator gradually becomes a main generator in the city. With the system grows up into a single big system, the system is afraid to be a brittle one as the nuclear generator system, which needs powerful huge security.

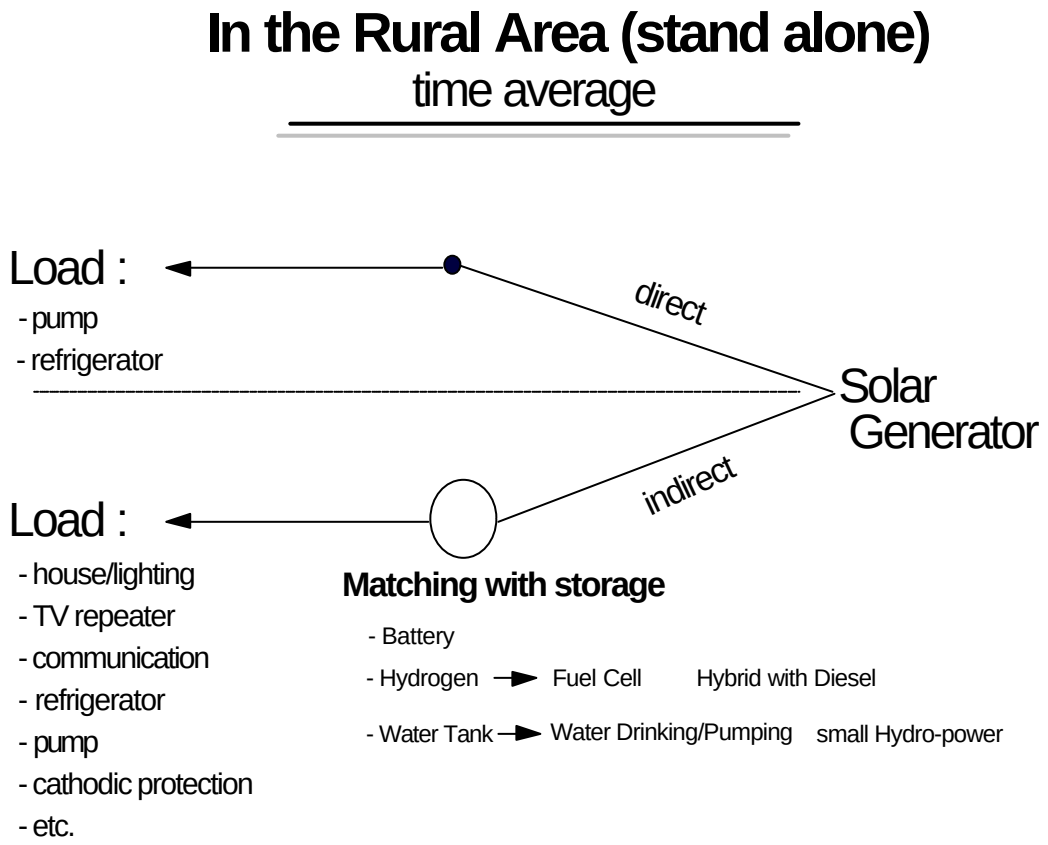

Figure 1.3: The solar generator is as the main generator.

1.1.2 Remote Area

In the rural area [25] and the space, solar energy is suitable as the main energy source, because the other energy source is limited. The intensity of the irradiation is highly fluctuating as mentioned above and utility grid cannot be used in the rural area, the energy storage in time is inevitable to match the variation of energy demand. In the Figure 1.3, the schema illustrates the solar generator as the stand alone of electric generator with some kinds of load. As the common electric storage, the battery is used but the size of the battery is too big compared with its capacity and it is not friendly to the environment. Hydrogen from the electrolysis of water is considered the promising storage as the fuel of fuel cell or diesel engine, but hydrogen is difficult to store or carry, and the hydrogen different from the water, gets out of the gravity area of the earth. This means the valuable and rare water goes out of the earth.

In this thesis, considering the countries such as Indonesia and Kochi, who have many islands or mountains, the photovoltaic pump (PVP) system of the hydraulic power generator is proposed as the energy storage, which is not only store the hydraulic energy but also supply the water drinking and watering places in the higher settlement area, where there are many places in the world and are waiting for the exploitation.

In the city solar energy is converted to the electricity by solar generators and collected through power utility grid, whereas in the rural area as illustrated in Figure 1.4, hopefully solar energy is stored in the pasture and collected by the cattle to the watering places constructed with the present system. With these procedures, entropy can be decreased and turned to power.

In Chapter 2, the PVP system is presented about the system loaded with two centrifugal pumps and without the battery. The small pump is set to operate in the morning and afternoon or low irradiation. The big pump is adjusted for the high irradiation or around noon.

In Chapter 3 and 4, the performance of the PVP system with maximum power tracker is presented for single pump. The measured data are evaluated and analyzed.

In Chapter 5, the PVP system with battery is proposed. The size of the battery based on the estimation and calculation with model are discussed.

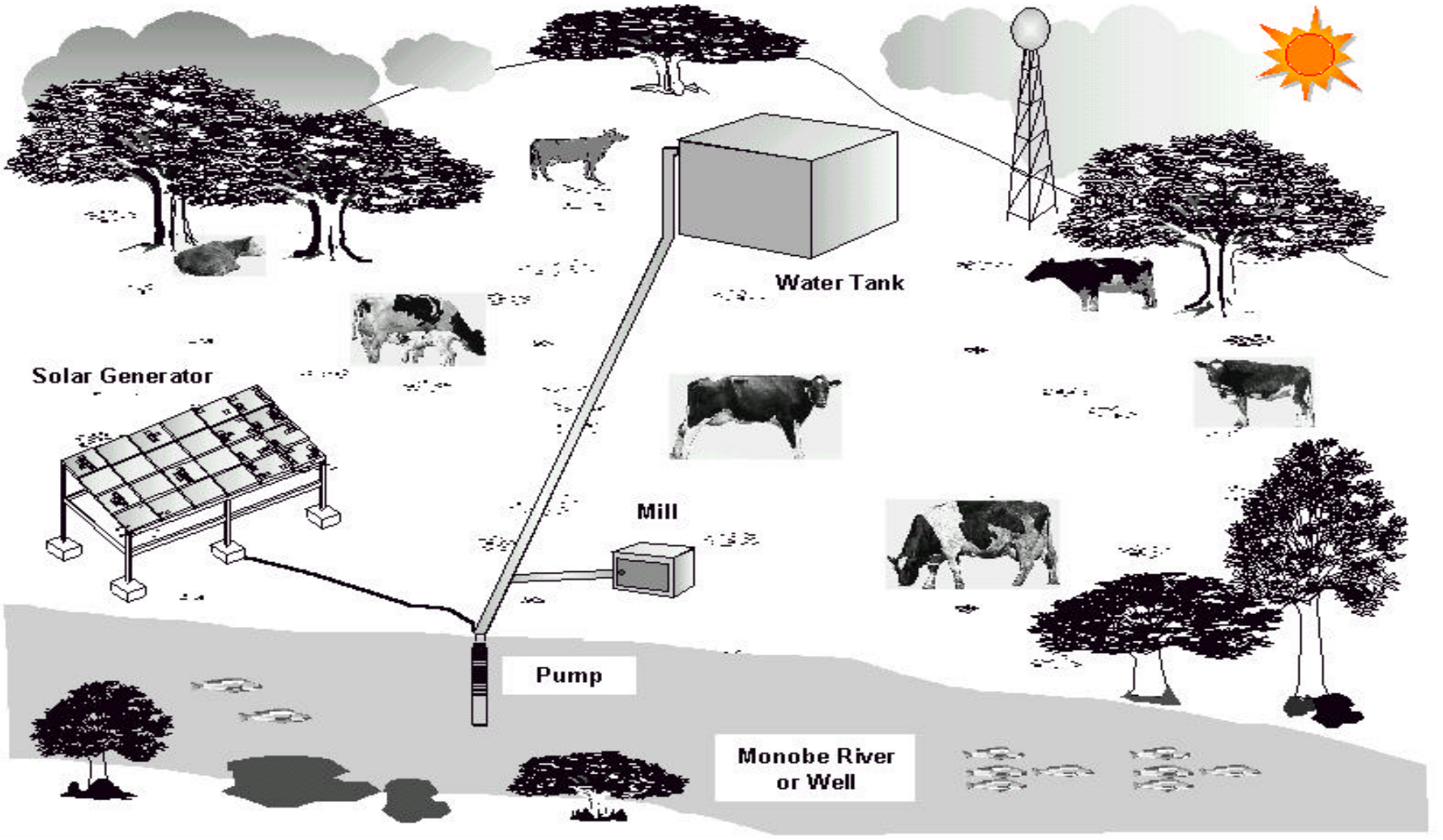

Figure 1.4 : Landscape in a village

Chapter 2

Double Pumps

2.1 Energy Output and Load

Exploiting the solar energy has been done to suffice the energy for the human life with directly or high process. One of applying the solar energy is the photovoltaic pump (PVP) system, which pumps the water from water source to the storage tank or the community. The solar cells made from the silicon material functions to change the solar energy into the electric energy. The solar generator consists of the some solar cells, which do converting the photonic energy into the electric energy. The power output of the solar generator is influenced by high-low irradiance intensity and temperature, but the temperature doesn't strongly affect the performance of the solar generator. The intensity of the sun radiation in one day is different value from 0 to 1000 Wm^{-2}. The radiation data of the every location is maybe different with the other location. The high-low radiation depends on the latitude and altitude of the location.

The power output of the solar-generator is written:

$$P_{SG} = I_{rr} \times A \times \xi_{cell} \quad (2.1)$$

where P_{SG} is power output of the solar-generator (Watt); I_{rr} the irradiance intensity of the sun radiation (0~1000 Wm^{-2}); A the area of the solar cells (m^2); ξ_{cell} the efficiency of the solar cell (poly-crystal $\xi_{cell} \leq 12\%$ and mono-crystal $\xi_{cell} \leq 15\%$).

From the Equation (2.1), while fluctuating the irradiance intensity, the power output is change or various. Commonly the PVP system is connected with a pump as the single

load and without the storage energy or the battery, which can be used to save the waste energy. When the irradiance intensity is low or high, the voltage (V) and current (I) output of the solar generator are different.

In the clear weather, the irradiance intensity has relationship to the time in one day. In the morning or low radiation, the system with the small load works well. Gradually the irradiance intensity rises and the power (current-voltage) output of the solar-generator is also swell. When the power output of the solar-generator is too bigger than the capacity load, the voltage output of the solar generator or the voltage input of the inverter/converter is over the maximum operating. According to the protection of the component in the inverter/converter for defection, the inverter/converter cuts automatically the connection from the solar-generator. The status of the inverter becomes in stand by. It causes that the pump doesn't run. The maximum irradiance intensity happened around 12 o'clock. After this time the irradiance intensity slowly decreases and the voltage output of solar generator also goes down. When the voltage output isn't over the voltage operating of the inverter/converter, the connector in the inverter is switch on and the pump runs back.

The PVP system with the big load only works at the high radiation or around noon. At the low irradiance intensity, this system doesn't operate, because the power output of the solar-generator is too smaller than the load capacity.

In one day the PVP system with the single load has the unbalancing between the power output of the solar-generator and the load capacity. The Unbalancing condition results the pump is stop and losing energy. It causes the performance of the PVP system isn't yet optimum.

2.2 Optimization with Double Pumps

In order to solve the problem of the PVP system, double pumps are loaded, which are different capacity. In the regulating and operating the loads, the small pump is run at the low irradiance intensity and the big pump is employed at the high irradiance intensity, as shown in Figure 2.1.

In the morning with the low irradiance intensity, the small load (pump I) is run. The irradiance intensity increases gradually with time. When the radiation is high, the

unbalancing energy occurs between the power output of the solar generator and the pump I. To balance this condition, the big load (pump II) is operated and the small pump (pump I) is stopped. Although the irradiance intensity is high, the PVP system works right. Because the capacity of the pump II is bigger, the water flow rate is also higher.

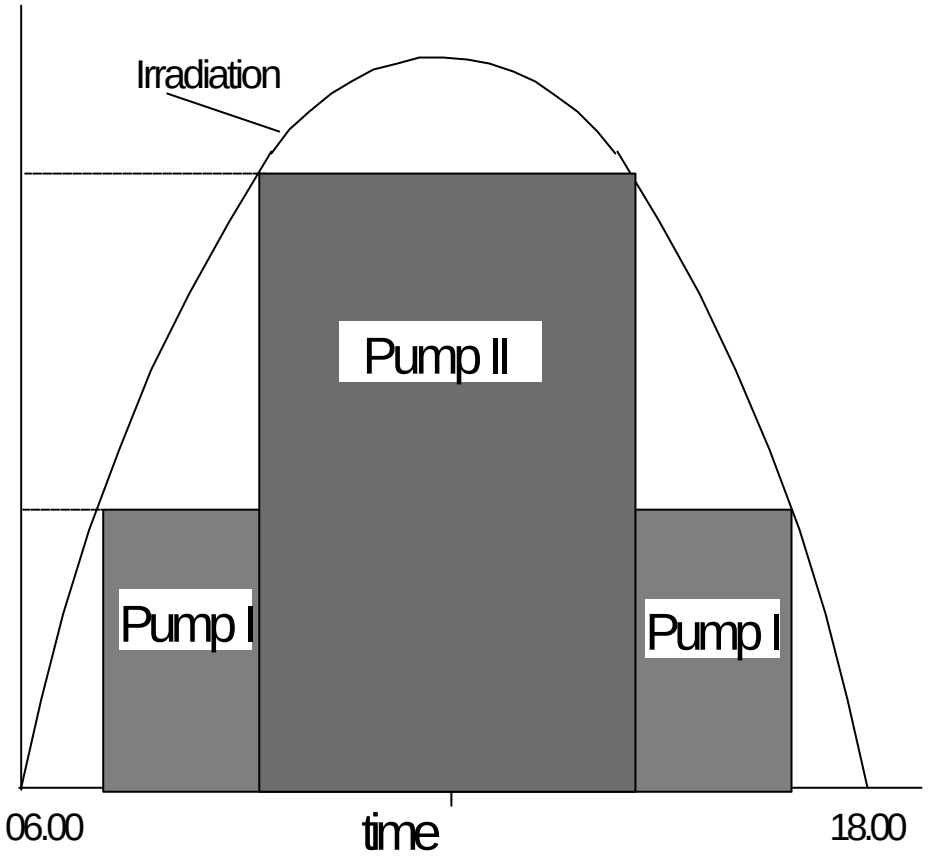

Figure 2.1: Operating area of the small and big pumps

In the clear weather, the maximum irradiance intensity is about 1000 Wm^{-2} around 12.00 o'clock. After 12 o'clock, the irradiance intensity goes down slowly. When the power output of the solar-generator doesn't balance with the pump II, the pump I is operated (pump II-off). Although the radiation relative low, the system operates yet with the small pump. In the cloud weather, the operating time of the small pump (pump I) is longer than the big pump (pump II).

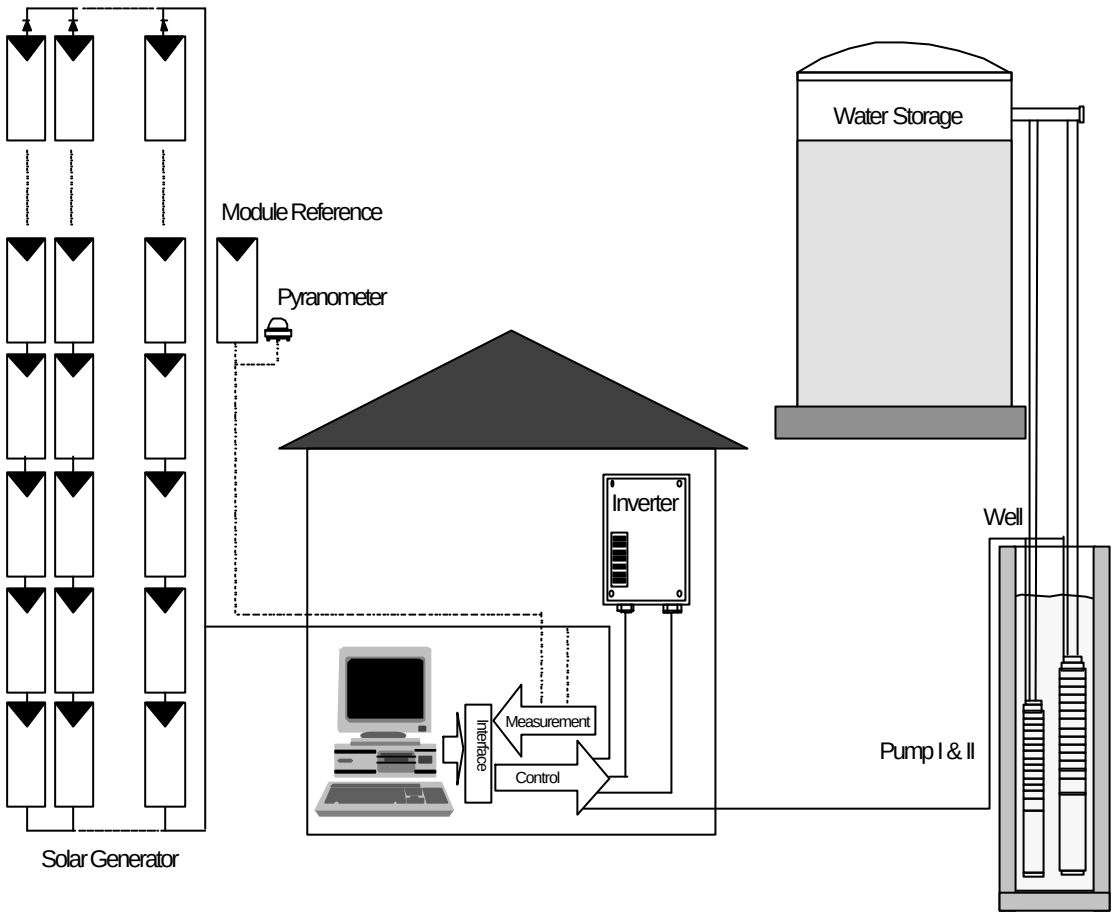

Figure 2.2: PVP system with double pumps.

2.3 Photovoltaic with Double Pumps

For the realizing of the PVP system with double pumps, some supplements of the equipment are necessary: personal computer, interface-card (PCL-718), sensor, transducer, software and etc. The c++ compiler is used to write and build the software, which made to: synchronizing between the computer and interface, reading the analog-digital signal and regulating-controlling the pump. The interface installed in the personal computer is possible to use for the data logger, because it is completed: 16 channels Analog-Digital (A/D) converter, 16 channels Digital-Digital (D/D) output and input. In addition, using for the data logger, this interface can be also applied for the controller, which is done by 2 channels Digital-Analog (D/A) output. These channels are functioned to operate the pump. The PVP system is monitored and

operated automatically by a personal computer, which is installed with the interface and software. For the accuracy of the regulation of the pump, the irradiance intensity is measured and averaged every minute. The computer using the interrupt handler reads the signal input from the interface. The measured data is averaged in a time period, which is adjusted in the program with unit: second, minute and hour. For the accuracy of the measured data and effective of the time, the time period is set for the one minute. One of the measured data is the irradiance intensity, which is used as a reference to regulate the pump operation. The PVP system in the clear weather starts to operate around 6:00 AM and stops around 18:00 PM. The location of the research is in UPT-LSDE Puspiptek, Serpong-Tangerang and the schema of the PVP system is shown in Figure 2.2. The equipment and component are installed in the PVP system with the double pumps:

2.3.1 Solar Generator

The solar-generator consists of 75 photovoltaic modules, which is 3.225-Watt peak. The modules are installed in series 18 pieces and in parallel 4. To optimize the power output of the solar generator in one year, the modules are put on the rig with angle 10 degree. The direction of the rig is north, because the Serpong's location is at South of the equator.

Specification of the photovoltaic module:

Nominal power	(P_n)	:	39	Wp
Nominal voltage	(V_n)	:	18.5	V
Nominal current	(I_n)	:	2.5	A
Open voltage	(V_{OC})	:	24.4	V
Short circuit	(I_{SC})	:	2.7	A
Module efficiency		:	10%	
Cell efficiency		:	11.5%	
Number cell		:	40	
Material		:	poly-crystal	

2.3.2 Inverter

The electric energy from the solar generator is direct current (dc) electric, but the load requires the alternating current (ac) power supply. To convert power from dc electric to the ac electric power, the inverter is necessary. The main component is the switcher and the pulse width modulation (PWM). Usually the switcher employs MOSFET or IGBT, which is driven and controlled by the PWM. The wave quality, frequency and voltage output of the inverter are also influenced by the PWM.

The voltage output of the solar generator fluctuates and depends on the irradiance intensity. To get optimum power output of the solar generator, the frequency of the inverter must be controlled. According to the capacity power, the three-phases inverter is chosen and installed in the PVP system.

The theory and illustration of the inverter are shown in Appendix C.1 to form the configuration of a three-phase inverter.

The specification of the inverter:

Capacity	:	3500 VA, 3 phase
Voltage input (V_{in})	:	135 ~ 300 V dc
Output voltage (V_{out})	:	13 ~ 127 V ac
Maximum input current (I_{in})	:	16 A dc
Average output current (I_{out})	:	14 A ac
Frequency	:	5~50 Hz
Wave	:	Sinuous

2.3.3 Motor

In the submersible pump, the motor is coupled directly with the pump in one unit. To suit the phase of the inverter and the size of the motor, the 3-phase induction motor is chosen. Three-phase induction motor is installed together with the centrifugal pump. Because this PVP system is without the battery, the power output of the solar generator depends on the irradiant intensity. It causes that the voltage and frequency output of the inverters are unsteady, however the starting and rotation of the three-phase induction motor have not problem. The maintenance of the induction motor is

relative low, because the rotor is squirrel cage type and without brush. The detail of the three-phase induction motor is shown in Appendix C.2.

The specification of the motor:

Motor I

product	:	Franklin Electric
nominal data at 50 Hz		
voltage input	:	3 x 127 V
average power	:	1100 Watt
current	:	8.5 Ampere
cos Φ	:	0.84
rpm	:	2835 per minute

Motor II

product	:	Franklin Electric
nominal data at 50 Hz		
voltage input	:	3 x 127 V
average power	:	2200 Watt
current	:	17 Ampere
cos Φ	:	0.84
rpm	:	2835 per minute

2.3.4 Pump

The type of the pump is centrifugal pump, which is connected with motor directly in one unit. The specification of the pump is appropriated with the head of the location. The head is measured from the source water to the water outlet of the pump with vertical direction. The detail of the centrifugal pump is illustrated and shown in Appendix C.3. The specification of the pump:

Pump I

Product	:	Groundfos
Type	:	SP 2A
Head	:	53 meter
Maximum flow	:	2 liter/second

Weight	:	15 kg

Pump II

Product	:	KSB
Type	:	UPA 100-4/22
Head	:	70 meter
Maximum flow	:	4 liter /second
Weight	:	19 kg

2.4 Regulating the Double Pumps

The regulating of the operation with the double pumps in the PVP system uses the analog-digital (A/D) output of the interface. Each signal output of D/A converter is 0 ~ 5 volt that it is connected to the switcher. The channel I is used to drive the connector between the inverter and the pump. The channel II is applied to steer the connector between the inverter and the solar-generator. Schematically the regulation is illustrated at the Figure 2.3. In the morning when the radiation is near 250 W/m^{-2} or around 7:30 AM, the PVP system starts to run with the small pump (pump I = 1.1 kW). Relationship to the time, the irradiance intensity increases little by little. When the irradiance intensity is high, the power output of the solar-generator and the voltage output of the module reference are also swell. While the voltage module reference is ≥ 2.3 volt, the voltage output of the channel I is +5 V (adjusting by the software).

With the signal +5 volt, the inverter- pump II is connected (pump II – on and pump I – off). When the moving of the connection from pump I to pump II is happened, the inverter in flash is without the load. As the protection, the inverter becomes in stand by. From stand by to ready condition, the inverter takes around 15 minutes. The reset inverter is required to cut the stand by time. When the output channel II is +5 volt, the connection between the inverter and the solar-generator is unconnected. The condition of the inverter from stand by to off necessitates 13 seconds. In order to protect the inverter, after 16 seconds, the output channel is +0 volt (adjusting in the software). This signal of the channel II causes the connecting between the inverter and the solar-generator. The PVP system with the pump II operates back. Because the capacity of the pump II is bigger than pump I, the water flow rate is also higher.

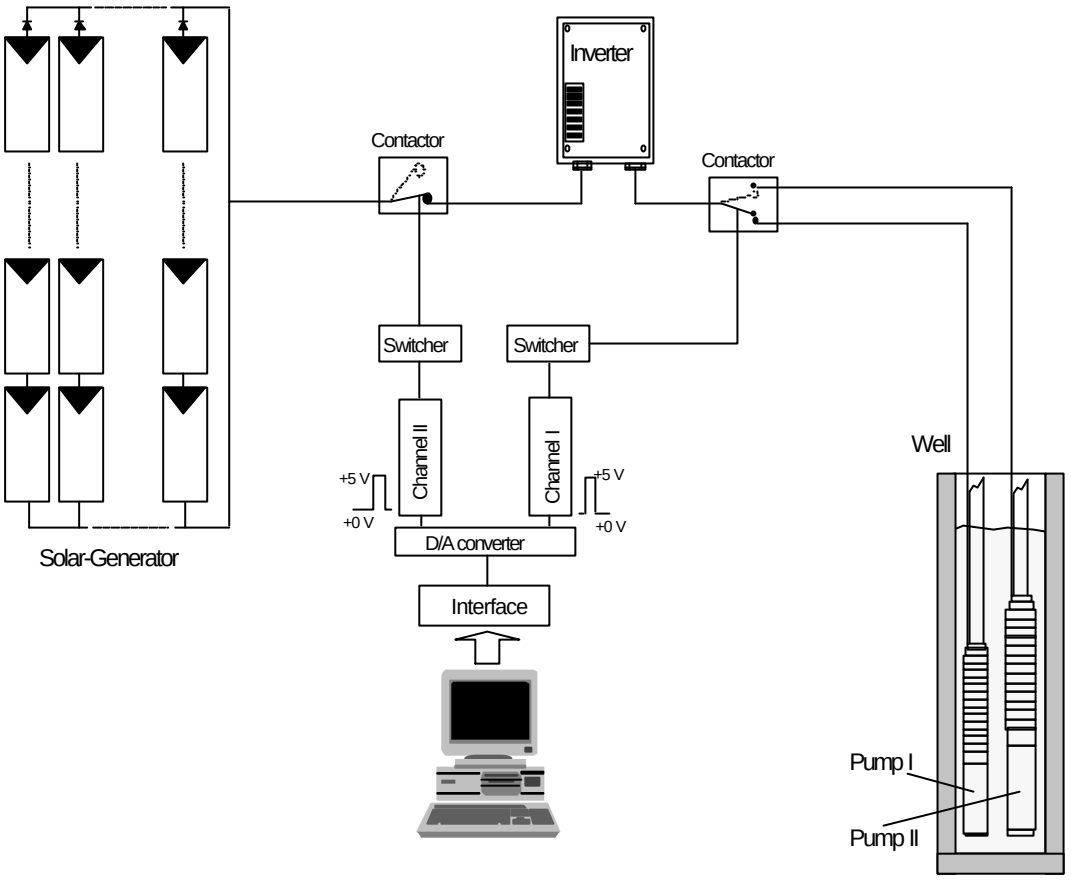

Figure 2.3: Schematic of the regulation of the pumps.

In good weather, the maximum irradiance intensity occurs around 12:00 AM. In the afternoon the irradiance intensity decreases gradually. When the voltage output of the module reference is ≤ 2 volt (radiation ≈ 550 Wm^{-2}) or around 15:00 PM, the output of the channel I is +0 volt. This signal causes the connecting between the inverter and pump I (pump II – off). When the load moves from pump II to pump I, in flash the inverter is without load. As the protection, the status of the inverter is in stand by. To reset the inverter, the output of the channel II is set +5 volt by the software. This signal causes the disconnecting between the inverter and the solar-generator. After 16 seconds, the output of the channel II is return +0 volt. The inverter and solar-generator is connected and the PVP system with the pump I (pump II-off) runs again. The irradiance intensity decreases continuously. When the radiation is < 200 Wm^{-2} or around 16:00 PM, the PVP system is stop. Because the power output of the solar-

generator is << the load capacity (pump I). The basic program of the regulation and measurement is shown in the Figure 2.7 (flowchart).

2.5 Performance and Measured Data

To evaluate and analyze the performance of the PVP system, some parameters of the system must be measured. A personal computer included the interface (PCL-718) is used as the data logger. The interface has 16 channels (single ended) analog-digital converter and 4 channels digital-digital output and input. The reading of the signal input of the measured data utilizes the interrupt handler in the computer. For the accuracy and effective of the time, the measured data is averaged every minute and saved directly to the hard disk.

The measured data is:

sun irradiation (E_c), output voltage of the solar generator (V_{out}), output current of the solar generator (I_{out}), hydrodynamic pressure (H), flow rate (Q), VAR power of the inverter (S_{var}), watt power of the inverter (P_{watt}) and output voltage of the reference module,

From this measured data, the other data is calculated,

sun irradiation per unit time ($kWhm^{-2}$ per day), power of the solar generator (kWh per day), water volume (m^3), total head (m), subsystem efficiency (%), system efficiency (%), VA power and factor power ($\cos \Phi$) inverter.

The measured data is displayed in the graphics, as shown in the Figure 2.4 and 2.6. From the Figure 2.4, the small pump (pump I) starts around 7: 30 AM or irradiance intensity ≈ 250 Wm^{-2}. The irradiance intensity increases slowly and the output solar-generator is also swell. When the irradiance intensity is around 700 Wm^{-2}, the PVP system operates with the big pump (pump II–on, pump I-off). Because the load capacity of the pump II is bigger than the pump I, the water flow rate is also faster. The maximum irradiance intensity is around 900 Wm^{-2} or about 12:00 AM. Afternoon the irradiance intensity decreases continuously. When the irradiance intensity is 550 Wm^{-2}, the PVP system operates with the small pump (pump I-on, pump II-off). The

irradiance intensity decreases gradually. When the power output of the solar-generator is << the load capacity of the pump I, the PVP system is stop.

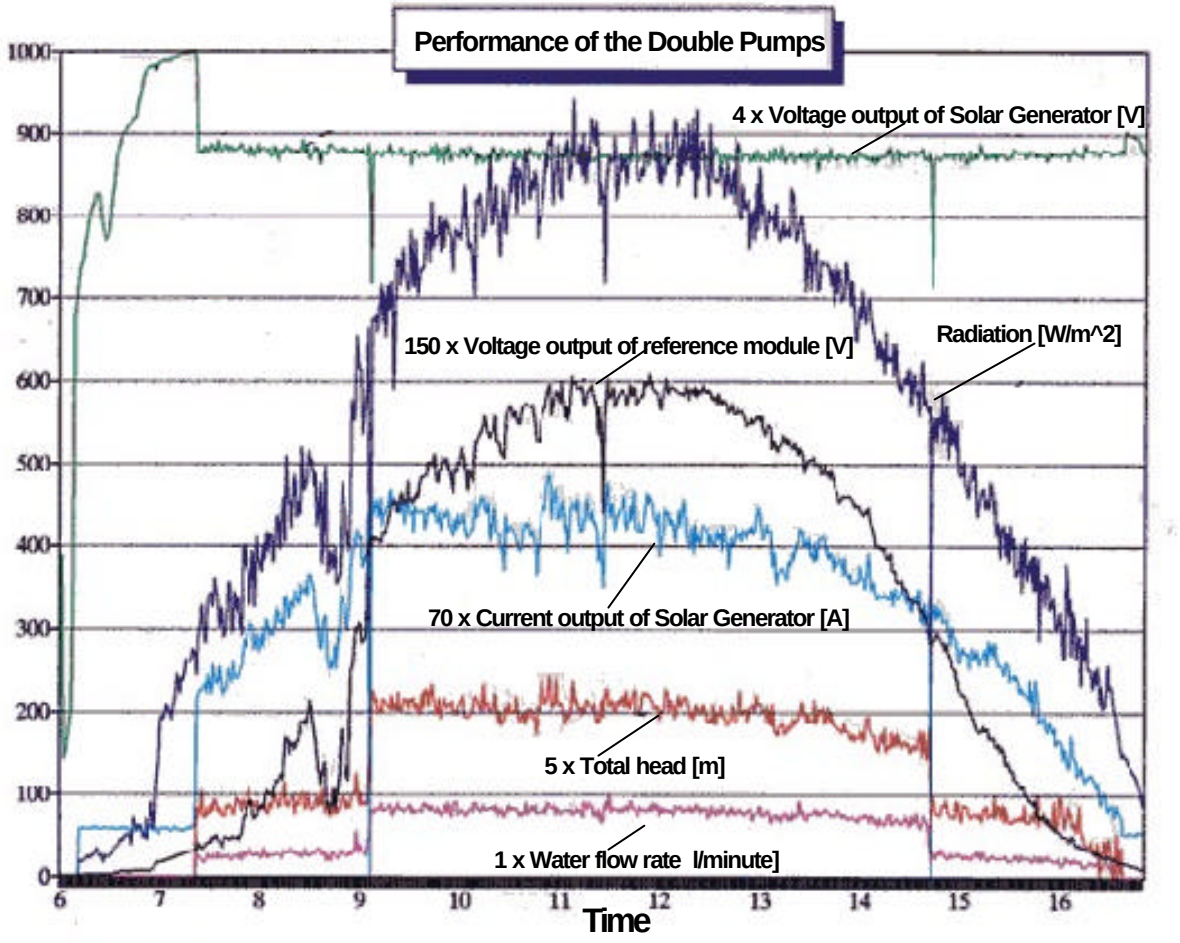

Figure 2.4: Performance of the double pumps in one day

From data in the Table 2.1, the performance of the PVP system with double pumps can be illustrated in the Figure 2.5. This figure shows the relationship between the hydraulic power (total head x water volume) and the insolation of the sun radiation. For the chance of the operation the small pump runs is longer than the big pump, because the insolation average is relative low. Therefore, this PVP system is only suitable for the location, where has the high insolation in one year. In the location with the low insolation, using double pumps isn't effective, because the big pump has small chance to run.

Table 2.1: Result of the performance of system

Insolation Wh/m^2 per day	Head H m	Water volume m^3	Inverter eff. %	Module eff. %	System eff. %	Power factor inverter	Hydroulic equivalent m^4
6453.04	30.16	31.936	80.287	6.348	2.690	0.509	963.32
5632.89	26.50	29.695	76.192	5.607	2.657	0.462	787.20
5378.07	27.59	24.390	64.689	6.026	1.075	0.450	673.06
5310.34	24.15	27.543	64.630	5.884	2.125	0.433	665.23
5035.07	27.72	23.816	78.074	5.349	2.337	0.471	660.30
4973.53	21.61	22.990	73.900	6.261	1.818	0.456	496.76
4559.44	20.04	11.628	59.385	5.485	1.007	0.407	233.12
3710.66	15.83	10.897	56.681	5.763	1.002	0.362	172.51

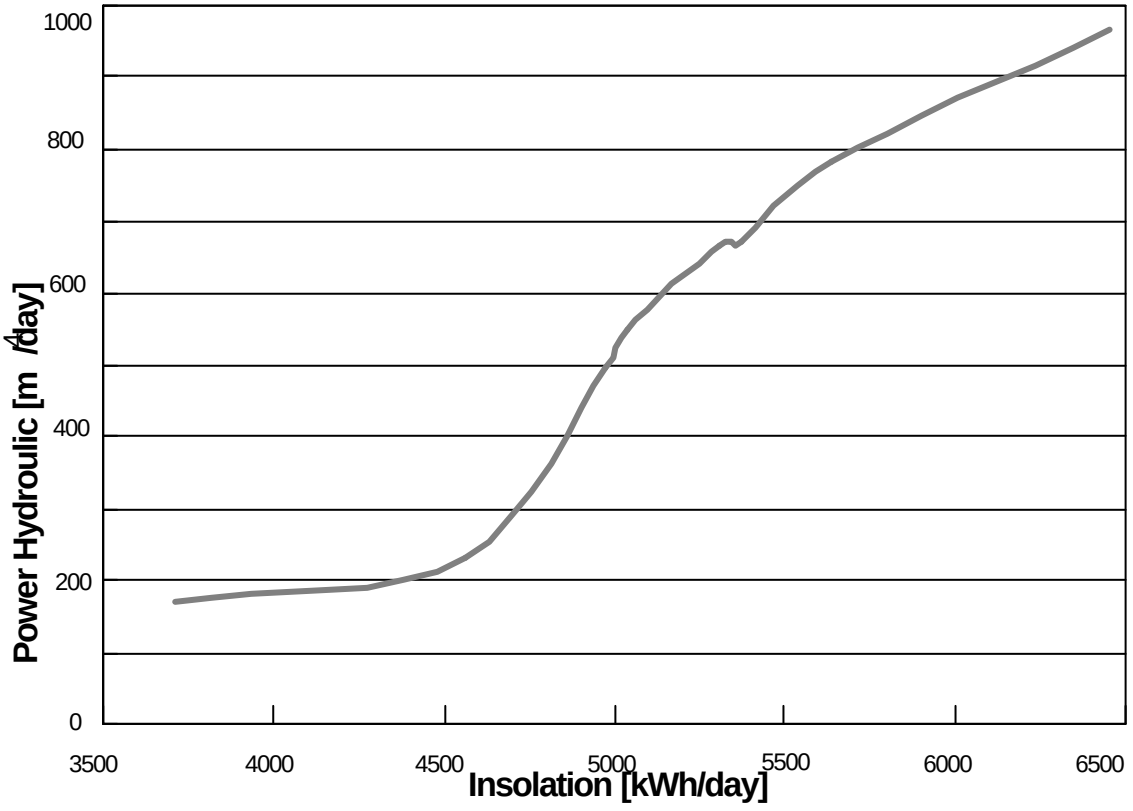

Figure 2.5: Power hydraulic of the double pumps at the various insolation

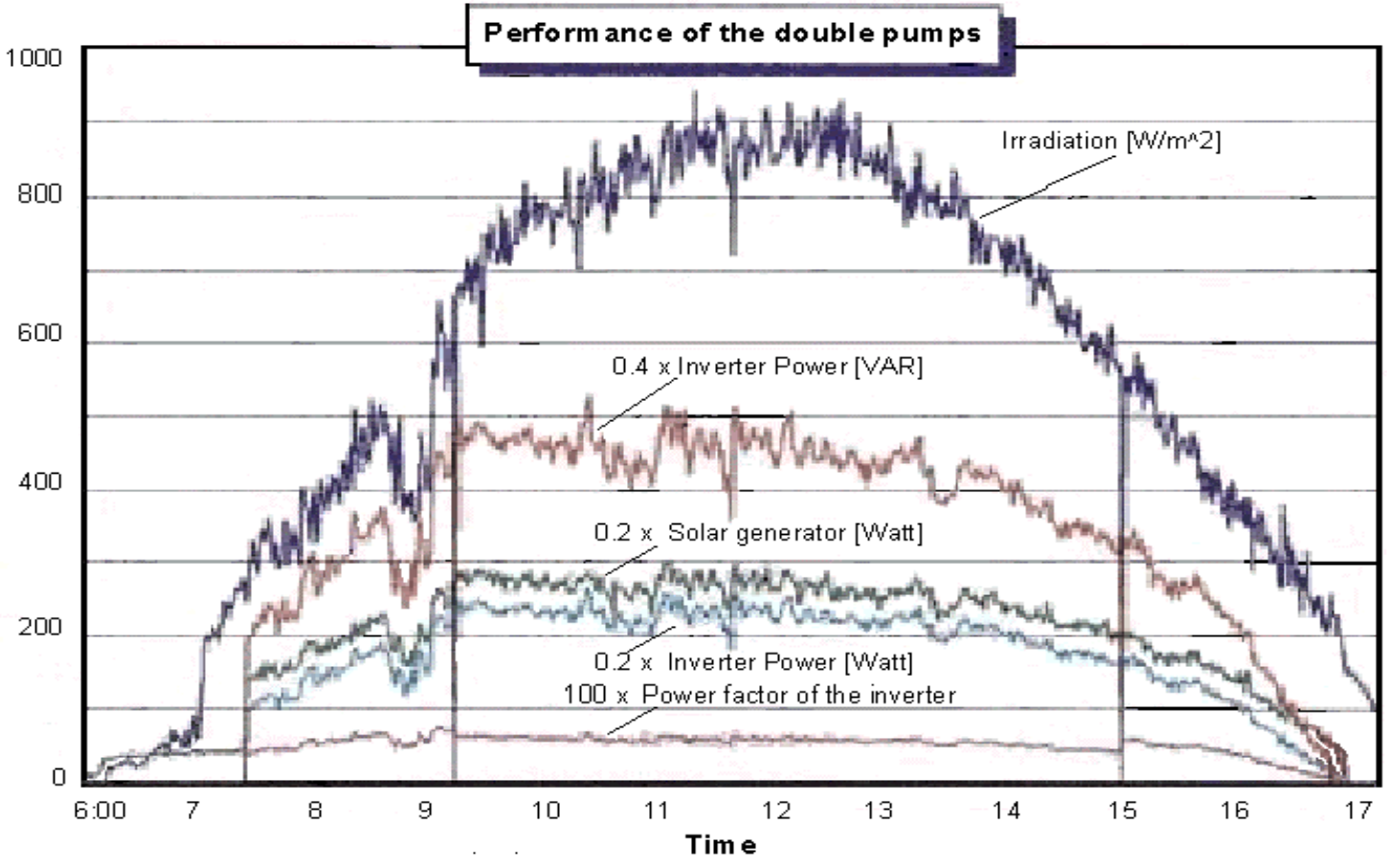

Figure 2.6: Performance of the double pumps in one day.

The regulation of the double pumps

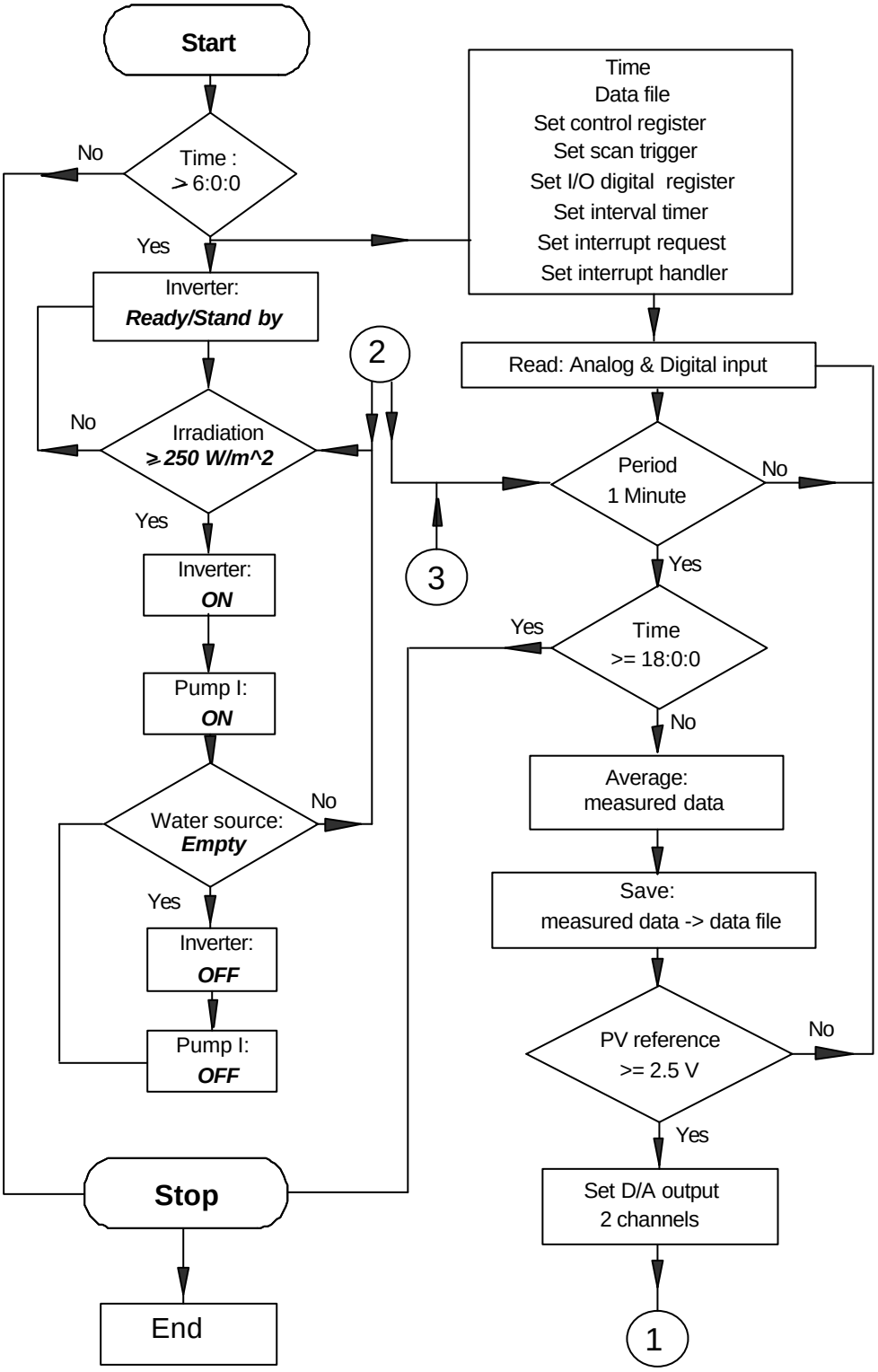

Figure 2.7: The basic program of the regulation and measurement.

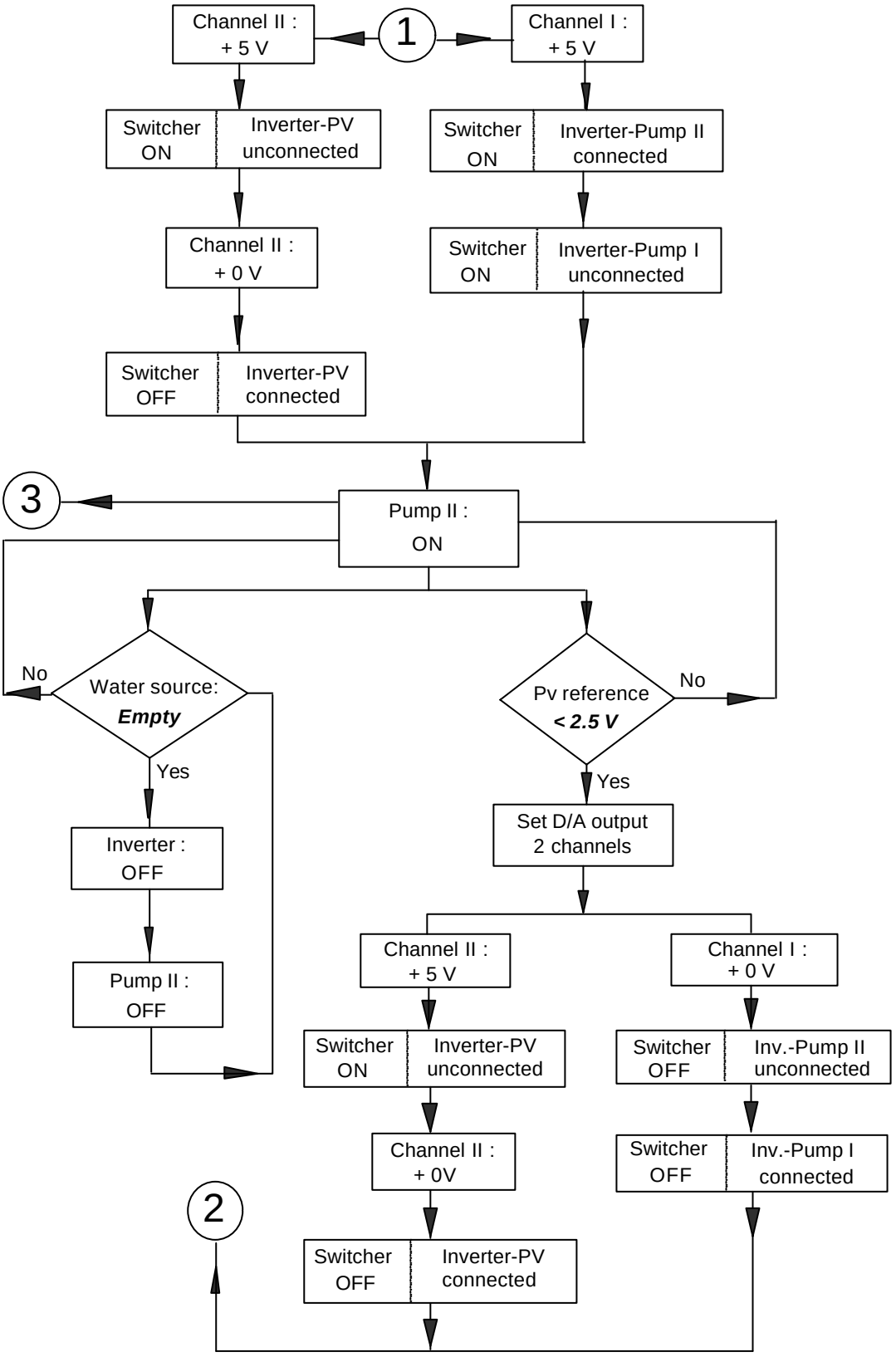
Channel II : + 5 V
1
Channel I : + 5 V
Switcher ON
Inverter-PV unconnected
Switcher ON
Inverter-Pump II connected
Channel II : + 0 V
Switcher ON
Inverter-Pump I unconnected
Switcher OFF
Inverter-PV connected
3
Pump II : ON
No
Water source: Empty
Yes
Pv reference < 2.5 V
No
Yes
Inverter : OFF
Set D/A output 2 channels
Pump II : OFF
Channel II : + 5 V
Channel I : + 0 V
Switcher ON
Inverter-PV unconnected
Switcher OFF
Inv.-Pump II unconnected
Channel II : + 0V
Switcher OFF
Inv.-Pump I connected
2
Switcher OFF
Inverter-PV connected

Chapter 3

Photovoltaic Module

3.1 Photovoltaic Model

The photovoltaic module consists of some solar cells, which is installed in series and parallel in the frame. Protecting for water, dash, humidity and heat, the solar cells are placed in the encapsulation, which has single or double flat glasses. Through the flat glass, the light possible radiates the surface of the solar cell. The solar cell functions to convert the photon energy to the electric energy. The electric energy resulted by the solar cell is direct current (dc) electric. Performance of the solar cell or photovoltaic module depends also on the efficiency. Maximum efficiency of the photovoltaic is approximate 15% for mono-crystal silicon and around 12% for poly-crystal silicon. Because the efficiency is relative low, to get the huge power capacity of the solar generator, many photovoltaic modules are required. The performance of the module can be identified with some methods, but one of the methods knows the model of the solar cell.

The model of the solar cell is declared in the exponential equation that includes constants and parameters, as the Equation (3.1)[1]:

$$j = (C_0 + C_1 T)G - C_{01} T^3 \exp\left[-\frac{e_o U_{gap}}{k T}\right]\left[\exp\left(\frac{e_o (V_c + j r_s)}{\alpha\, kT}\right) - 1\right]$$

$$- C_{02} T^{5/2} \exp\left[-\frac{e_o U_{gap}}{2 kT}\right]\left[\exp\left(\frac{e_o (V_c + j r_s)}{\beta kT}\right) - 1\right] - \frac{V_C + j r_S}{r_{sh}} \quad (3.1)$$

where U_{gap} is band gap (set constant to 1.14 V); e_o charge of an electron (1.6021 x 10^{-19} As); k Boltzmann constant (1.3854 x 10^{-23} JK^{-1}); α (1.0) β (3.1) diode parameter, and T cell temperature in Kelvin; G irradiation; j current density; V voltage; C_0; C_1;C_{01}; C_{02} constants; r_{sh}, r_s shunt and series resistance. Each solar cell in the module is considered to have similar performance. To get the parameters of the model, the module is radiated and loaded with a load simulator. While being irradiated, the load simulator is regulated gradually from zero until maximum load by a personal computer. The regulated load simulator results various output current-voltage of the module. The testing is repeated under the low-high irradiation and various temperatures.

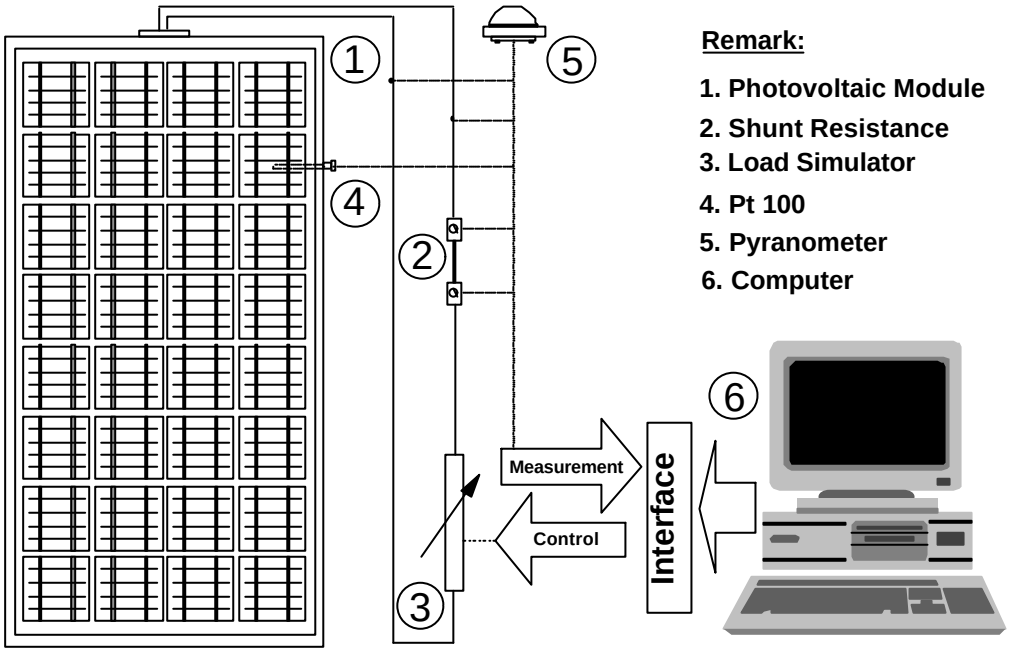

Figure 3.1: Testing of a photovoltaic module

The measured data (radiation (G) and cell temperature (T)) and the output current-voltage of the module are recorded and saved in the hard disk. The radiation (G) and cell temperature (T) of the recorded data are as input data for the model and the recorded I-V output of the testing as reference for the I-V output of the model. The values of the parameters (C_0, C_{02}, C_1, r_{sh}) are obtained from the linear simultaneous

equations, and log linear simultaneous equations for (C_{01}, r_s) by use of least square method and iteration. After the best fit, the results from the model coincided with those from measurement, and the values of the parameters are considered appropriate.

Because the equation of the model is exponential, the values of the I-V output are solved by iteration. The value of the maximum output voltage (V_{max}) is fixed firstly with entry the value of the output current equal zero (I=0). To find the value of the current (I_n), the value of the maximum voltage (V_{max}) is decreased small by small ($V_n=V_{max} - n\,\Delta V$). The calculation is continually done until the value of the voltage equal zero ($V_n=0$) and the maximum output current (I_{max}) is established. The calculation is reiterated for the other value of the radiation (G) and cell temperature (T) from the recorded data. Some results of the measured I-V curve are shown in Figure 3.2 (shown by lines with symbols).

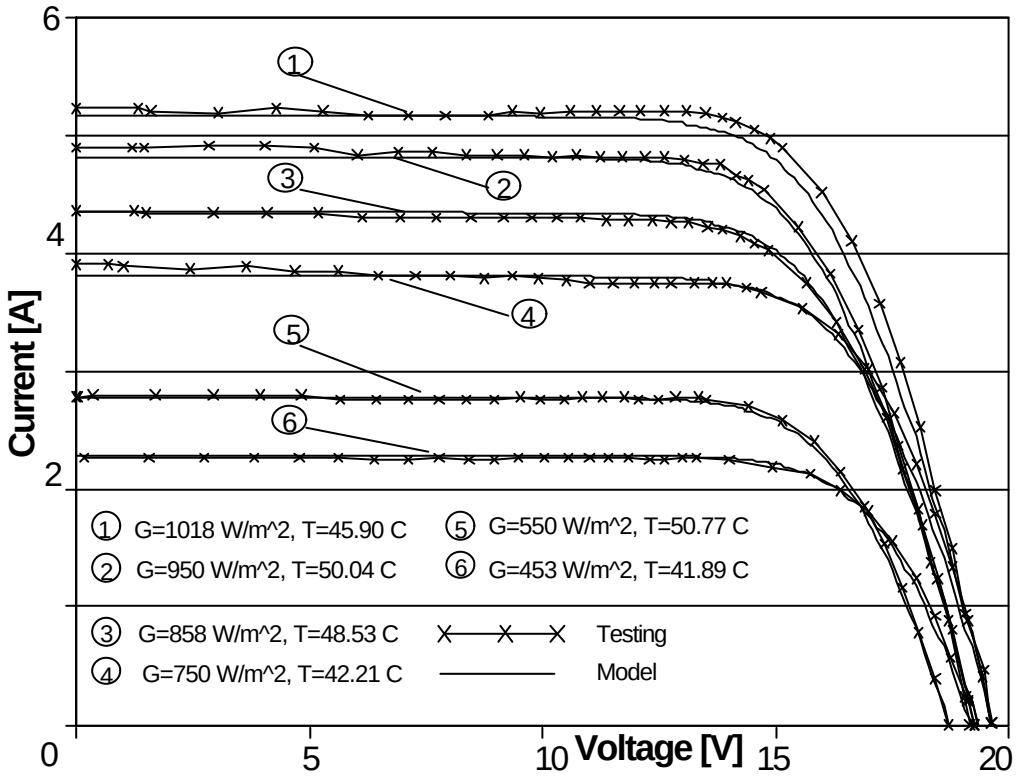

Figure 3.2: I-V curve of the measurement and model of a photovoltaic module.

The values of the I-V model are approached to the I-V output of the measurement, the value of the parameters are as: $\alpha = 1$; $\beta = 3.1$; $r_s = 1.3660 \times 10^{-04}\ \Omega\ m^{-2}$; $r_{sh} = 0.913\ \Omega\ m^{-2}$; $Co = 0.45100\ V^{-1}$; $C_1 = 0.1786 \times 10^{-04}\ V^{-1}\ K^{-1}$; $C_{01} = 38.1786\ A\ m^{-2}\ K^{-3}$; $C_{02} = 0.1220\ A\ m^{-2}\ K^{-5/2}$.

The value of the parameters depends on the quality and efficiency of the solar cell.

The performance of the photovoltaic module is easy identified by the model simulation with the various radiation (0 ~ 1000 Wm^{-2}) and temperature, as shown Figure 3.2. The voltage output is relative constant at the various radiations, but the current output is proportionally with the radiation.

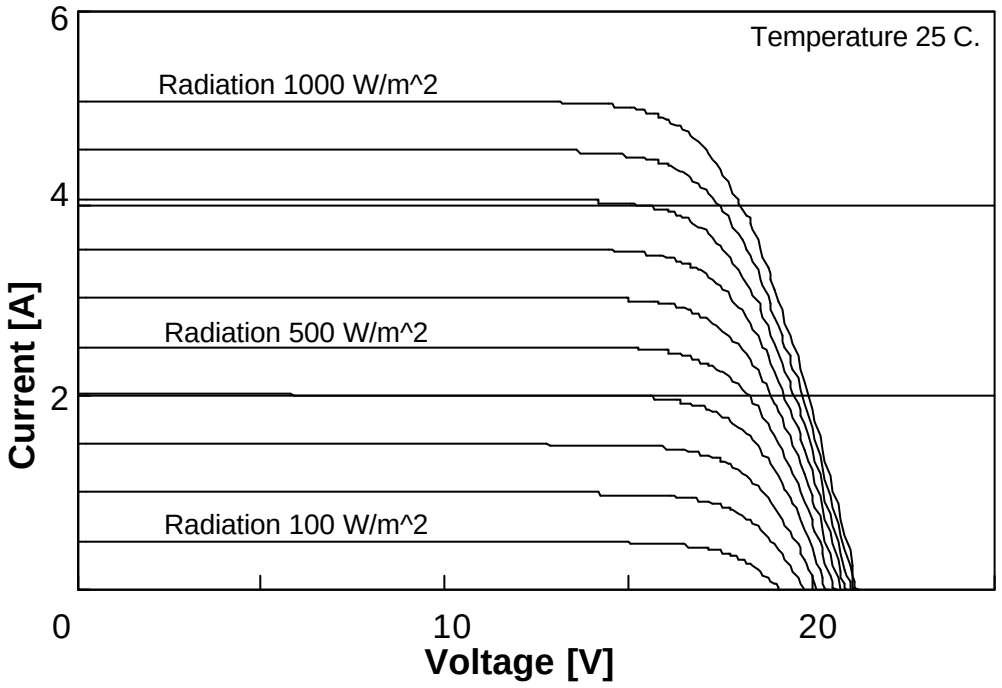

Figure 3.3: I-V curve with the values of radiation.

The cell temperature affects the performance of the I-V output of the module. By the simulation model, the I-V curve is illustrated with the various cell temperature and constant radiation, as shown Figure 3.4.

At the Figure 3.4, the graphic shows relationship between the cell temperature and I-V output of the module. The Effect of the cell temperature is due to the exponential increases in the saturation current with an increase in temperature.

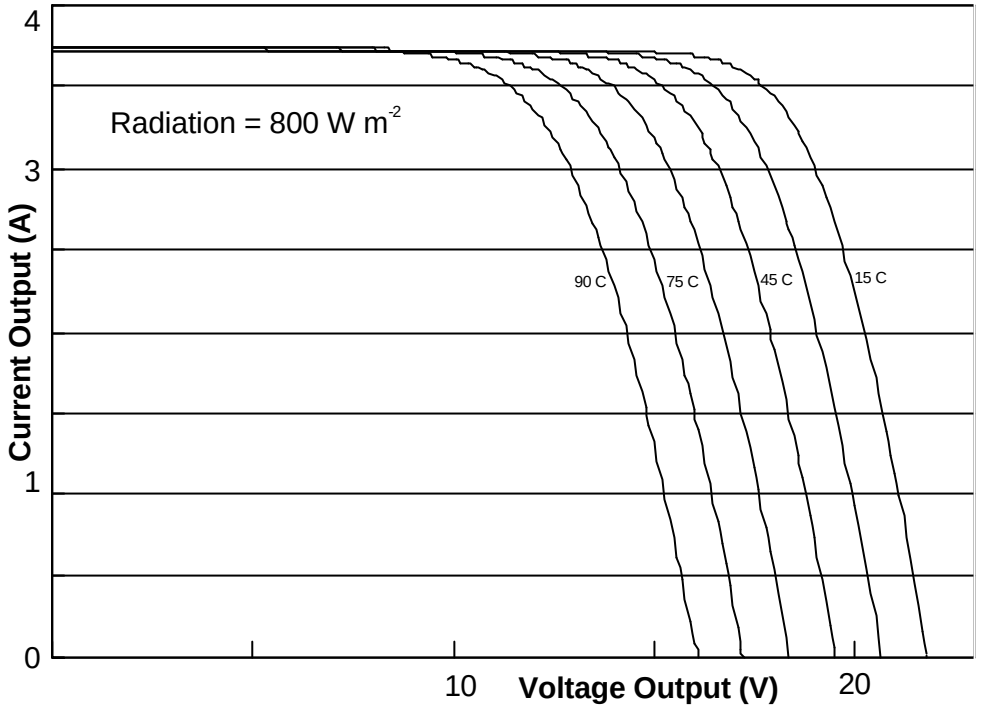

Figure 3.4: I-V curve with the various cell temperatures.

3.2 Solar Generator

The photovoltaic system with the big capacity power requires some photovoltaic modules. The voltage output of the solar-generator depends on the photovoltaic modules in series. In order, the power of the solar-generator is bigger than the power of one individual module, the modules are connected in parallel.

3.2.1 Modules in Series

In an ideal case when numbers (n) of the identical photovoltaic module are connected in series, the open-circuit voltage equal to n^{th} the voltage of one individual module:

$$V_{SG} = \sum_{n}^{1} V_n = V_1 + V_2 + V_3 + ... + V_n \qquad (I > 0)$$

$$V_{SG} = nV_{OC1} = nV_{OC2} = nV_{OC3} = ... = nV_{OCn} \qquad (I = 0) \qquad (3.2)$$

The result of the ideal characteristic of n identical modules in series by the simulation model is presented in the Figure 3.5.

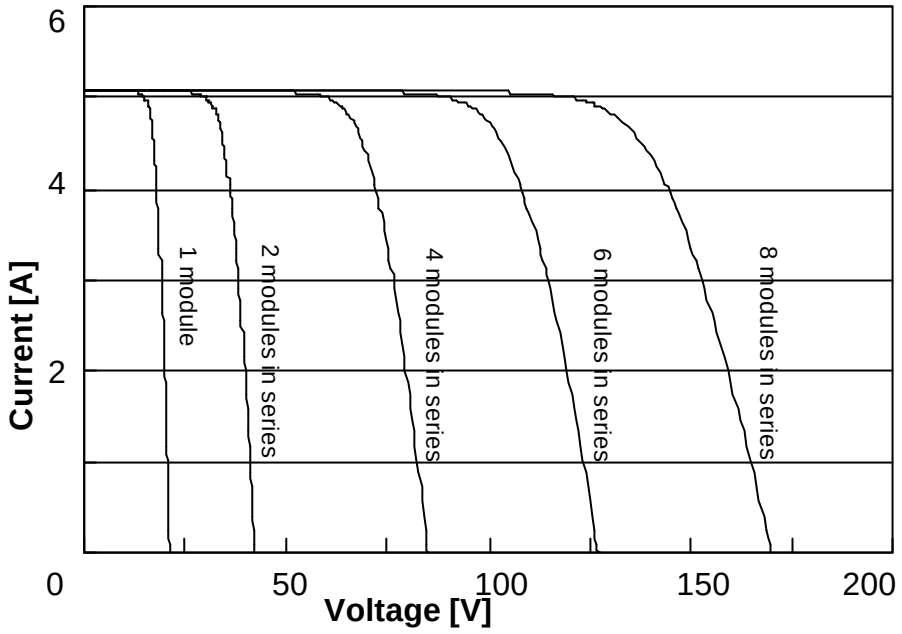

Figure 3.5: The photovoltaic modules in series.

3.2.2 Module in parallel

The numbers (n) of the identical module are jointed in parallel. The resulting voltage (V_{SG}) is the same for each module and the resulting current (I_{SG}) is the sum of the respective currents I_1 until I_n of the module:

$$I_{SG} = \sum_{n}^{1} I_n = I_1 + I_2 + I_3 + ... + I_n$$

$$V_{SG} = V_1 = V_2 = V_3 = ... = V_n \qquad (3.3)$$

The simulation model illustrates the ideal resulting of characteristic of the modules in parallel in the Figure 3.6.

The solar-generator of the photovoltaic system with the big capacity is built by the some modules, which are connected in series and parallel. The integrated assembly of the photovoltaic modules together with support structure (foundation, tracking, box junction, cable and other components) is defined as the photovoltaic array.

The current and voltage output of the solar-generator in the photovoltaic array are:

$$V_{out} = \sum_{n}^{1} V_n = V_1 + V_2 + V_3 + ... + V_n \qquad (3.4)$$

$$I_{out} = \sum_{m}^{1} I_m = I_1 + I_2 + I_3 + ... + I_m \qquad (3.5)$$

The power of the solar-generator (P_{out}) is written in the Equation (3.6):

$$P_{out} = \sum_{n}^{1} V_n \sum_{m}^{1} I_m = (V_1 + V_2 + V_3 + \ldots . V_n)(I_1 + I_2 + I_3 \ldots . I_m) \quad (3.6)$$

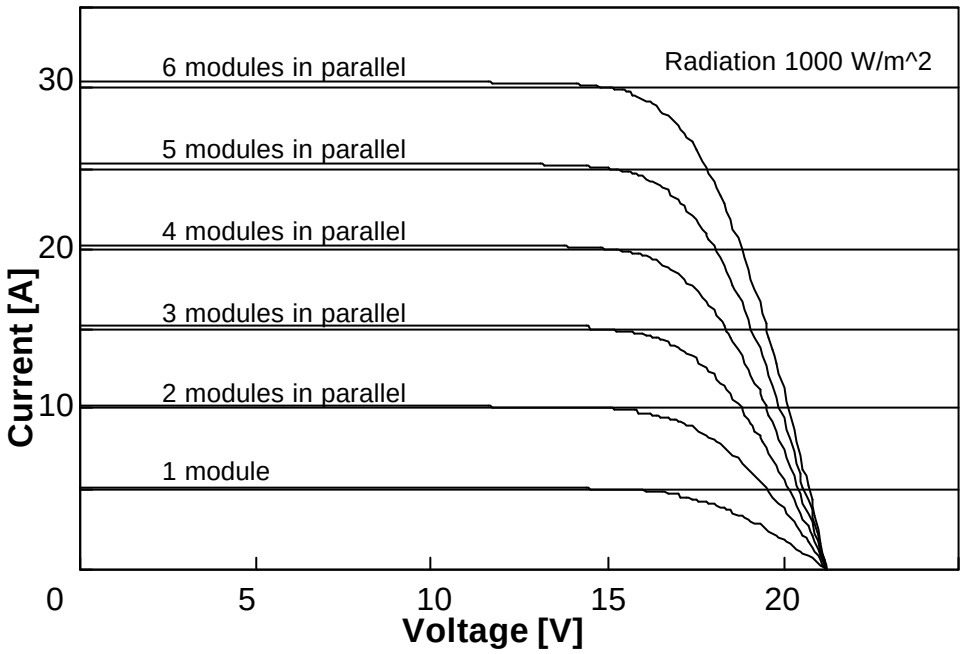

Figure 3.6: The modules in parallel.

3.3 Maximum Power Point

The maximum power point (MPP) is a vertex point between the current line and the voltage line at the I-V curve with the widest area. The changing of the radiation and cell temperature moves the position of the MPP. In the Figure 3.7, a line connects from the MPP at the radiation 100 Wm^{-2} until the MPP at the radiation 1000 Wm^{-2} at the I-V curve. Because the module consists of the solar cell, the current and voltage output of the module are found by the Equation (3.1) and the MPP of the module is calculated:

$$P_{md-max} = V_{md} \cdot I_{md} \quad (3.7)$$

$$V_{md} = m_{cl} \; V_{cl} \quad (3.8)$$

$$I_{md} = n_{cl} \; I_{cl} \quad (3.9)$$

Substitution Equations (3.7), (3.8) and (3.9)

$$P_{md-max} = m_{cl}\, n_{cl}\, V_{cl}\, I_{cl} \quad (3.10)$$

where $P_{md\text{-}max}$ is the maximum power output of the module; V_{md} the voltage output of the module; I_{md} the current output of the module; V_{cl} the voltage output of the one cell; I_{cl} the current output of the one cell; m_{cl} the number of the cell in series in the one module; n_{cl} the number of the cell in parallel in the one module.

The MPP of the photovoltaic module is calculated with using the Equation (3.1) and (3.10) by simulation model. The maximum voltage (V_{max}) is computed with the current equal zero (I=0). The relationship between the current (I_n) and voltage (V_n) is found with decreasing the maximum voltage step by step ($V_n=V_{max} - n\ \Delta V$). The result of the power calculated by Equation (3.7) is always compared with the previous power (P_{n-1}). With this method, the maximum power (P_{max}) is found.

In the Figure 3.7, the highest of the maximum power (P_{max}) at the radiation 1000 W m^{-2} is shown with ABCD area. The point B is a vertex between the current line and voltage line of the maximum power point (MPP).

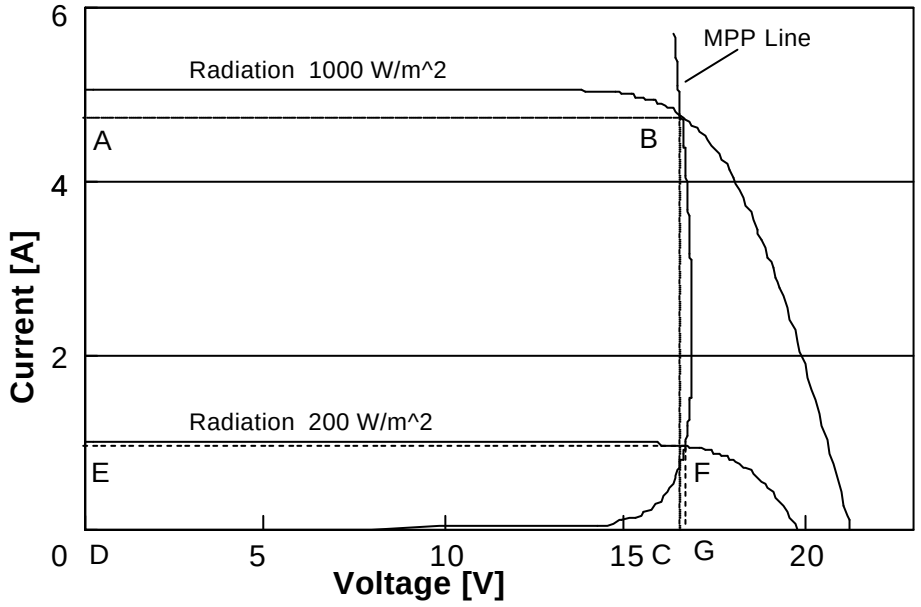

Figure 3.7: The MPP line of the photovoltaic module.

Chapter 4

Single Pump

4.1 Photovoltaic System

One of the method of increasing the efficiency of the photovoltaic system is replacing the sub-component or the component with higher efficiency. Usually the PVP system uses the centrifugal pump, but in the current experiment operates the piston pump as the new sub-component. The PVP system consists of the main component: photovoltaic array, converter, motor, pump and other supporting of the equipment. The PVP systems in the current experiment are installed in two locations: Subang and Serpong, West Java-Indonesia. The components and the equipment supporting the PVP systems at the two locations are similar. The experimental setup is illustrated schematically in Figure 4.1. The solar generator part consists of 24 modules with 36 mono-crystal solar cells in each module. The parallel number of the solar cell in each module is 1. The parallel number of the module in the photovoltaic array is 3. The capacity of the solar generator is 2040-watt peak. A 510-watt dc motor is used as a mechanical driver that is connected by the belt to a flywheel. The rated power of the motor is chosen smaller than the generator capacity to enable the PVP system to run under low irradiation. To track the optimum power output of the solar generator, a Maximum Power Point (MPP) Tracker and a 1400-watt dc-dc converter are installed. The MPP Tracker controls and adjusts the voltage output. Because the motor is connected directly to the MPP tracker without the stored energy (battery), the speed of the motor is relative not constant. The fluctuant of the radiation causes the change of

current and voltage output of the solar-generator. The head of the pump is used the head simulator that exploits the adjusting valve. The head of the piston pump is set to work from 15 to 35 meters. The experiments are carried out under the clear weather starting from about 8.00 AM or when the irradiation is approximately 180 W/m^2 until around 16.00 PM.

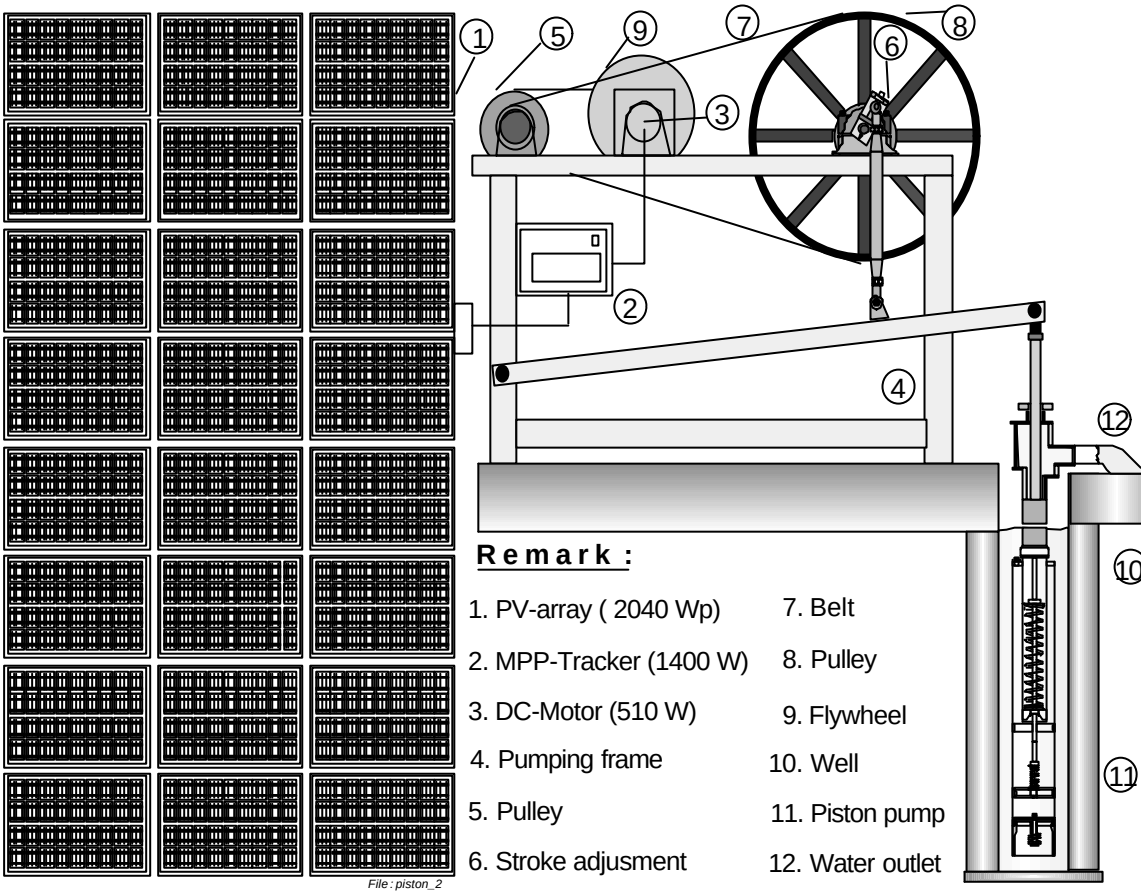

Figure 4.1: Schema of the mechanical piston pump system

4.2 Solar Generator

The solar-generator consists of the photovoltaic modules 24 pieces with type BP 585F. The modules are connected in series 8 pieces and in parallel 3 arrays. To protect the module from the animal, people and shadow, the modules put on the supporting or the rig that is 1-2 meter high. The latitude of the position of two locations (Subang and Serpong) is around 107 degree and the altitude is about 10 degree South. Because the location in the south of the equator, the module is directed to north and the angle is

around 10 degree. The direction and angle is fixed, in order to get the optimum of the radiation during one year. Besides the radiation intensity, the shadow and dust at the photovoltaic module can influence the power output of the solar-generator. Therefore, the location of the photovoltaic array must be free from tree, building and something, which are higher than the high PV array. For the dust, the glass of the photovoltaic module should be cleared 2 times in one year. The lifetime of the photovoltaic module is estimated for 15 years.

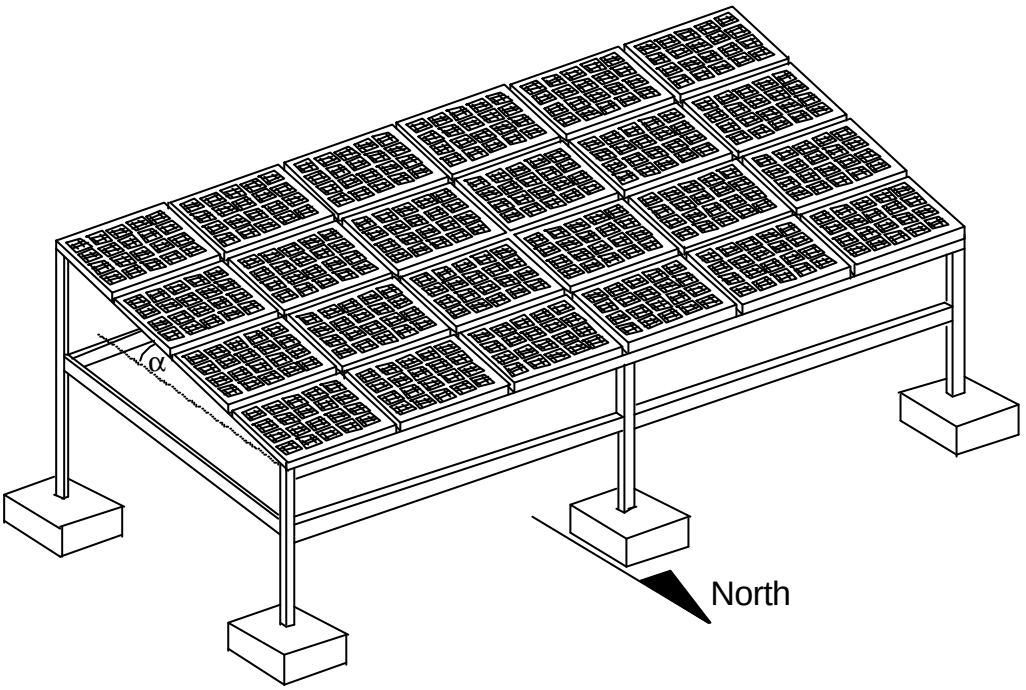

Figure 4.2: The photovoltaic array with 24 modules.

The specification of the photovoltaic module:

Module type	:	BP 585F
Crystal	:	mono-crystal
Nominal peak power	:	85.00 W
Peak power voltage (V_{mp})	:	18.00 V
Peak power current (I_{mp})	:	4.72 A
Short circuit current (I_{sc})	:	5.00 A
Open circuit voltage (V_{oc})	:	22.03 V
Minimum power (P_{min})	:	80.00 W

Number cell	:	36 cells
Total area cell	:	0.45 m^2
Weight	:	7.5 kg

4.3 DC-DC Converter [16]

The dc-dc converter or dc chopper protects the condition of the voltage output in the photovoltaic system. In addition to regulating the voltage output, the dc-dc converter functions as the maximum power point (MPP) tracker. Because the radiation intensity changes, the current and voltage output of the solar-generator always fluctuate and the MPP of the solar-generator also moves. With the MPP tracker, the power output of the solar-generator is near optimum. The dc chopper can be used as switching-mode regulators to convert a dc voltage normally unregulated, to a regulated dc voltage output. The regulation is normally achieved by pulse-width modulation (PWM) at a fixed frequency and the switching device is commonly a power IGBT or MOSFET.

4.3.1 Buck Regulator

In a Buck regulator, the average output voltage V_a is less than the input voltage V_s hence the name "buck ", a popular regulator. The circuit diagram of a buck regulator using a power IGBT is shown in Figure 4.3-a, and this like a step-down chopper. The circuit operation can be divided into two modes. Mode 1 begins when transistor Q_1 is switched off at t = 0. The input current, which rises, flows through filter inductor L, filter capacitor C and load resistor R. Mode 2 begins when transistor Q_1 is switched off at $t = t_1$. The diode D_m conducts due to energy stored in the inductor and the inductor current continues to flow through L, C, load and diode D_m. The inductor current falls until transistor Q_1 is switched on again in the next cycle. The equivalent circuits for the modes of operation are shown in Figure 4.3.b. The waveforms for the voltages and currents are shown in Figure 4.3.c for a continuous current flow in the inductor L. Depending on the switching frequency, filter inductance and capacitance, the inductor current could be discontinuous.

The voltage across the inductor L is in general,

$$e_L = L\frac{di}{dt}$$

Assuming that the inductor current rises linearly from I_1 to I_2 in time t_1,

$$V_s - V_a = L\frac{I_2 - I_1}{t_1} = L\frac{\Delta I}{t_1} \qquad (4.1)$$

or

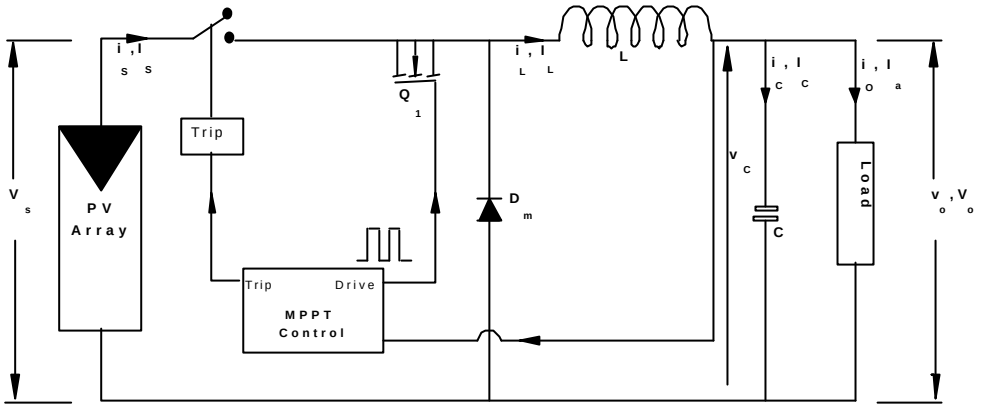

(a) Circuit diagram

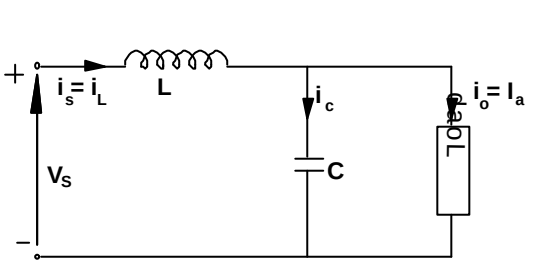

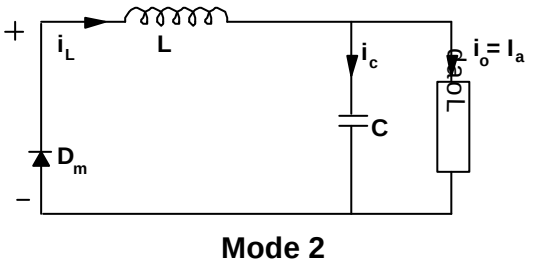

(b) Equivalent circuits

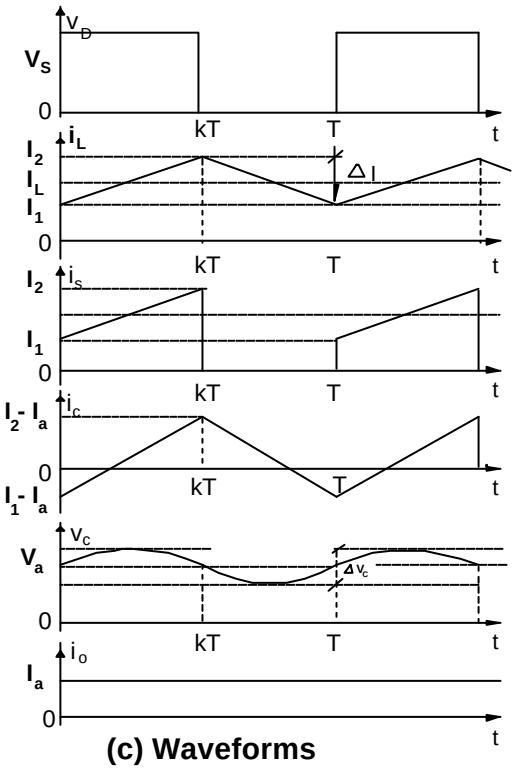

(c) Waveforms

Figure 4.3: Buck regulator

$$t_1 = \frac{\Delta I\, L}{V_s - V_a} \tag{4.2}$$

and the inductor current falls linearly from I_2 to I_1 in time t_2,

$$-V_a = -L\,\frac{\Delta I}{t_2} \tag{4.3}$$

or

$$t_2 = \frac{\Delta I\, L}{V_a} \tag{4.4}$$

where ΔI is the peak-to-peak ripple current of the inductor L. Equating the value of ΔI in Equation 4.1 and 4.3 gives

$$\Delta I = \frac{(V_s - V_a)\, t_1}{L} = \frac{V_a\, t_2}{L} \tag{4.5}$$

Substituting $t_1 = kT$ and $t_2 = (1\text{-}k)T$ yields the average output voltage as

$$V_a = k\, V_s \tag{4.6}$$

Assuming a loss less transistor switch, $V_s\, I_s = V_a\, I_a = k\, V_a\, I_a$ and the average input current,

$$I_s = k\, I_a \tag{4.7}$$

The switching period T can be expressed as

$$T = \frac{1}{f} = t_1 + t_2 = \frac{\Delta I\, L}{V_s - V_a} + \frac{\Delta I\, L}{V_a} = \frac{\Delta I\, L\, V_s}{V_a (V_s - V_a)} \tag{4.8}$$

which gives the peak-to-peak ripple current as

$$\Delta I = \frac{V_a\,(V_s - V_a)}{f\, L\, V_s} \tag{4.9}$$

or

$$\Delta I = \frac{V_s\, k\,(1-k)}{f\, L} \quad . \tag{4.10}$$

Using Kirchhoff's current law, the load current can be written as

$$i_L = i_c + i_o.$$

If the load ripple current, Δi_o, is very small and negligible, $\Delta i_L = \Delta i_c$. The average capacitor current, which flows for $\frac{t_1}{2} + \frac{t_2}{2} = \frac{T}{2}$, is

$$I_c = \frac{\Delta I}{4}.$$

The capacitor voltage is expressed as

$$v_c = \frac{1}{C}\int i_c\,dt + v_c \quad (t=0)$$

and the peak-to-peak ripple voltage of the capacitor is

$$\Delta V_c = v_c - v_c\,(t=0) = \frac{1}{C}\int_0^{T/2}\frac{\Delta I}{4}\,dt = \frac{\Delta I\,T}{8C} = \frac{\Delta I}{8fC} \quad . \tag{4.11}$$

Substituting the value of ΔI from equation (4.9) or (4.10) in equation (4.11) yields

$$\Delta V_c = \frac{V_a\,(V_s - V_a)}{8LCf^2 V_s} \tag{4.12}$$

or

$$\Delta V_c = \frac{V_s\,k(1-k)}{8LCf^2} \quad . \tag{4.13}$$

The buck regulator requires only one transistor, is simple and has high efficiency. The di/dt of the load current is limited by inductor L. However, the input current is discontinuous and a smoothing input filter is normally required. It provides one polarity of output voltage and unidirectional output current. It requires a protection circuit in case of possible short circuit of the diode path.

The specification of the dc-dc converter:

Type	:	Maximizer 1200 P
Power	:	1400 W
Input current	:	0 ~ 12 A
Output current	:	0 ~ 20 A
Input voltage	:	20 ~ 165 V dc
Output voltage adjustment	:	13 ~ 132 V dc

With these devices, maximum power can be tracked by changing the value of k to be optimum I x V. In the present experiment, Buck Regulator was used.

The other regulator (boost regulator) is shown in Appendix C.4.

4.4 Motor

The motor changes the electric energy into the mechanical energy. The kind of the motor is the dc motor, which has couple brushes and couple permanent magnets. The using the permanent magnet increases the efficiency motor, because the stator doesn't

require the electric power, which is used to excite the magnet field in the stator. The motor with the permanent magnet is only suitable for the small capacity, but for the big capacity, it is not effective. The detail of the dc motor is shown in Appendix C.5.

The specification of the dc motor:

Type	:	WSM3
Capacity	:	510 W
Input voltage	:	43 ~ 190 V dc
Nominal input current	:	16.8 A
Maximum input current	:	140 A
Nominal rotation	:	750 per minute
Maximum rotation	:	4500 per minute
Efficiency	:	71%
Weight	:	21 kg

4.5 Pump

The new type of the pump installed in PVP system is piston pump or Bohner's pump. Schematic of the piston pump is shown in the Figure 4.4. The pump consists of the main component: cylinder, piston, springs and valves. When the piston, Pt, moves up, the valve, VL_1, is open, whereas the valve, VL_2, is close ($P_2 > P_1$), the water flows up through the valve, VL_1. The piston, Pt, goes up until the top position that is adjusted with the stroke of the pump. On the contrary, when the piston, Pt, moves down, the valve, VL_2 is open (VL_1 is close), the water flows through the valve VL_2 at the piston.

The flowing water in the pump is needed the work in the equation as:

$$W = (P_2 - P_1)\, A\, \Delta l \tag{4.14}$$

where W is the work; P_1 & P_2 the water pressure; A the cross area of the cylinder and Δl the length of the piston displacement.

The efficiency of the piston pump is higher than the centrifugal pump. Because the size of the piston pump is relative big and requires the supporting, the installing of the PVP system with the piston pump is relative more difficult than with the centrifugal pump.

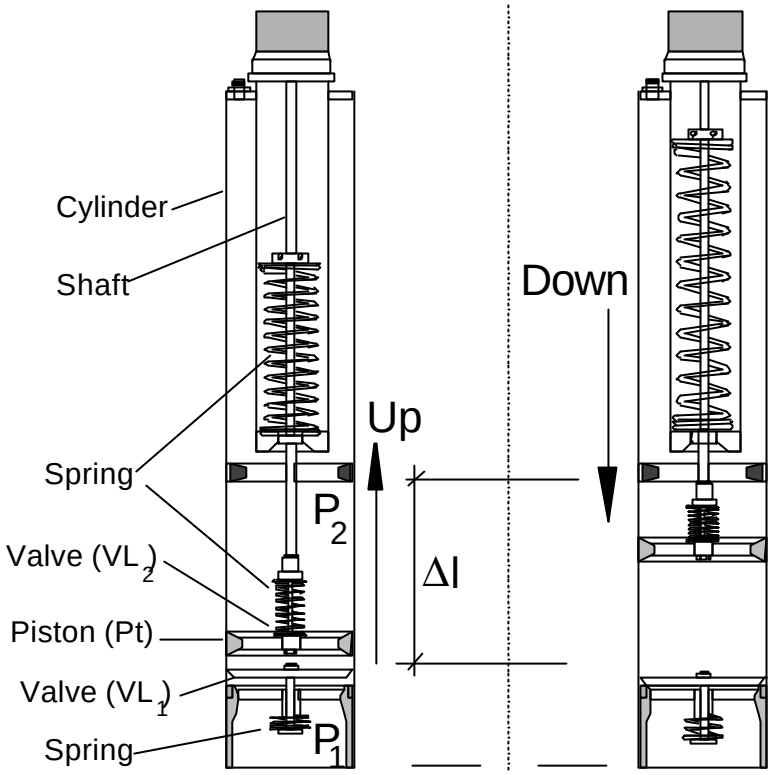

Figure 4.4: Schematic of the piston pump

The specification of the piston pump:

Type	:	piston/Bohner's pump
Piston diameter (on demand)	:	50 ~ 130 mm
Stroke (adjustable)	:	100 ~ 240 mm
Rotational speed	:	10 ~ 120 rpm
Water head (static)	:	15 ~ 100 m
Daily yield	:	25 ~ 170 m3 per day
Well diameter	:	6 inch

4.6 Measured Data

The data logger does the reading and recording of the measured data. The recording of the measured data is possible adjusted in minute and hour. To get the accuracy of the measured data, the recording is set in every minute. By a personal computer via the RS 232 port, the measured data is transferred in the hard disk.

The measured data :

- Irradiation W m^{-2}
- Voltage of the solar generator V
- Current of the solar generator A
- Temperature of the solar cell ^{o}C
- Ambient temperature ^{o}C
- Rotation of the motor rpm
- Pressure outlet pump bar
- Level of the water source bar
- Water flow l/sec.
- Temperature of the MPP tracker ^{o}C
- Temperature of the motor ^{o}C
- Efficiency of the solar generator %
- Efficiency subsystem %
- Efficiency system %
- Total head m
- Water total m^3
- Hydraulic output m^4
- Water flow rate per rotation

4.7 Evaluations and Analysis

The photovoltaic model with the parameters is known and the measured data of the photovoltaic system is obtained as mentioned in previous Chapters. In order to get the performance of the PV system, the evaluating and analyzing with the model and the measured data is presented. With the simulation program in the personal computer, the performance of the PV system (maximum power of the solar-generator, impedance load, efficiency subsystem and efficiency system) is simply known.

4.7.1 Maximum Power Solar-Generator

The purpose of the calculating of the maximum power is to know between the loading and the power of the solar-generator under the radiation. The maximum power output of the solar generator is expressed by the equation:

$$P_{SG-max} = V_{SG} \cdot I_{SG} \quad (4.15)$$

Substitution equation (3.10) and (4.15), the maximum power output of the solar generator:

$$P_{SG-max} = m_{cl}\, n_{cl}\, m_{md}\, n_{md} V_{cl} \cdot I_{cl} \quad (4.16)$$

where $P_{SG\text{-}max}$ is the maximum power output of the solar generator; V_{SG} the voltage output of the solar generator; I_{SG} the current output of the solar generator; m_{md} the number of the module in series; n_{md} the number of the module in parallel.

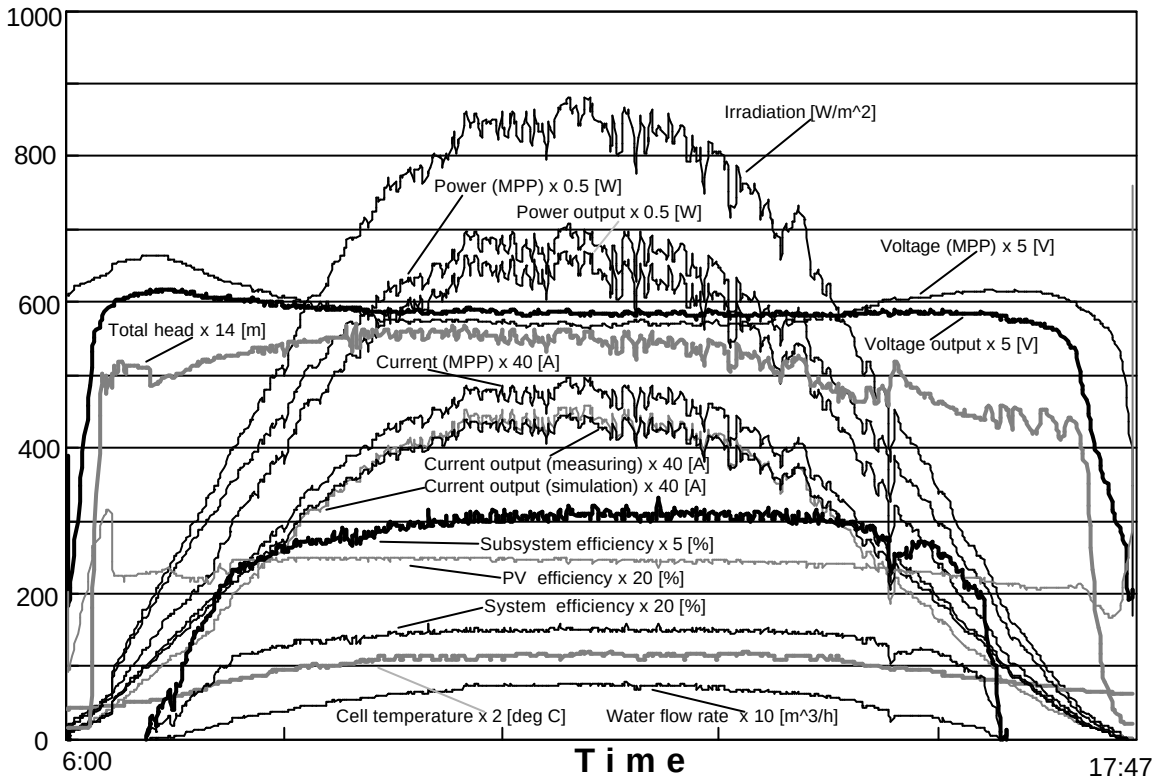

Figure 4.5: Performance of PVP System

With the simulation program of the solar-generator model and the measured data (radiation (G) and cell temperature (T)), the relationship between the current and voltage (I-V) output of the solar-generator is found. In order to get the maximum voltage $(V_{SG})_{max}$ of the solar-generator under the radiation (G) and temperature (T), the current solar-generator is set equal zero ($I_{SG} = 0$). To find the maximum power, the value of the maximum voltage is decreased little by little ($V_{SG}[n] = V_{SG\ Max} - n$

ΔV) and the current ($I_{SG}[n]$) is gotten. The power ($P_{SG}[n] = V_{SG}[n] \times I_{SG}[n]$) must be compared to the previous power ($P_{SG}[n-1]=V_{SG}[n-1] \times I_{SG}[n-1]$). With this method, the maximum power of the solar-generator under the radiation (G) and temperature (T) is obtained. The calculating of the maximum power of the solar-generator is repeated for the other measured data (G,T). The Figure 4.5 shows the correlation between: radiation (G), cell temperature (T), current ($I_{SG\ MPP}$), voltage ($V_{SG\ MPP}$) and maximum power ($P_{SG\ MPP}$) of the solar-generator.

The values of the maximum power ($P_{SG\ MPP}$) and the current ($I_{SG\ MPP}$) are little bigger than the power and current output of the solar-generator from the measured data. It means that the PVP system with the piston pump is near optimum.

4.7.2 Impedance Load [10]

To know the performance of the PV system, one of the methods calculates the impedance load (r_L). The impedance load is equivalent of the capacity of the load under radiation (G). To get the impedance load, the numerator of the last term of equation (3.1), V_C+jr_S, is replaced by V_C+jr_L. The model with the load can be written:

$$j = (C_0 + C_1 T)G - C_{01} T^3 \exp\left[-\frac{e_o U_{gap}}{k T}\right]\left[\exp\left(\frac{e_o (V_c + j r_s)}{\alpha\, kT}\right) - 1\right]$$

$$- C_{02}\, T^{5/2} \exp\left[-\frac{e_o U_{gap}}{2\, kT}\right]\left[\exp\left(\frac{e_o (V_c + j r_s)}{\beta\, kT}\right) - 1\right] - \frac{V_C + j(r_S + r_L)}{r_{sh}} \quad (4.17)$$

The $r_L >> r_S$, the equation becomes:

$$j = (C_0 + C_1 T)G - C_{01} T^3 \exp\left[-\frac{e_o U_{gap}}{k T}\right]\left[\exp\left(\frac{e_o (V_c + j r_s)}{\alpha\, kT}\right) - 1\right]$$

$$- C_{02}\, T^{5/2} \exp\left[-\frac{e_o U_{gap}}{2\, kT}\right]\left[\exp\left(\frac{e_o (V_c + j r_s)}{\beta\, kT}\right) - 1\right] - \frac{V_C + j\, r_L}{r_{sh}} \quad (4.18)$$

The r_L is the equivalent impedance load, which indicates the load capacity of the PVP system, and estimated from the experimental data of current output at large irradiation. With this constant parameter, r_L, the current output of the experimental data coincided well with the calculated values over a wide range of irradiation as shown in Figure 4.5. The calculated maximum power also overlaps with the measured data over a long range of time. The value of constant r_L is almost same for other experiments of same system and condition. With this model, the system could be well evaluated, and the MMP tracker is shown to work well, but the lifetime of the motor is relatively short. This might be due to the mismatch of the capacity of the motor and the solar generator, and the large and immediate fluctuation in the irradiation intensity. However, this still needs further investigation.

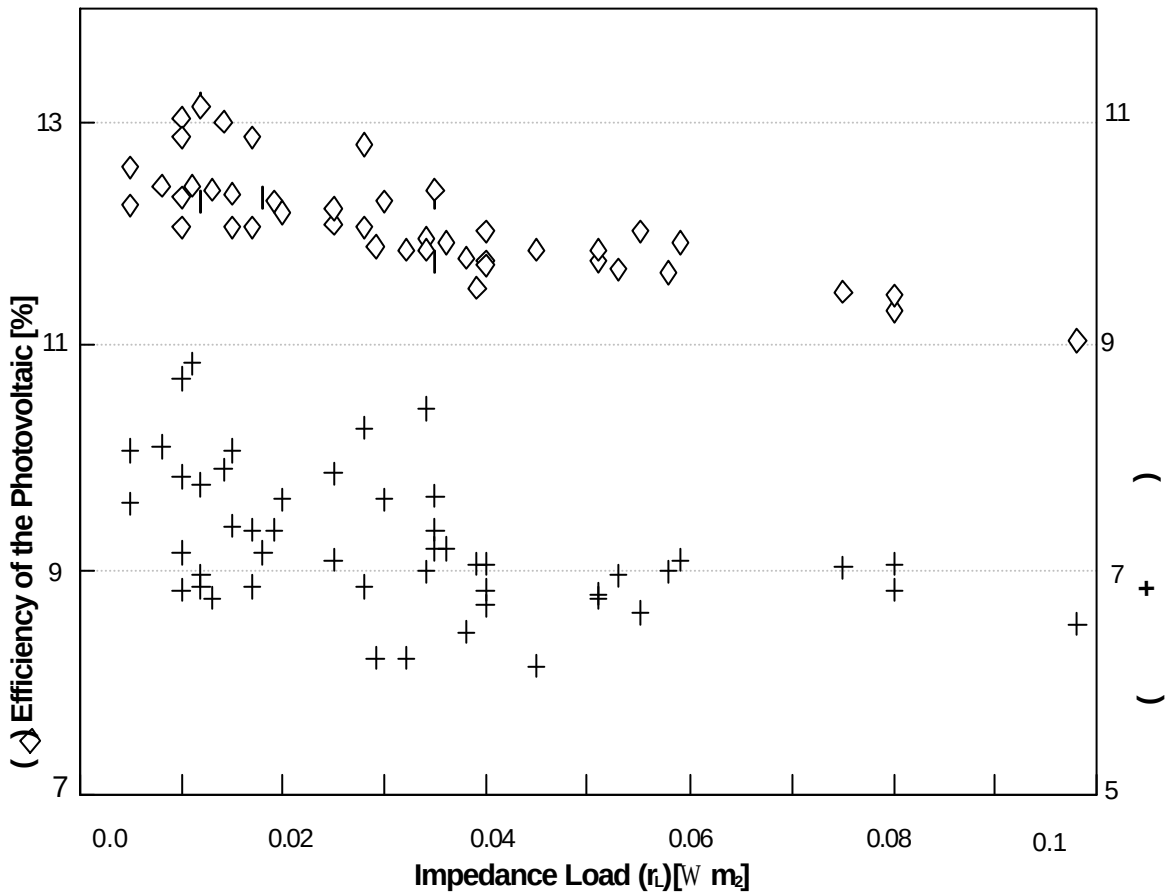

Figure 4.6: Correlation: impedance load (r_L) – efficiency (ξ)

4.7.3 Efficiency

The performances of the PVP system can be explained in term of its efficiency. Based on the measured data, the efficiency is categorized in this study into photovoltaic efficiency (ξ_{pv}), subsystem efficiency (ξ_{Sub}) and total efficiency or system efficiency (ξ_{sys}).

The photovoltaic efficiency (ξ_{pv}) is the comparison between energy output of the solar generator and irradiation. The pv efficiency depends on the quality and kind of the crystal. The mono-crystal had the efficiency higher than the poly-crystal. The

The PV efficiency is written by the following equation:

$$\xi_{PV} = \frac{V_{SG} \times I_{SG}}{G \times A_{PV}} 100\% \qquad (4.19)$$

where A_{pv} is total area of the solar generator [m^2]; V_{SG} voltage output [V] and I_{SG} current output [A] of the solar generator. From the measured data, the average of the PV efficiency is 12.5 %, and the PV efficiency is also dependent on the impedance load (r_L) as shown in Figure 4.6.

The subsystem efficiency (ξ_{Sub}) is the ratio between the hydraulic power and the power of the solar generator. The value of ξ_{Sub} reflects the efficiencies: dc-dc converter, motor and pump. The subsystem efficiency is:

$$\xi_{Sub} = \frac{Q \times H}{0.367 \times V_{SG} \times I_{SG}} 100\% \qquad (4.20)$$

The value of ξ_{Sub} can be calculated from the measured data shown in Figure 4.9. The mean subsystem efficiency is 60%. This value is higher than that of the PVP system with the centrifugal pump.

The total efficiency (ξ_{sys}) is the comparison between the energy output and the energy input to the system. The total efficiency is an integration of several efficiencies: PV efficiency and subsystem efficiency, and can be written as:

$$\xi_{sys} = \xi_{PV} \text{ x } \xi_{Sub} = \frac{Q \text{ x } H}{0.367 \text{ x } G \text{ x } A_{PV}} 100\% \qquad (4.21)$$

The total efficiency (ξ_{sys}) of this system is approximately 8% as shown in Figure 4.6

The correlation between the motor temperature (T_m) and the impedance load (r_L) is shown as Figure 4.7. The motor used in the PVP system is the dc motor 510 watt. Because the motor capacity is too small than the pump, the motor temperature is average 50 ^oC degree. The impedance load follows the increasing of the motor temperature.

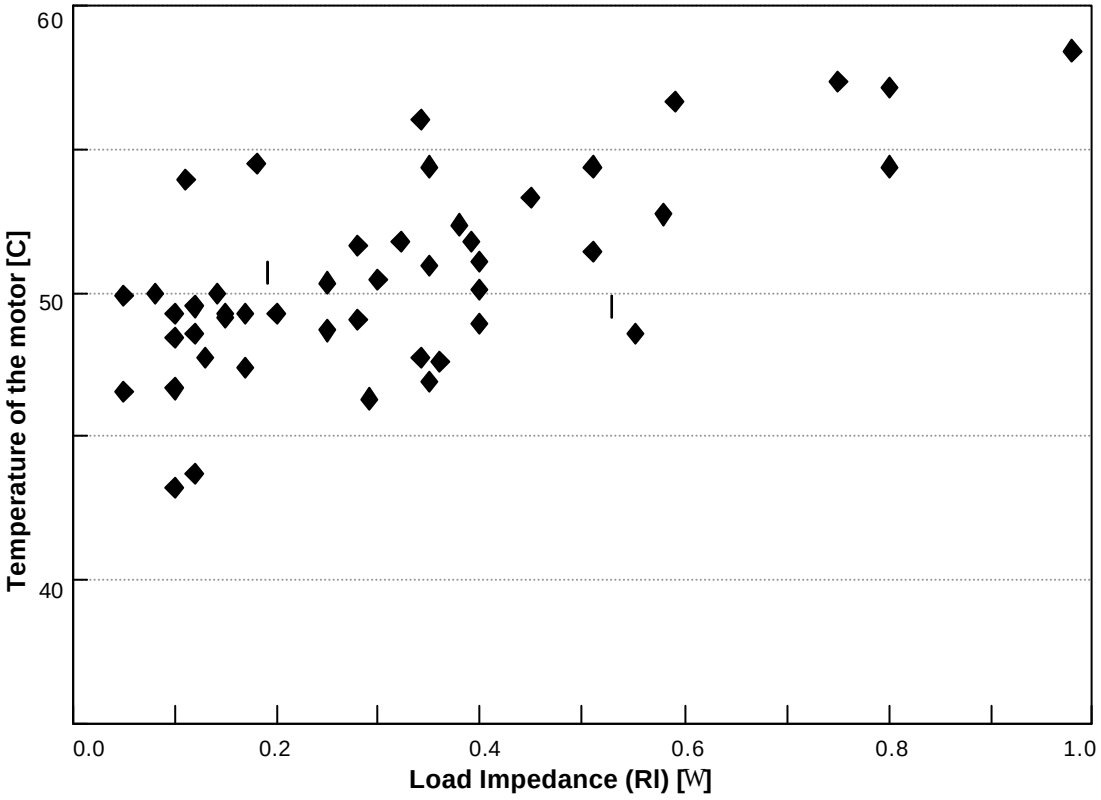

Figure 4.7: Correlation: impedance load (r_L) – motor temperature (T_m)

Figure 4.8 and 4.9 are the relationship between the irradiation and the efficiency of the piston pump and the centrifugal pump. The efficiency of the centrifugal pump (including the inverter) is approximately 37% at the irradiation around 600-1000 W m^{-2}. The performance of the centrifugal pump is well only at the high irradiation (>600 Wm^{-2}), but at the low irradiation, it is relative bad or not running.

The efficiency of the piston pump (including dc-dc converter) is near 64% at the irradiation around 400~1000 Wm^{-2}. Although the irradiation is relative low (150< irradiation <400 Wm^{-2}), the piston pump can be operating. Base on this result, the performance of the piston pump is better than the centrifugal-pump and its efficiency is also higher.

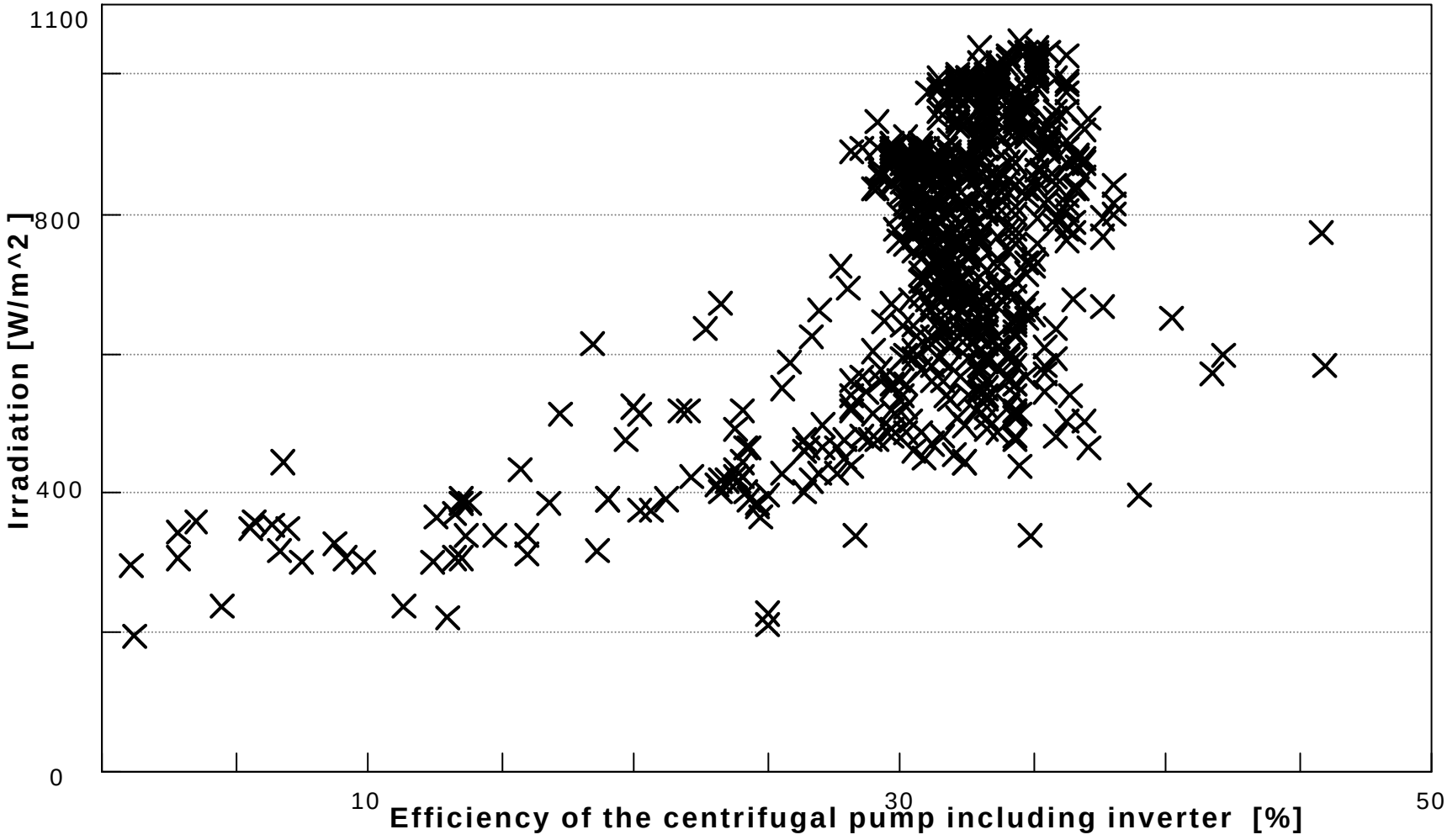

Figure 4.8: Performance of the centrifugal pump

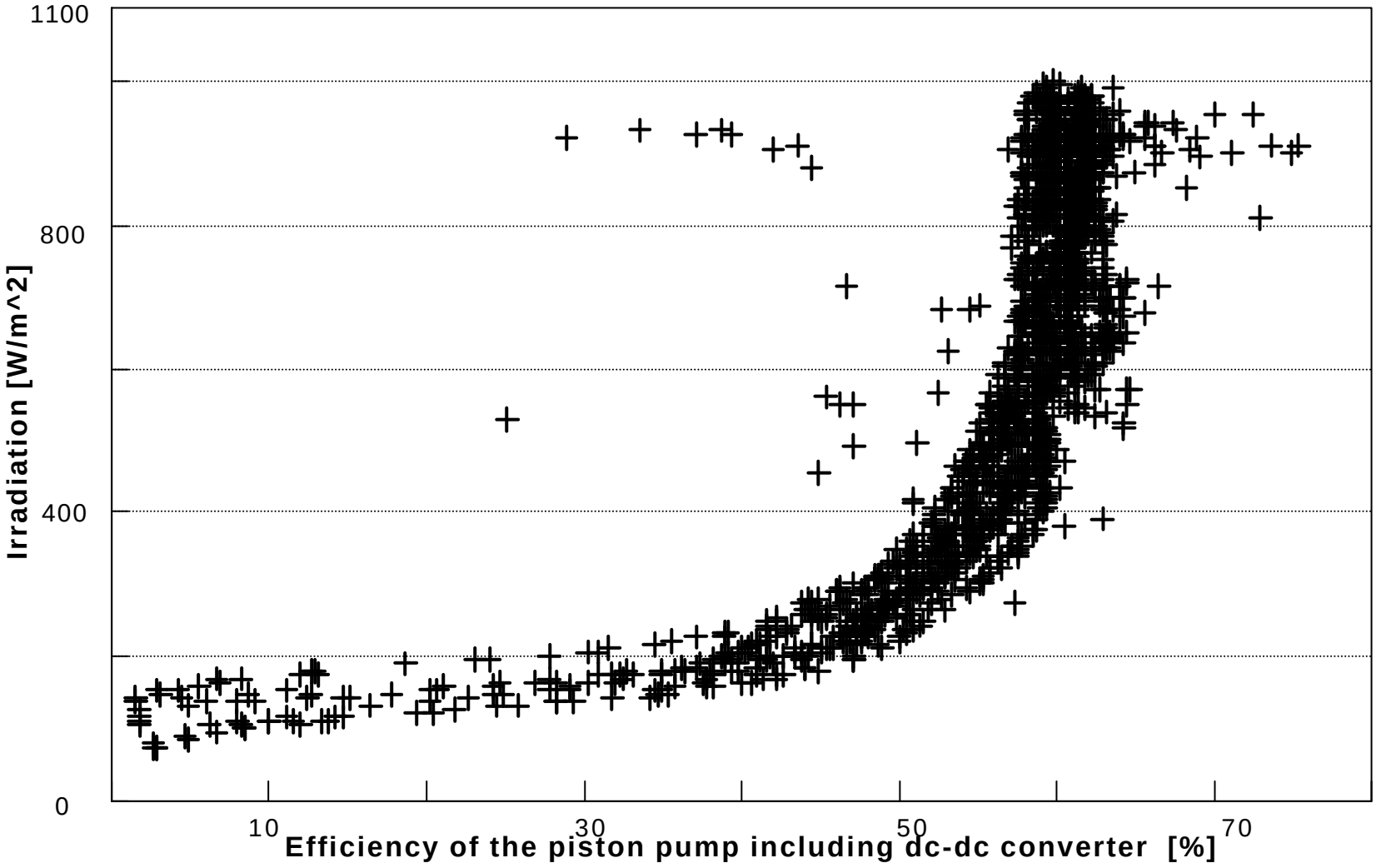

Figure 4.9: Performance of the piston pump

Chapter 5

Single Pump with Battery

5.1 Background

The average efficiency of the photovoltaic pump system is still low. To increase the efficiency, and reducing the motor temperature, the battery will be installed in the photovoltaic piston pump (PVPP) system. The battery is necessary to store the surplus energy, when the power output of the solar generator is greater than the load. As the backup, when the power output of the solar generator is smaller than the load, the some energy is taken from the battery. The other effect, the voltage system and the speed of the motor become relative constant. Using the ac motor, which is without the brush, is low for the maintenance and easy to find the spare part. The current output of the solar-generator is the dc current, but the load is the ac motor. To solve this problem, the inverter is used, which changes the dc current to the ac current. The capacity of the solar-generator is 2040-Watt peak with 24 photovoltaic modules. The valve simulated the head simulator of the pressure pump outlet, which can be adjusted to 20 - 60 meters. According to the head of the pump specification is 40 meters, in the current experiment the head simulator will be set to 40 meters. By the constant head, the measured data of the performance will be evaluated and analyzed easier.

As the controller and data logger, the personal computer will be used that is completed with the interface-card (PCI-9118HG), sensor, transducer, software and etc. The interface has 2 channels digital-analog output, 4 channels digital-digital output-

input and 16 channels (single ended) analog-digital converter. The visual C++ windows 98 will be used to build the software that functions to: synchronizing between computer-interface, reading the signal input of the interface and saving for the measured data in the hard disk. Schematically, the PVPP system with the battery is illustrated in Figure 5.1. In the current experiment, the system will be installed in location: UPT-LSDE, Puspiptek-Serpong, Tangerang.

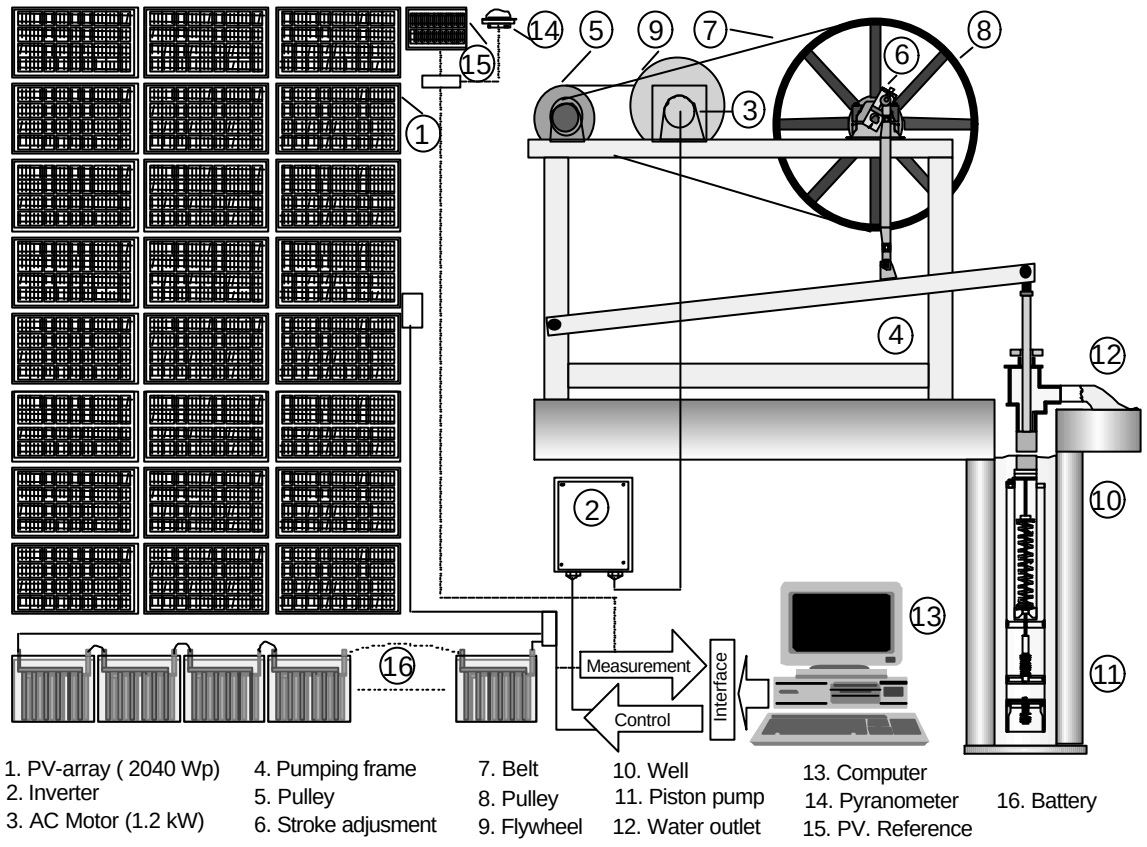

Figure 5.1: Schematic of the piston pump with the battery and measuring system.

5.2 Load-Battery Capacity

In order to get the optimum of the PVPP system, the balancing among the solar generator output, the load capacity and the sizing of the battery must be found. The power output of the solar-generator is influenced by the irradiance intensity. Therefore, fixing of the load capacity and the battery references to the radiation and the temperature data from the location where the system will be installed.

The maximum power output of the solar-generator is calculated with the program simulation, which consists of the photovoltaic model with the equation (3.1) and

(4.16). The radiation and temperature from the measured data are the input data by the simulation program. Because the relationship between the current (I) and the voltage (V) in the photovoltaic model is the exponential equation, the solution can be obtained only possible with the iteration.

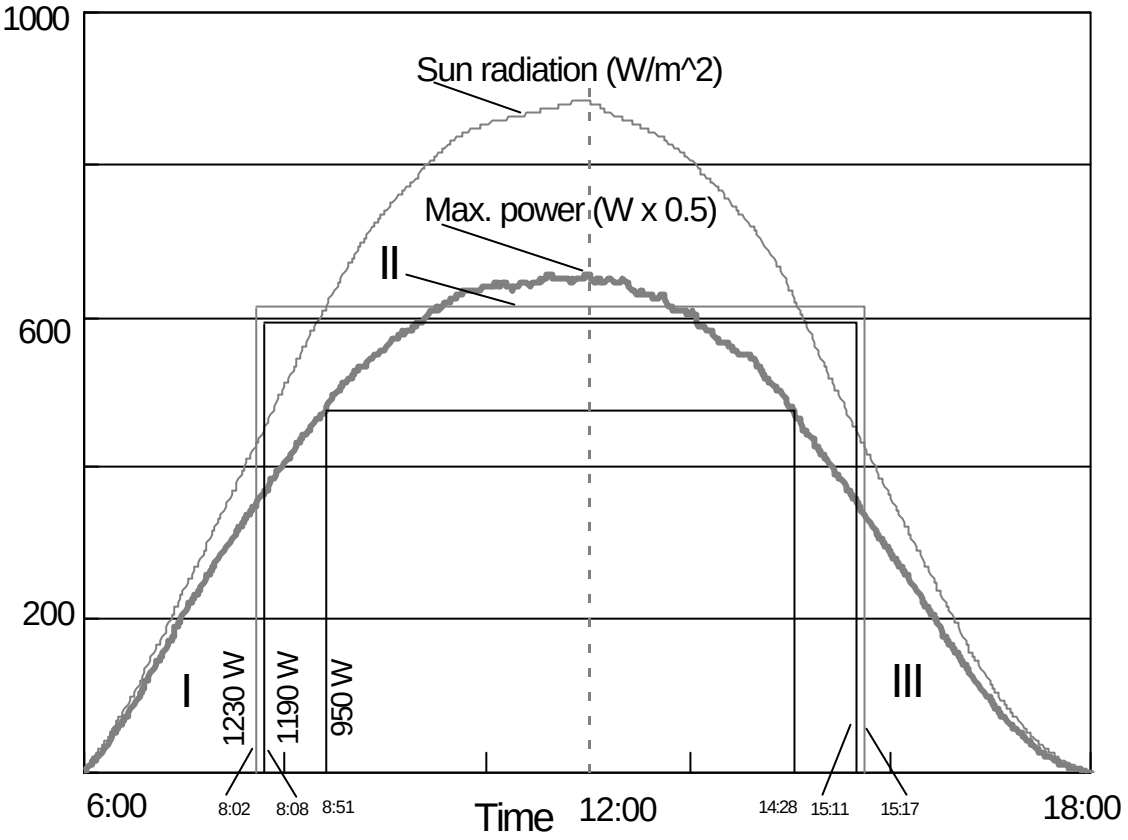

Figure 5.2: Optimizing the load and the maximum power of the solar generator.

5.2.1 Load Capacity

The load and battery capacities depend on the capacity of the solar generator and the weather particularly irradiance intensity. By the model and its parameters with the simulation program, the power output of the solar generator can be calculated. As input datum (irradiance intensity and temperature) for the simulation program the real datum are used, which are taken from the measured data of every minute period. With this period and real data, the output of the simulation is hoped with the high accuracy result. To find the load capacity, the load is put from 500 watt ~ 1300 watt. The principle of the calculation of the optimum basic load for every datum input (radiation and temperature) that the basic load must be smaller than the power output of the solar

generator, as shown in the Figure 5.2. The basic load is set smaller than the power output of the solar generator, in order to avoid the unbalance energy or the deficient energy. By this method, the using energy for the load, the waste energy and starting-stopping time can be calculated. The result of the calculation is shown in the Figure 5.3. The relationship among the load capacity, the waste energy and the basic load is shown in Figure 5.3. The optimum basic load is around 950 watt. It is also has the widest area.

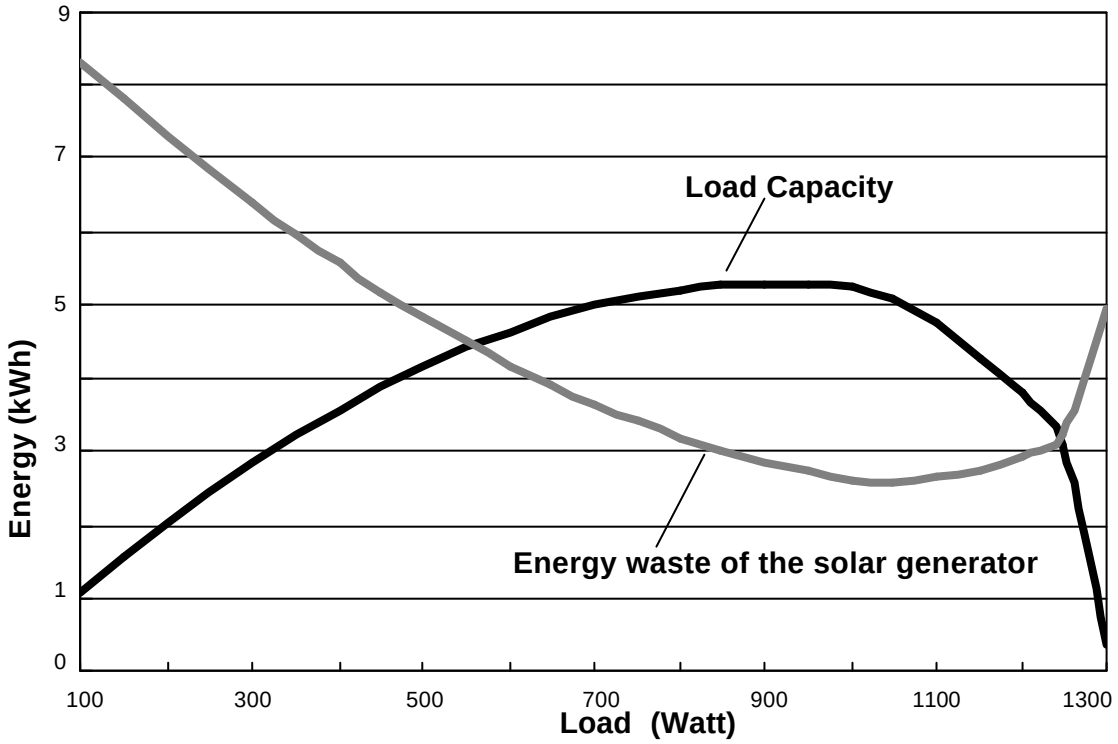

Figure 5.3: Correlation of the load capacity, the waste energy and the basic load

5.2.2 Battery Capacity

The battery capacity in the photovoltaic system is determined from the charge-discharge energy and the factor value of the deep of discharge (DOD). The battery functions to save the energy, when the energy is surplus and as the backup, when the power is deficient or the power output of the solar generator is lower than the load. The battery in the ideal condition is always full charge (100% energy capacity), but it is impossible, because charging-discharging the energy into or from the battery happens always. To maintain the lifetime of the battery and the energy condition in the battery, the charge-discharge must be limited. The limiting of the energy

discharging is called deep of discharge (DOD), which is declared with percent (%) from the full capacity. The DOD value is depends on the quality and kind of the battery. For example, the DOD of the block's battery is higher than the car battery.

In the photovoltaic pump system, the battery has functions:

- Storage energy:

  When the power output of the solar generator is greater than the load, the surplus energy is saved into the battery. This situation happens, while the irradiance intensity is high or the pump is not running.

- Energy Back-up

  The power output of the solar generator is influenced by the weather especially the sun radiation. When the weather is a little cloudy, the energy is deficient and the energy is taken from the battery.

- Constant Voltage

  The characteristic motion of the piston pump is: slow, smooth and continuous. Therefore, the rpm of the motor must be as possible adjusted constant. With the battery, the voltage input of the motor is not fluctuation and the rpm of the motor is relative stable.

The optimum basic load is known L = 950 Watt as presented above. In this case, by use of battery the starting point t will change. At the optimum, (L_0, t_0) would not change with the small change of the battery capacity. Then from the Figure 5.4, the equation (5.1) yields:

$$\frac{\Delta y}{\Delta t} = \frac{L_0}{t_0 / 2}$$

$$\Delta t = \frac{\Delta y \times t_0}{2 \times L_0} \qquad (5.1)$$

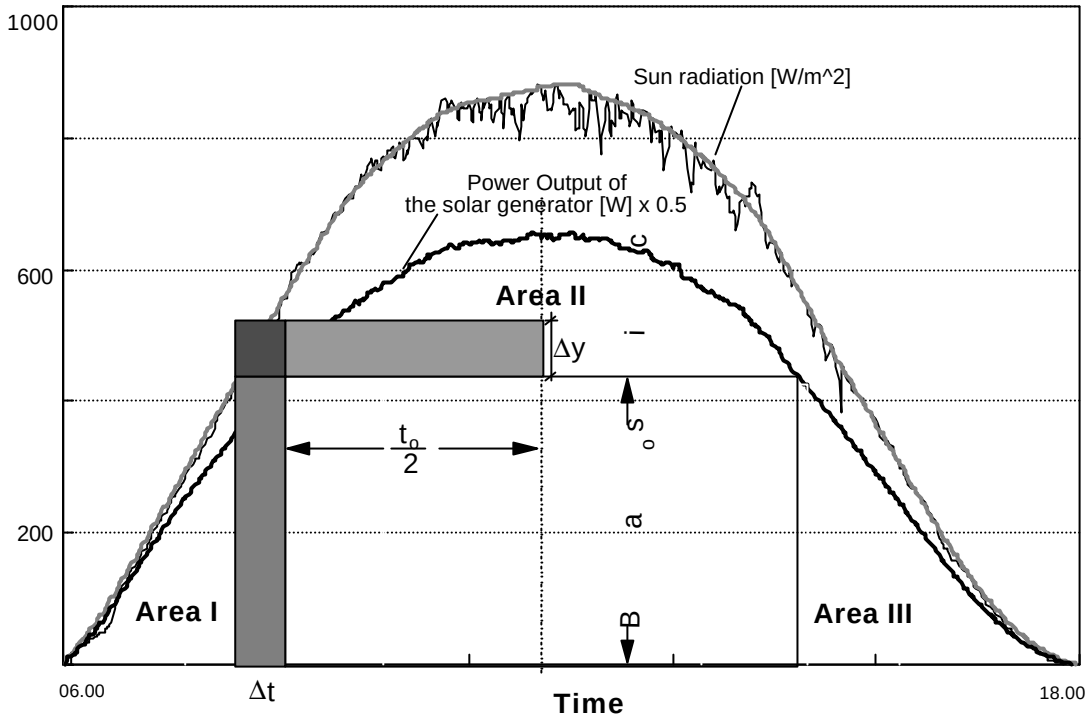

Figure 5.4: Calculating the total load.

where Δt is the change of starting time of the total load; L_0 basic Load; Δy increasing load (50, 100, 150, 200,…etc.); t_0 operation time of the basic load.

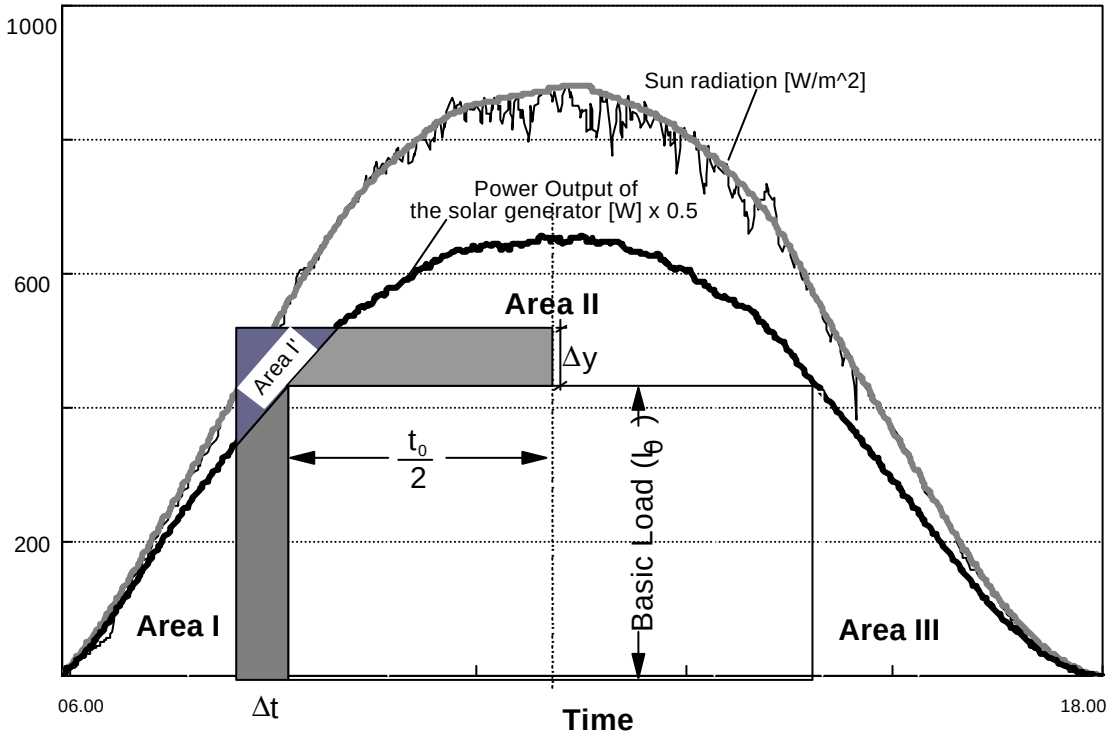

Figure 5.5: Basic calculation of the battery and the total load capacities

To find the total load, which is suitable, the Δy is increased with 50, 100, 150, 200 watt. The area I (surplus energy) and the area I' (deficient energy) must be equal illustrated in the Figure 5.5, because the surplus energy at the area I is saved in the battery. Considering the efficiency of the battery, Δy, varies with the battery efficiency. The saved energy in the battery and Δy at the basic load 950 watt is presented in the Figure 5.6.

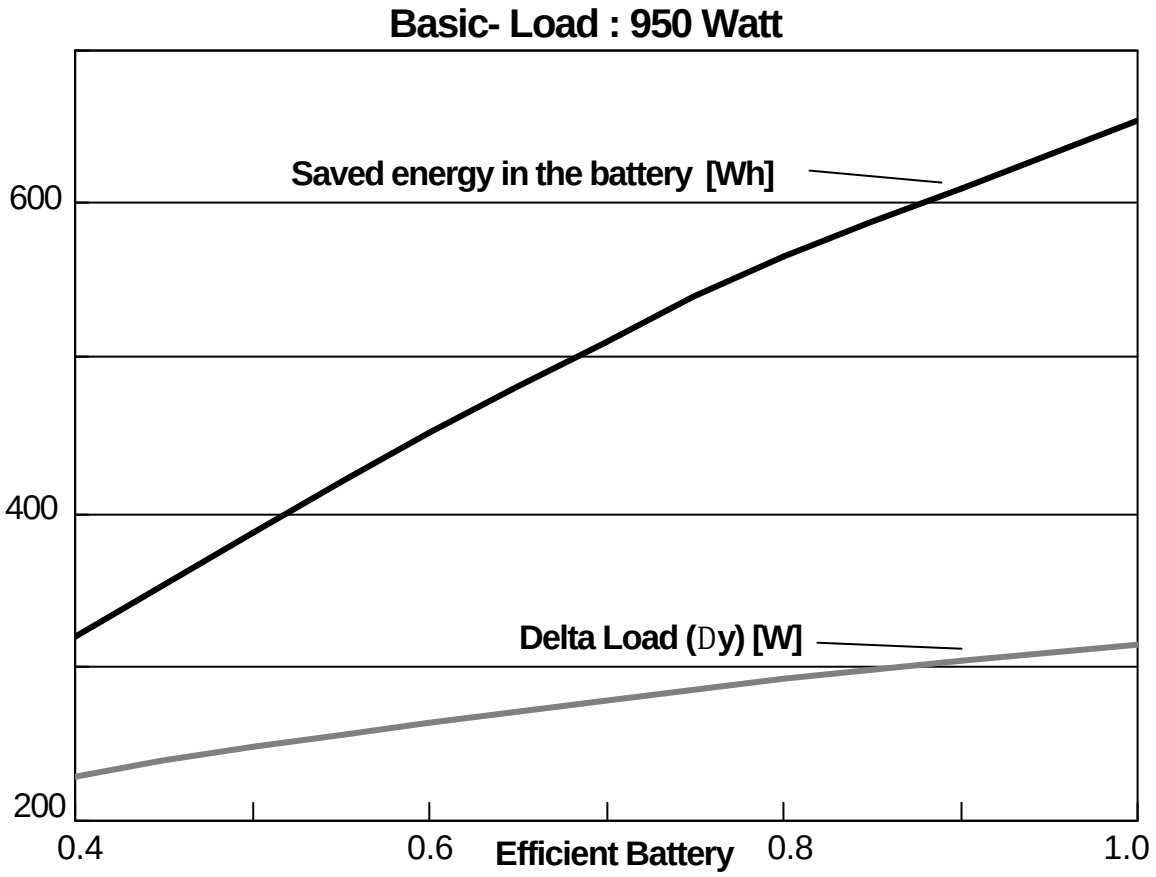

Figure 5.6: The waste energy at the basic load 950 watt.

The battery capacity can be found,

$$BC = \frac{\text{Area I'}}{\text{DOD}} \tag{5.2}$$

where BC is the battery capacity in ampere hour (Ah); DOD deep of discharge (%); area I' the deficient energy.

Area I' << area I, the battery capacity can be written,

$$BC = \frac{\text{Area I}}{\text{DOD}} \qquad (5.3)$$

For the other optimum basic load L_0 of other sun models, the total load is shown in the Figure 5.7. From this figure and at the DOD, the battery capacity can be decided .To reduce the cost, the car battery would be used with DOD 15%-20%.

In the followings, some devices necessary for the planning future experiments will be noted.

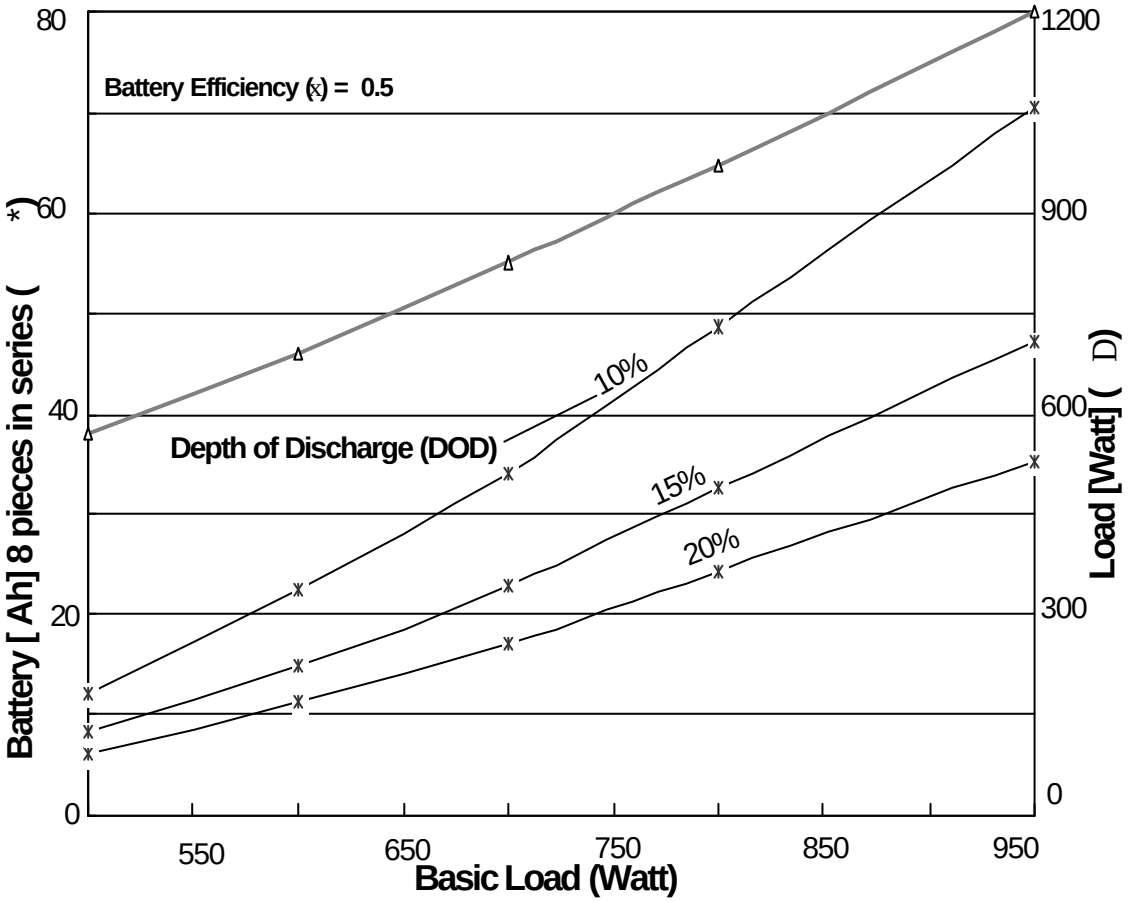

Figure 5.7: The battery capacity for DOD 10%-20%

5.3 Battery Charge Regulator

The photovoltaic system with the battery must be equipped with the battery charge regulator (BCR). The BCR protects the battery condition from over charging and over discharging. At this photovoltaic system, the function of the BCR will be replaced by

a personal computer, which will be equipped with the interface, sensor and transducer, as shown Figure 5.8.

In the clear weather, the current output of the solar-generator flows to the load and battery, because the current output of the solar-generator (I_{SG}) is bigger than the load (I_L). According to Kirchoff's current law, the current output of the solar generator is,

$$I_{SG} = I_B + I_L \tag{5.4}$$

where I_{SG} is the current output of the solar generator; I_B the battery current and I_L the load current.

The energy is surplus and the current battery (I_B) is positive. It is named the battery charging. In this condition, the energy stored in the battery is raising that makes swell the battery voltage. The maximum voltage battery (V_B) is 2.34 volt per cell. At this voltage, the lead acid in the battery starts to gassing or over charging. To protect the over charging, the power supply from the solar-generator must be disconnected.

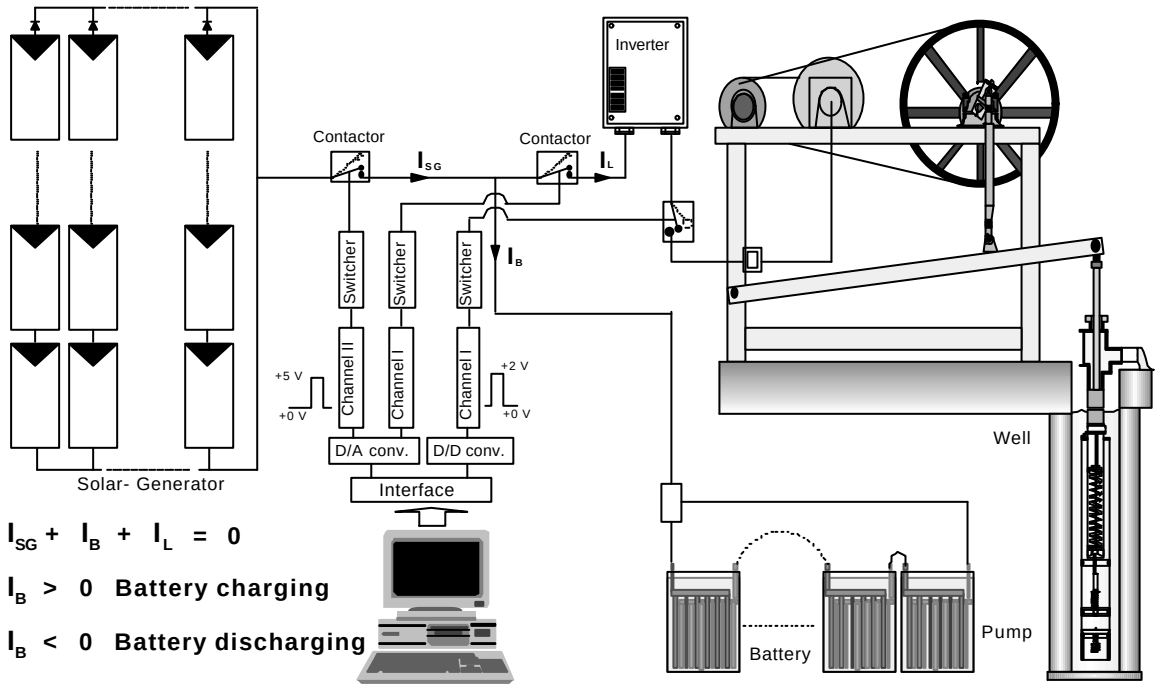

Figure 5.8: Basic of the battery charge regulator (BCR).

With the interface-card, the signal of the channel II D/A is set +5 volt. The signal is connected to the switcher, which is a connector between the solar-generator and the battery. Because the signal +5 volt drives the switcher, the switcher is off. It causes disconnecting the solar generator-the battery and the over charging can be voided.

When the system is operating in the cloud weather or low radiation and the power output of the solar-generator is smaller than the load, some energy is taken from the battery. When the minus energy occurs, the some energy is taken from the battery as the backup energy. The current battery (I_B) is negative that is defined the battery discharging.

$$I_L = I_B + I_{SG} \tag{5.5}$$

The some energy is taken from the battery and the current battery is negative. The deficient energy decreases the energy in the battery and the voltage battery. The battery discharging must be limited until the minimum voltage, which is 1.9 volt per cell. The border of the battery discharge is defined the depth of discharging (DOD) which is sized with percent unit (%). When the voltage battery is 1.9 volt (DOD around 20%), the connection between the battery and the load must be disconnected. In this situation, the signal of the channel I D/D converter is set +2 volt. This signal is continued to the switcher, which is a connector between the battery and the load. With the signal +2 causes the switcher off and disconnecting between the battery and the load and the over discharging can be stopped. The time operation is set in the program. When the time operation starts, the signal output of the channel I A/D converter is set +5 volt. The signal is continued to the switcher that the battery and the inverter are contact and the pump is running. When the time operation is over, the signal of the channel I A/D converter is +0 volt and the pump is stopping.

The program in the computer regulates the operating of the system automatically. The basic of the regulation is the condition of the weather (radiation), the energy in the battery, the water source and the time operation, as shown in Figure 5.10 (flowchart).

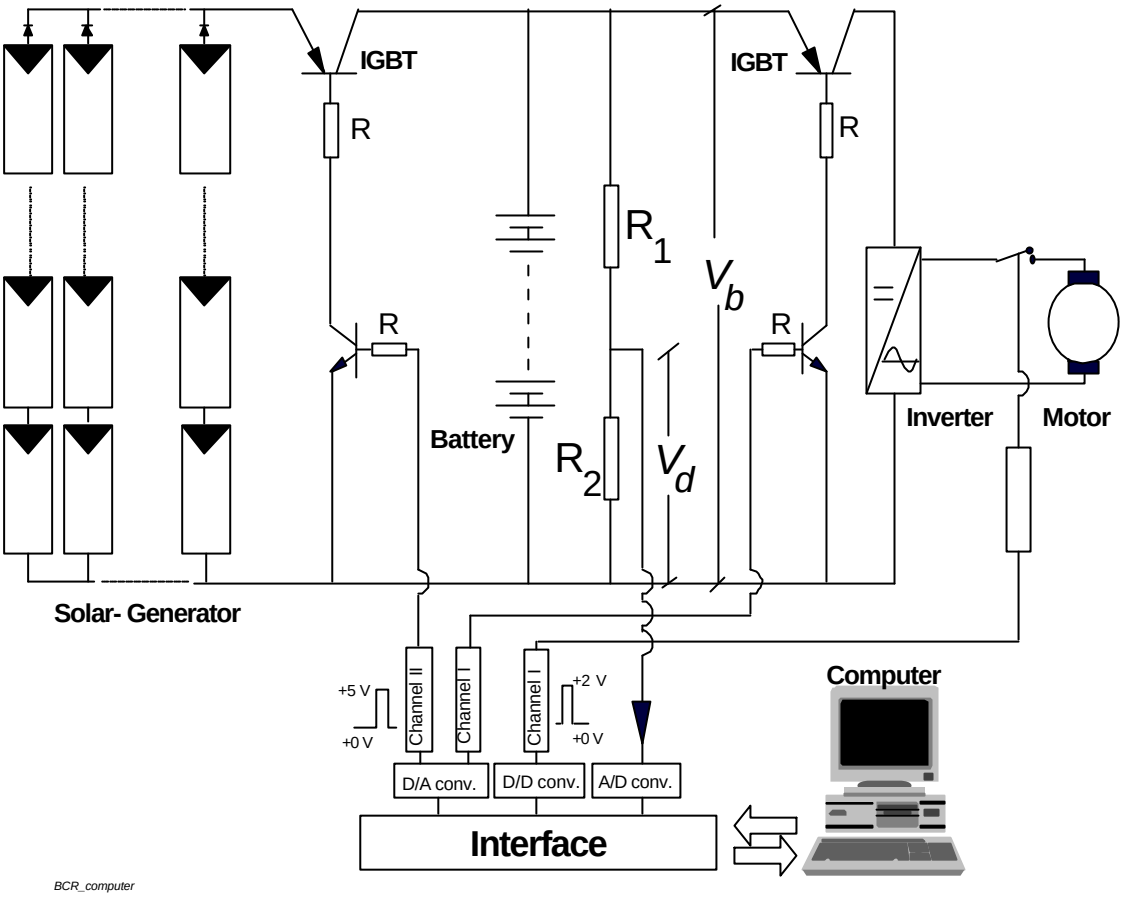

Figure 5.9: Personal computer functions as the battery charge regulator.

5.4 Data in the Next Research

In addition to regulating charge-discharge energy for the battery with one of the above-mentioned regulators, the personal computer with the PCI-9118HG interface can be used as the data logger. The channel is exploited: 16 channels Analog-Digital (A/D) input and 4 channels Digital-Digital (D/D) input. In order to getting the parameters of the photovoltaic system, some sensor and transducer will be required. Interrupt handler system is exploited to read the signal input from the interface. The measured data is averaged in the time period and saved in the hard disk. The time period is possible adjusted in every second, minute and hour. For the accuracy and effective, the time period is set every 1 (one) minute. The datum will be measured: sun irradiation, voltage of the solar-generator, current of the solar-generator, voltage of the battery, current of the battery, cell temperature, ambient temperature, pressure of the pump, water flow rate and rpm of the motor

To know the performance of the photovoltaic system, the evaluating and analyzing will reference to the measured data. The performance of the system is planning to display in the graphics and table.

The regulation of the single pump with the battery

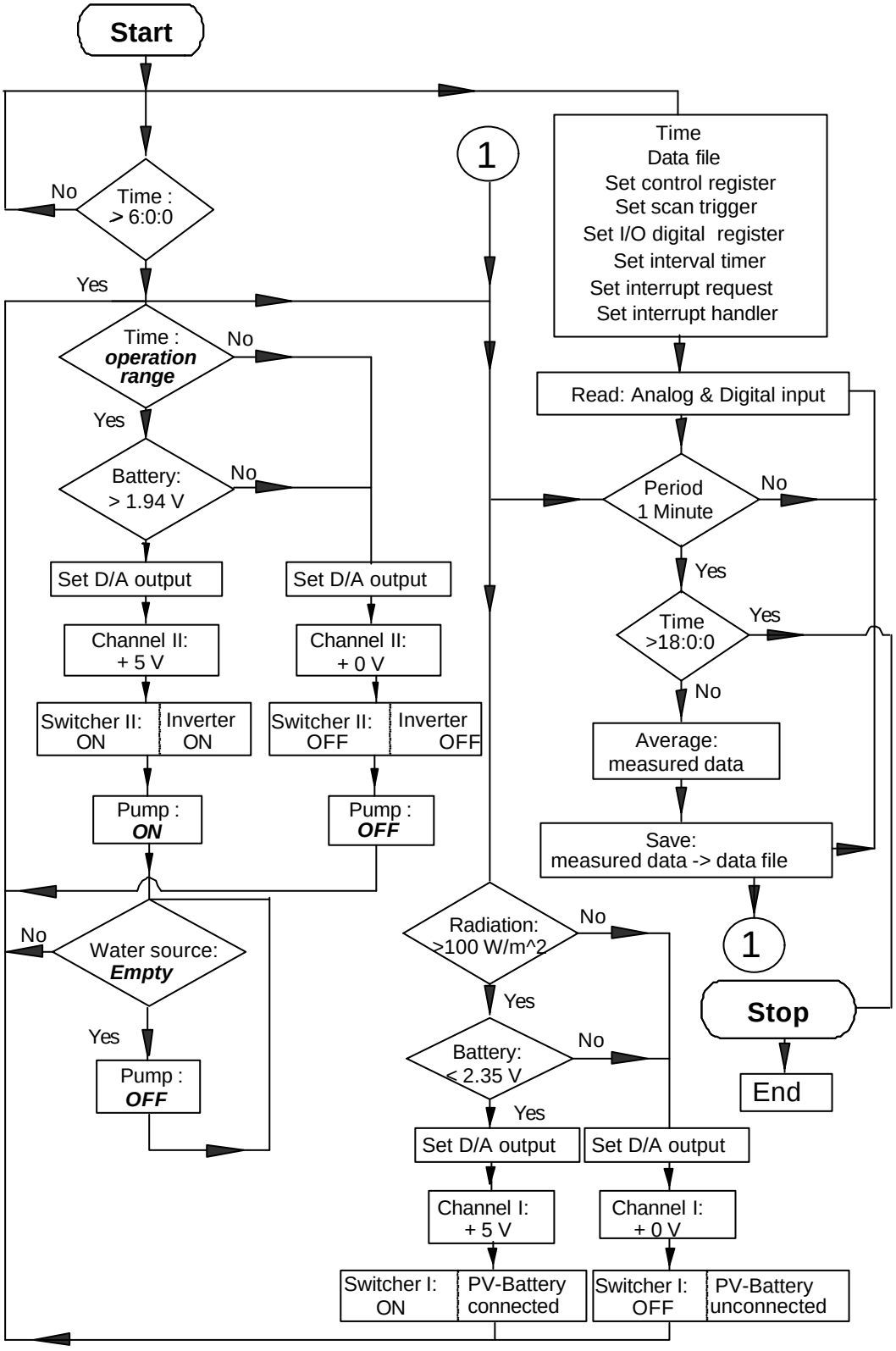

Figure 5.10: Basic program of the regulation and measurement

Conclusion

1. The PVP system with double pumps is suitable for the large irradiation and big capacity of the solar generator. The small pump is set to run in the morning and afternoon or at the low irradiation. At the high irradiation or around noon, the small pump is stopped and the big pump is operated. The location of the low insolation isn't suitable for double pumps system, because the probability of the big pump running is small. Therefore, the PVP system loaded with the single pump is more effective.

2. The efficiency of piston pump (including dc-dc converter) (64%) is better than the efficiency of centrifugal pump (including inverter) (37%). The photovoltaic pump system loaded with the piston pump always runs well, whereas the photovoltaic pump system with the centrifugal pump has good performance only at the high irradiation.

3. The output current of the solar generator is found well estimated using a exponential equation mathematical model.
   The simulation program using the model is applied also to evaluate performance of the PVP system. From the comparison between the maximum power of the model and the power output of the measured data, performance of the PVP system is found optimum.

4. The photovoltaic efficiency and the efficiency of the total system are well correlated by the impedance load, which has a relationship to the motor temperature.

5. To reduce the overheating of the motor temperature and increase the efficiency, the battery should be installed as the storage of the surplus energy and backup energy. Even the small capacity battery is found very effective for the PV water pumping system.

Problems

1. The efficiency of photovoltaic system is still relative low or under 10 percent. To increase the efficiency, the new components are replaced with higher efficiency. For the example: usually the PVP system uses the centrifugal pump, but in the current experiment, the piston pump is used. Because the size of the piston pump is bigger than the centrifugal pump, the PVP system with the piston pump needs more the construction for the supporting.

2. When the weather is clear and the irradiance intensity is high, the power output of the solar generator is greater than the load ($I_{SG} >> I_L$). The waste energy causes the damages to the system

3. The price of the photovoltaic module is relative expensive. The photovoltaic system can't be competitive with the other system. Therefore, the photovoltaic system is used in the rural area as the alternative power supply. In order to get the competitive photovoltaic system, the accuracy design and high performance is necessary.

4. The lifetime of the photovoltaic module is estimated 15 years. However, the result of the experiment finds that some module installed less than 15 years occurred at the solar cell: color ring, power degradation and cracking.

Appendix A

A simple basic design of a small photovoltaic pumping-up power system is shown here as an example obtained by this thesis.

Usually this power generator system is large plant. The pump and turbine of the system is the same device called as the pump-turbine of centrifugal type. But as shown in Chapter 4 the efficiency of the small centrifugal pump is not good. So in this thesis the pump and mill are not the same one but selected separately. The capacity of the power generator is set to be W=500W as presented in Chapter 4. The schematic diagram of the system is shown as Figure A1. The size of the photovoltaic module system is about 7 x 4m. A piston pump of 500W at the water source can pump up the water with $7m^3\,h^{-1}$ for 7 hours a clear day. Then a water tank of 4x4x3m is installed at H=30m above the water source of river or well. The pump is connected to the water tank with d=10cm dia. pipe. For the generation of the electric power, the efficiency of small turbine is low and about η_t =0.7. The efficiency of the generator and the transducer is η_g =0.7. Then from the equation

$$W = \eta_t \eta_g H Q \qquad \text{(a.1)}$$

The flow rate can be obtained as Q=3.3l/s. The head loss h_l of the pipe l=100m long with friction loss λ =0.03 is

$$h_l = \frac{\lambda l}{2 d w^2 g} \qquad \text{(a.2)}$$

and is small as 1m.

The revolution speed of turbine is set n=3000 rpm. Then the specific speed of the turbine n_s is

$$n_S = \frac{n\,Q^{0.5}}{H^{0.75}} \qquad \text{(a.3)}$$

n_s =13 . Then Pelton or cross flow mill should be chosen in this system.

Appendix B

The rice field of 1000 m^2 produces about rice 480 kg for 6 months.

Effective insolation time for one day is assumed 3 hours (including cloudy days).

As 1 kg (rice) = 5000 k calorie.

Total energy (TE) = 480 x 5000 k calorie

= 10080000 k W sec.

6 months ≈ 6 x 30 x 3 x 3600 = 1944000 seconds

Total energy per day: $\frac{TE}{time} = \frac{10080000}{1944000}\,kW = 5.18518\,kW$ for area 1000 m^2.

= 5.18518 Wm^{-2}.

Maximum irradiation is about 1 kWm^{-2}, then the storage efficiency of rice can be roughly estimated:

$$\eta_S = \frac{5.18518}{1000} \approx 0.5 \quad .$$

Appendix C

C.1 Inverter [18]

Inverter converts power from direct current (dc) source to alternating current (ac) power at a specified output voltage and frequency. Based on the phase, the inverter has two kinds: single phase and three phases, but in this topic the three-phases inverters are only discussed.

Three-phase inverters are normally used for high-power applications. The three-phase inverter should be selected considering with the power output and the load. Three single phase half (or full)-bridge inverter can be connected in parallel as shown in Figure c.1.(a) to form the configuration of a three-phase inverter.

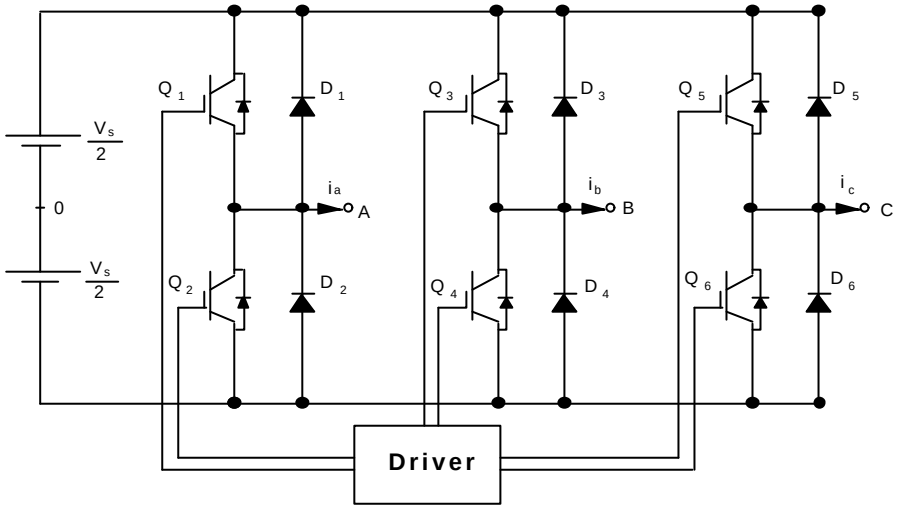

(a) Circuit of the three-phase inverter

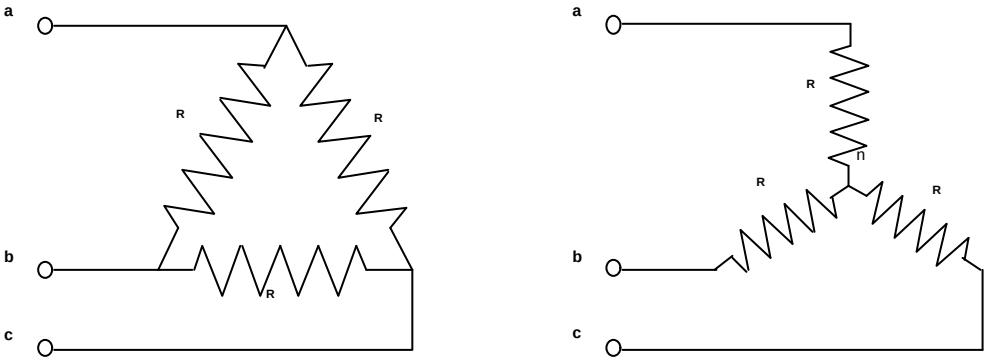

(b) Delta connection (c) Wye connection

Figure c.1: Three-phase circuit and connection of the inverter.

The gating signals of single-phase inverters should be advanced or delayed by 120^o with respect to each other in order to obtain three-phase balanced (fundamental) voltages. The transformer primary windings must be isolated from each other, while the secondary windings may be connected in wye or delta. The transformer secondary is normally connected in wye to eliminate triple n harmonics (n = 3, 6, 9, ……) appearing on the output voltages and the circuit arrangement. This arrangement requires three single-phase transformers, 12 transistors (or thyristors) and 12 diodes. If the output voltages of single-phase inverters are not perfectly balanced in magnitudes and phases, the three-phase output voltages will be unbalanced. A three-phase output can be obtained from a configuration of six transistors and six diodes as shown in Figure c.1.(a). When transistor Q_1 is switched on, terminal a is connected to the positive terminal of the dc input voltage. When transistor Q_4 is switched on, terminal a is brought to the negative terminal of the dc source. There are six modes of operation in a cycle and the duration of each mode is 60^o. The transistors are numbered in the sequence of gating of the transistors (e.g. 123, 234, 345, 456, 561, 612) and each transistor conducts for 180^o. The gating signals are shifted from each other by 60^o to obtain three-phase balanced (fundamental) voltages.

The load may be connected in wye or delta as shown in Figure c.1.(b) & (c). For delta-connected load, the phase currents can be obtained directly from the line-to-line voltages. Once the phase currents are known, the line currents can be determined. For a wye-connected load, the line-to-neutral voltages must be determined to find the line (or phase) currents. There are three modes of operation in a half-cycle and the equivalent circuits are shown in Figure c.2 (a).

During mode 1 interval $0 \le \omega t \le \frac{\pi}{3}$,

$$R_{eq} = R + \frac{R}{2} = \frac{3R}{2}$$

$$i_1 = \frac{V_S}{R_{eq}} = \frac{2V_S}{3R}$$

$$\upsilon_{an} = \upsilon_{cn} = \frac{i_1 R}{2} = \frac{V_S}{3}$$

$$\upsilon_{bn} = - i_1 R = -\frac{2 V_S}{3}$$

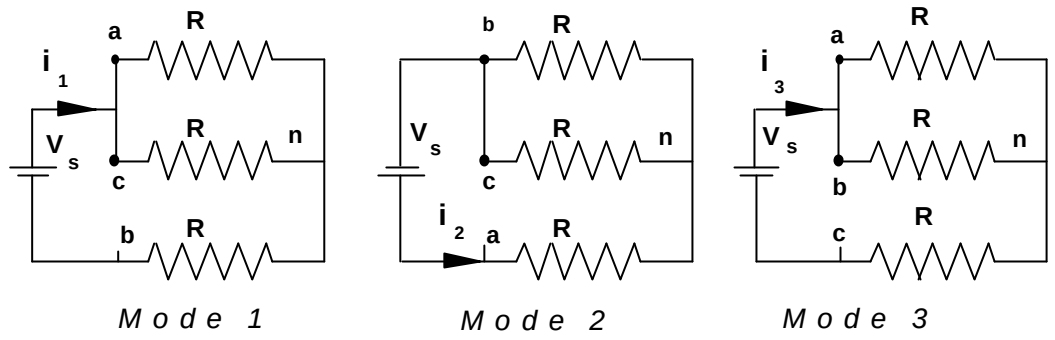

(a). Equivalent circuit

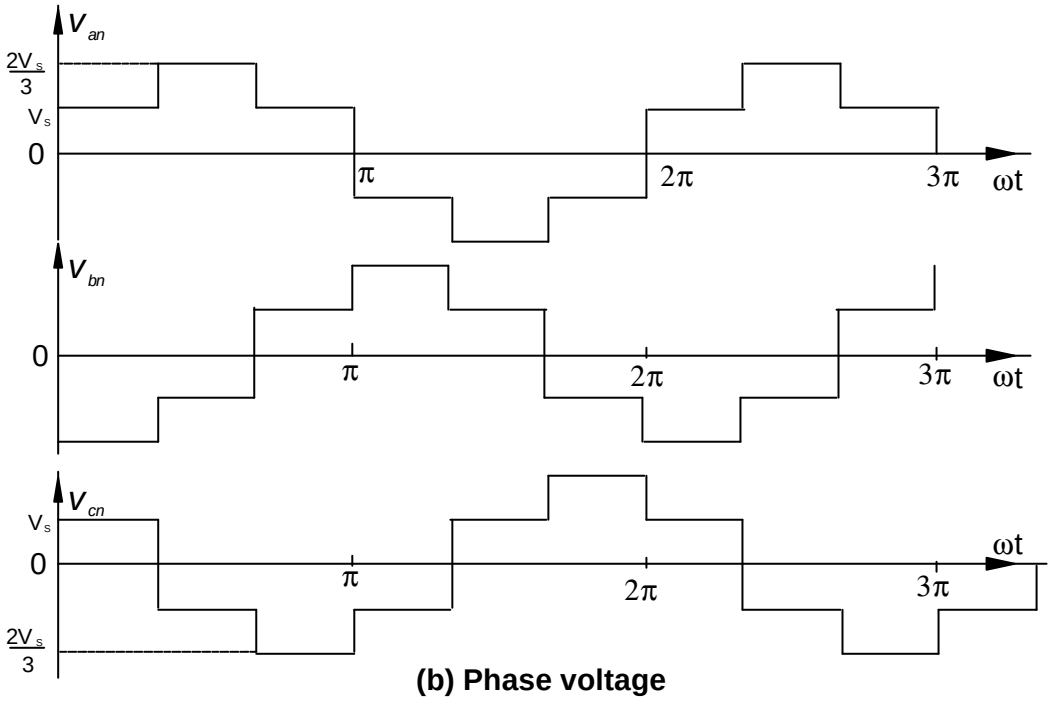

(b) Phase voltage

Figure c.2: Equivalent circuits for wye-connected resistive load.

During mode 2 interval $\frac{\pi}{3} \le \omega t \le \frac{2\pi}{3}$,

$$R_{eq} = R + \frac{R}{2} = \frac{3R}{2}$$

$$i_2 = \frac{V_S}{R_{eq}} = \frac{2V_S}{3R}$$

$$\upsilon_{an} = i_2 R = \frac{2 V_S}{3}$$

$$\upsilon_{bn} = \upsilon_{cn} = -\frac{i_2 R}{2} = -\frac{V_S}{3}$$

During mode 3 interval $\frac{2\pi}{3} \le \omega t \le \pi$,

$$R_{eq} = R + \frac{R}{2} = \frac{3R}{2}$$

$$i_3 = \frac{V_S}{R_{eq}} = \frac{2V_S}{3R}$$

$$\upsilon_{an} = \upsilon_{bn} = \frac{i_3 R}{2} = \frac{V_S}{3}$$

$$\upsilon_{cn} = -i_3 R = -\frac{2 V_S}{3}$$

The line-to-neutral voltages are shown in Figure c.2.(b). The instantaneous line-to-line voltage, υ_{ab} , can be expressed in a Fourier series, recognizing that υ_{ab} is shifted by $\pi/6$ and the even harmonics are zero,

$$\upsilon_{ab} = \sum_{n=1,3,5,.....}^{\infty} \frac{4 V_S}{n\pi} \cos\frac{n\pi}{6} \sin n\left(\omega t + \frac{\pi}{6}\right) \qquad \text{(c.1)}$$

υ_{bc} and υ_{ca} can be found from Equation (c.1) by phase shifting υ_{ab} by 120^o and 240^o, respectively,

$$\upsilon_{bc} = \sum_{n=1,3,5,.....}^{\infty} \frac{4 V_S}{n\pi} \cos\frac{n\pi}{6} \sin n\left(\omega t - \frac{\pi}{2}\right) \qquad \text{(c.2)}$$

$$\upsilon_{ca} = \sum_{n=1,3,5,.....}^{\infty} \frac{4V_S}{n\pi} \cos\frac{n\pi}{6} \sin n\left(\omega t - \frac{7\pi}{6}\right) \qquad \text{(c.3)}$$

From Equation (c.1), (c.2) and (c.3) that the triple n harmonics (n = 3, 9, 15, …..) would be zero in the line-to-line voltages. The line-to-line rms voltage can be found from

$$V_L = \left[\frac{2}{2\pi}\int_0^{2\pi/3} V_S^2 \, d(\omega t)\right]^{1/2} = \sqrt{\frac{2}{3}}\, V_S = 0.8165\, V_S \; . \qquad \text{(c.4)}$$

From n = 1, the rms value of fundamental component can be found from the peak magnitude in Equation (c.1):

$$V_{L1} = \frac{4V_S \cos 30^0}{\sqrt{2}\,\pi} = 0.7797\, V_S \quad . \qquad \text{(c.5)}$$

The rms value of line-to-neutral voltages can be found from the phase voltage,

$$V_p = \frac{V_L}{\sqrt{3}} = \frac{\sqrt{2}\, V_S}{3} = 0.4714\, V_S \quad . \qquad \text{(c.6)}$$

With resistive loads, the diodes across the transistors have no functions. If the load is inductive, the current in each arm of the inverter would be delayed to its voltage. When transistor Q_4 in Figure c.1 (a) is off, the only path for negative line current i_a is through D_1. Hence the load terminal a is connected to the dc source through D_1 until the load current reverses its polarity at $t = t_1$. During the period for $0 \le t \le t_1$, transistor Q_1 will not conduct. Similarly, must be continuously gated, since the conduction time of transistors and diodes depends on the load power factor.

C.2 AC motor [18]

Three-phase induction motor is commonly used in adjustable-speed drives and it has three-phase stator and rotor windings. The stator windings are supplied with balanced three-phase voltage, which produce induced voltages in the rotor windings due to transformer action. It is possible to arrange the distribution of stator winding so that there is an effect of multiple poles, producing several cycles of magneto motive force (mmf) (or field) around the air gap. This field establishes a spatially distributed

sinusoidal flux density in the air gap. The speed of rotation of the field is called the synchronous speed, which is defined by

$$\omega = \frac{2\omega}{p} \tag{c.7}$$

where p is the number of poles and ω is the supply frequency in rad/s.

A stator phase voltage, $\upsilon_s = \sqrt{2}\, V_s \sin \omega t$, produces a flux linkage (in the rotor) given by

$$\phi(t) = \phi_m \cos(\omega_m t + \delta - \omega_s t) \tag{c.8}$$

the induced voltage per phase in the rotor winding is

$$\begin{aligned} e_r &= N_r \frac{d\phi}{dt} = N_r \frac{d}{dt}\left[\phi_m \cos(\omega_m t + \delta - \omega_s t)\right] \\ &= N_r \phi_m (\omega_s - \omega_m) \sin\left[(\omega_s - \omega_m) t - \delta\right] \\ &= -s E_m \sin(s\omega_s t - \delta) \\ &= -s\sqrt{2} E_r \sin(s\omega_s t - \delta) \end{aligned} \tag{c.9}$$

where N_r is number of turns on each rotor phase, ω_m angular speed of rotor, δ relative position of the rotor, E_r rms value of the rotor induced voltage and s is slip, defined as

$$s = \frac{\omega_s - \omega_m}{\omega_s}. \tag{c.10}$$

The equivalent circuit for one phase of the rotor is shown in Figure c.3 (a), where R'_r is the resistance per phase of the rotor windings, X'_r is the leakage reactance per phase of the rotor at the supply frequency and E_r represents the induced phase voltage when the speed is zero (or s = 1). The rotor current is given by

$$I'_r = \frac{s E_r}{R'_r + j s X'_r}$$

$$I_r' = \frac{E_r}{\frac{R_r'}{s} + j X_r'} \qquad \text{(c.11)}$$

where R'_r and X'_r are referred to the rotor winding.

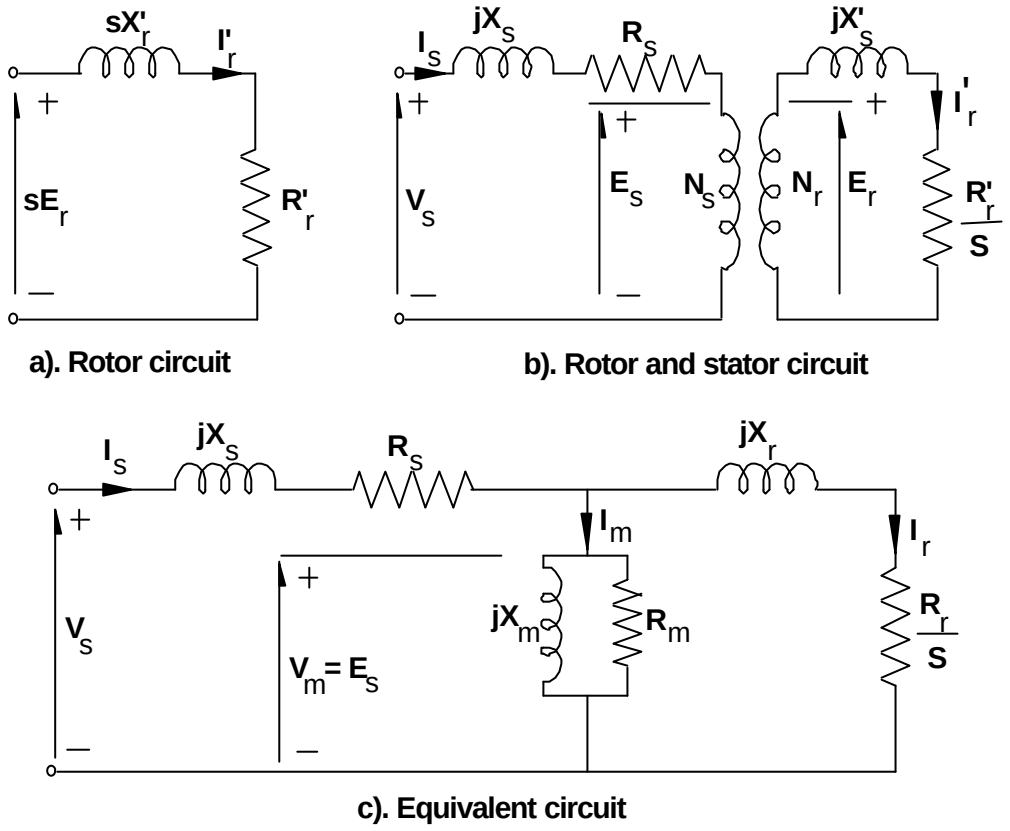

Figure c.3: Circuit model of induction motors.

The per phase circuit model of induction motors is shown in Figure c.3 (b), where R_s and X_s are the per phase resistance and leakage reactance of the stator is shown in Figure c.3 (c), where R_m represents the resistance for excitation (or core) loss and X_m is the magnetizing reactance. There will be stator core loss, when the supply is connected and the rotor core loss depends on the slip. The friction and wind age loss, $P_{no\ load}$, exists when the machine rotates. The core loss, P_c may be included as a part of rotational loss, $P_{no\ load}$.

The rotor current I_r and stator current I_s can be found from the circuit model in Figure c.3 (c) where R_r and X_r are referred to the stator windings. Once the values of I_r and I_s are known, the performance parameters of the motor can be determined as follows:

Stator copper loss,

$$P_{su} = 3\, I_s^2\, R_s \tag{c.12}$$

Rotor copper loss,

$$P_{ru} = 3\, I_r^2\, R_r \tag{c.13}$$

Core loss,

$$P_c = \frac{3V_m^2}{R_m} \approx \frac{3V_s^2}{R_m} \tag{c.14}$$

Gap power,

$$P_g = 3I_r^2 \frac{R_s}{\omega_s} \tag{c.15}$$

Developed power,

$$P_d = P_g - P_{ru} = 3I_r^2 \frac{R_r}{s}(1-s)$$

$$= P_g\,(1-s) \tag{c.16}$$

Developed torque,

$$T_d = \frac{P_d}{\omega_m}$$

$$= \frac{P_g(1-s)}{\omega_s(1-s)} = \frac{P_g}{\omega_s} \tag{c.17}$$

Input power,

$$P_i = 3V_s\, I_s \cos\theta_m$$

$$= P_c + P_{su} + P_g \tag{c.18}$$

where θ_s is angle between I_s and V_s. Output power,

$$P_o = P_d - P_{no\ load}\ .$$

Efficiency,

$$\eta = \frac{P_o}{P_i} = \frac{P_d - P_{no\ load}}{P_c + P_{su} + P_g} \tag{c.19}$$

If $P_g >> (P_c + P_{su})$ and $P_d >> P_{no\ load}$, the efficiency becomes

$$\eta \approx \frac{P_d}{P_g} = \frac{P_g (1 - s)}{P_g} = 1 - s \tag{c.20}$$

The value of X_m is normally large and R_m, which is much larger, can be removed from the circuit model to simplify the calculations. If $X_m^2 >> (R_s^2 + X_s^2)$, then $V_s \approx V_m$ and the magnetizing reactance X_m may be moved to the stator winding to simplify further. This is shown in Figure c.4.

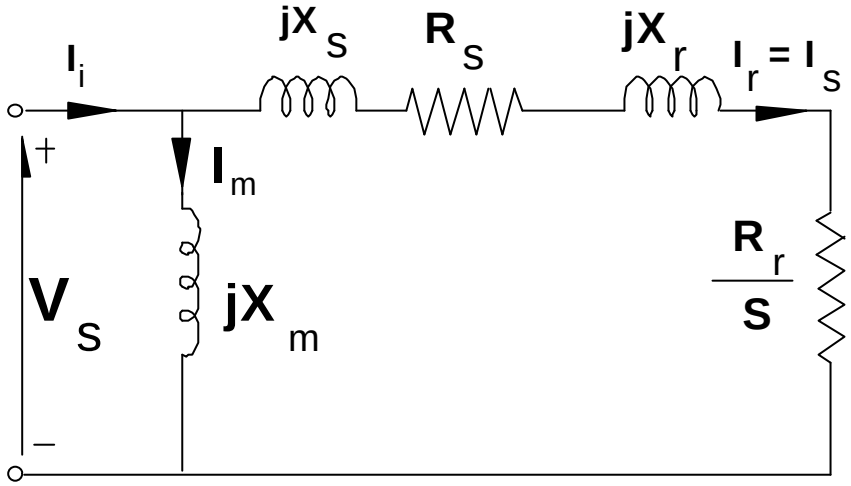

Figure c.4: Approximate per-phase equivalent circuit.

The input impedance of the motor,

$$Z_i = \frac{-X_m (X_s + X_r) + jX_m \left(R_s + \frac{R_r}{s} \right)}{R_s + \frac{R_r}{s} + j (X_m + X_s + X_r)} \tag{c.21}$$

and the power factor angle of the motor,

$$\theta_m = \pi - \tan^{-1}\frac{R_s + \frac{R_r}{s}}{X_s + X_r} + \tan^{-1}\frac{X_m + X_s + X_r}{R_s + \frac{R_r}{s}} \quad . \qquad \text{(c.22)}$$

From Figure c.4, the motor current,

$$I_r = \frac{V_s}{\left[\left(R_s + \frac{R_r}{s}\right)^2 + (X_s + X_r)^2\right]^{1/2}} \quad . \qquad \text{(c.23)}$$

Substituting Equation (c.23) in Equation (c.15) and (c.17) yields

$$T_d = \frac{3R_r V_s^2}{s\omega_s\left[\left(R_s + \frac{R_r}{s}\right)^2 + (X_s + X_r)^2\right]} \quad . \qquad \text{(c.24)}$$

If the motor is supplied from a fixed voltage at a constant frequency, the developed torque is a function of the slip and torque-speed characteristics can be determined from Equation (c.24).

C.3 Centrifugal Pump [16]

The mechanical load characteristics can be described by

$$\tau_L = \tau_o + (\tau_{nL} - \tau_o)\left(\frac{S}{S_o}\right)^x \qquad \text{(c.25)}$$

where x = 0 for a constant torque; x = 1 for viscous friction; x = 2 for a centrifugal pump at constant head.

Hence, for a centrifugal pump

$$\tau_L = \tau_o + (\tau_{nL} - \tau_o)\left(\frac{S}{S_o}\right)^2 \quad .$$

For simplicity, this Equation is written as

$$\tau_L = A + B\,S^2 \qquad \text{(c.26)}$$

where

$$A = \tau_o$$

$$B = \frac{\tau_{nL} - \tau_o}{S_o^2} \quad .$$

The pump is modeled by the characteristic surface of H, Q and S where H is the head (m), Q is the flow (m^3) and S (rev. min^{-1}) is the speed and these parameters have the relationship,

$$H = f(Q,S) \; .$$

Alternatively, the Equation may be written as

$$H = A_1\,Q^2 + 2\,B_1\,SQ + C_1\,S^2 \qquad \text{(c.27)}$$

where A_1, B_1 and C_1 are constant for a given pump and could be found either from the test data or from the manufacturer's specifications.

C.4 DC-DC Converter

C.4.1 Boost Regulator

In a boost regulator, the output voltage is greater than the input voltage hence the name "boost". A boost regulator using a power MOSFET is shown in Figure c.5.(a), and this similar to a step-up chopper. The circuit operation can be divided into two modes. Mode 1 begins when transistor Q_1 is switched on at t = 0. The input current, which rises, flows through inductor L and transistor Q_1. Mode 2 begins when transistor Q_1 is switched off at $t = t_1$. The current, which is flowing through the transistor, would now flow through L, C, load and diode D_m. The inductor current falls until transistor Q_1 is turned on again in the next cycle. The energy stored in inductor L is transferred to the load. The equivalent circuits for the modes of

operation are shown in Figure c.5.(b). The waveforms for voltages and currents are shown in Figure c.5.(c) for continuous load current.

Assuming that the inductor current rises linearly from I_1 to I_2 in time t_1,

$$V_s = L\frac{I_2 - I_1}{t_1} = L\frac{\Delta I}{t_2} \qquad \text{(c.28)}$$

or

$$t_1 = \frac{\Delta I\, L}{V_s} \qquad \text{(c.29)}$$

and the inductor current falls linearly from I_2 to I_1 in time t_2,

$$V_s - V_a = -L\,\frac{\Delta I}{t_2}. \qquad \text{(c.30)}$$

Substituting $t_1 = kT$ and $t_2 = (1\text{-}k)T$ yields the average output voltage,

$$V_a = \frac{V_s}{1-k}. \qquad \text{(c.31)}$$

Assuming a loss less transistor $V_s I_s = V_a I_a = V_s I_a/(1\text{-}k)$ and the average input current is

$$I_s = \frac{I_a}{1-k} \quad . \qquad \text{(c.32)}$$

The switching period T can be found from

$$T = \frac{1}{f} = t_1 + t_2 = \frac{\Delta I\, L}{V_s} + \frac{\Delta I\, L}{V_a - V_s} = \frac{\Delta I\, L\, V_a}{V_s\left(V_a - V_s\right)} \qquad \text{(c.33)}$$

and this gives the peak-to-peak ripple current,

$$\Delta I = \frac{V_s\left(V_a - V_s\right)}{f\, L\, V_a} \qquad \text{(c.34)}$$

or

$$\Delta I = \frac{V_s\, k}{f\, L} \quad . \qquad \text{(c.35)}$$

When the transistor is on, the capacitor supplies the load current for t = t_1. The average capacitor current is $I_c = I_a$ and the peak-to-peak ripple voltage of the capacitor is

$$\Delta V_c = v_c - v_c(t=0) = \frac{1}{C}\int_0^{t_1} I_a \, dt = \frac{I_a \, t_1}{C} \quad . \tag{c.36}$$

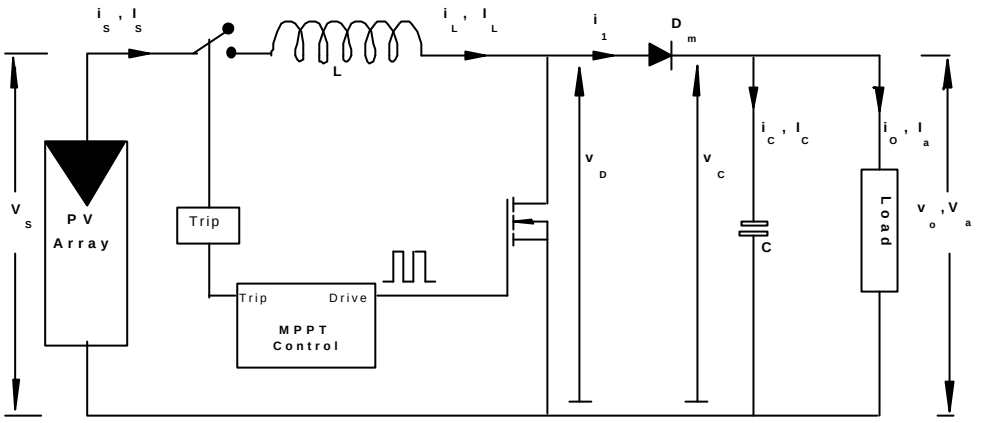

(a) Circuit diagram

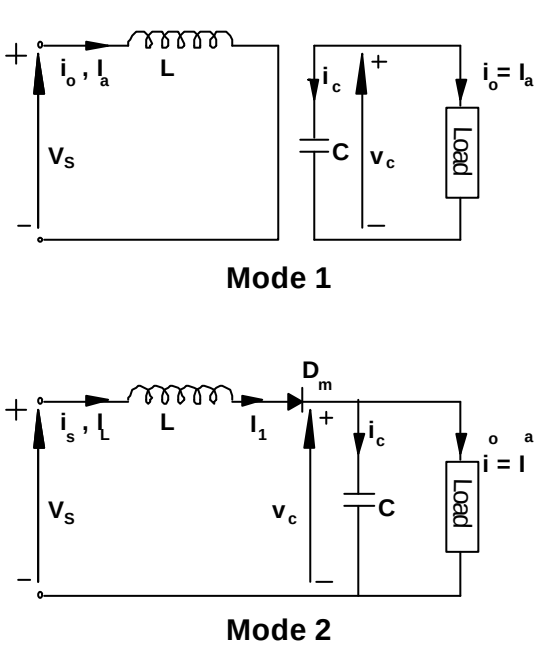

(b) Equivalent circuits

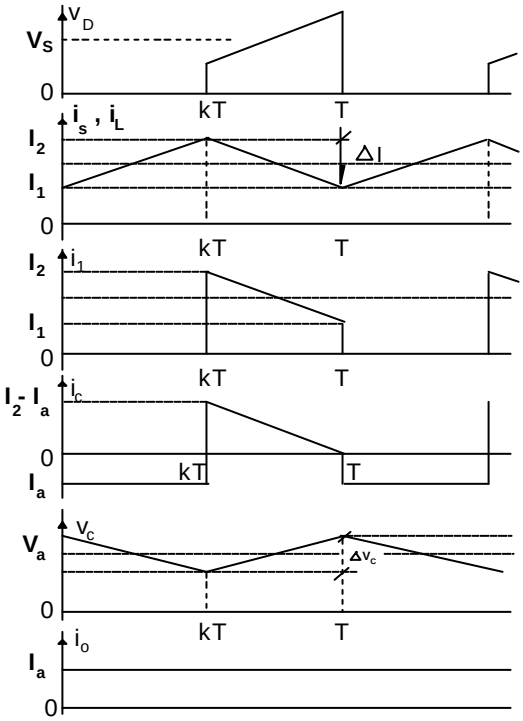

(c) Waveforms

Figure c.5: Boost regulator.

Equation c.31 gives $t_1 = (V_a - V_s)/(V_a f)$ and substituting t_1 in equation c.36 gives

$$\Delta V_c = \frac{I_a (V_a - V_s)}{V_a f C} \quad \text{(c.37)}$$

or

$$\Delta V_c = \frac{I_a k}{f C} \quad . \quad \text{(c.38)}$$

A boost regulator can step up the output voltage without a transformer. Due to single transistor, it has high frequency. The input current is continuous. However, a high peak current has to flow through the power transistor. The output voltage is very sensitive to changes in the duty cycle k and with the load circuit. The average output current is less than the average inductor current by a factor of (1-k) and a much higher rms current would flow through the filter capacitor, resulting in the use of a larger filter capacitor and a larger induction than those of a buck regulator.

C.5 DC Motor [16]

The equivalent circuit for a separately excited dc motor is shown in Figure c.6. When a separately excited motor is excited by a field current of i_f and an armature current of i_a flows in the armature circuit, the motor develops a back emf and a torque to balance the load torque at a particular speed. The field current, i_f, of a separately excited motor is independent of the armature current, i_a and any change in the armature current has no effect in field current. The field current is normally much less than the armature current. The equations describing the characteristics of a separately excited motor can be determined from Figure c.6. The instantaneous field current, i_f, is described as

$$\upsilon_f = R_f i_f + L_f \frac{di_f}{dt} \quad .$$

The instantaneous armature current can be found from

$$\upsilon_a = R_a i_a + L_a \frac{di_a}{dt} + e_g \quad .$$

The motor back emf, which is also known as speed voltage, is expressed as

$$e_g = K_v \omega i_f \quad .$$

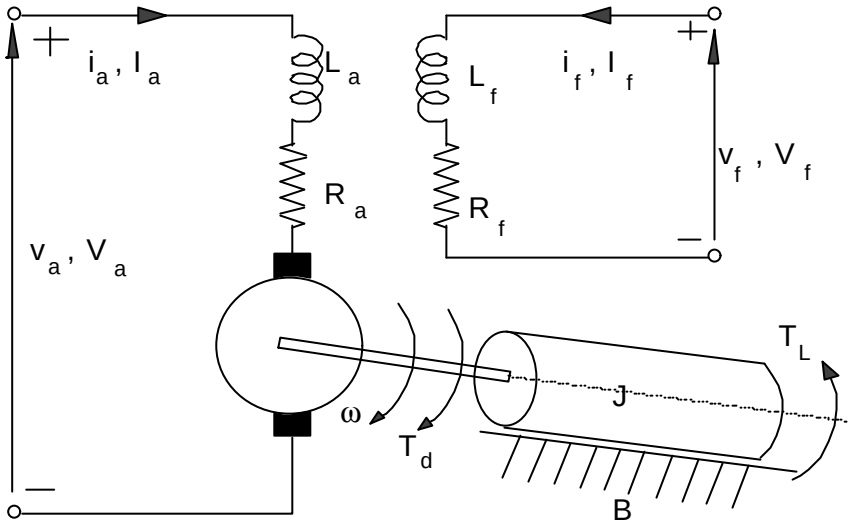

Figure c.6: Equivalent circuit of separately excited dc motors.

The torque developed by the motor is

$$T_d = K_t i_f i_a \quad .$$

The developed torque must be equal to the load torque:

$$T_d = J\frac{d\omega}{dt} + B\omega + T_L$$

where ω is motor speed, rad/s; B viscous friction constant, N.m/rad/s; K_v voltage constant, V/A-rad/s; K_t=K_v torque constant; L_a armature circuit inductance, H; L_f field circuit inductance, H; R_d armature circuit resistance, Ω; R_f field circuit resistance, Ω; T_L load torque, N.m.

Under steady-state conditions, the time derivatives in these equations are zero and the steady-state average quantities are

$$V_f = R_f I_f \quad . \tag{c.39}$$

$$V_a = R_a I_a + E_g \quad . \tag{c.40}$$

$$E_g = K_v \omega I_f \quad . \tag{c.41}$$

$$T_d = K_t I_f I_a \quad .$$

$$= B\omega + T_L \tag{c.42}$$

The develop power is

$$P_d = T_d \omega \ . \tag{c.43}$$

The relationship between the field current, I_f, and the back emf, E_g, is nonlinear due to magnetic saturation. This relationship is known as magnetization characteristic of the motor. The speed of separately excited motor can be found from

$$\omega = \frac{V_a - R_a I_a}{K_v I_f} = \frac{V_a - R_a I_a}{K_v V_f} R_f \quad . \tag{c.44}$$

The motor speed can be varied by (1) controlling the armature voltage, V_a, know as voltage control; (2) controlling the field current, Ị, known as field control; or (3) torque demand, which corresponds to an armature current, I_a, for a fixed field current, I_f. The speed, which corresponds to the rated armature voltage, rated field current and rated armature current, is known as the base speed.

Bibliography

[1] Araujo, G.L., Sánchez, E., Marti, M. *Determination of the two-exponential solar cell equation parameters from empirical data*, Solar Cells 5 2 (199-204) 1992.

[2] Arrouf M., Goedel Pr. C., *Photovoltaic pumping system for induction machine with hysterisis array current control*, IEEE, pp. 853-855, 1996.

[3] Beckman W.A., *Units and symbols in solar energy*, Solar Energy 21 volume 1 pp. 65-68, 1967.

[4] Bergmann R.B, Rinke T.J, Schmidt J. and Werner H., *Advances in monocrystalline Si thin film solar cells by laser transfer*, Technical digest of the international PVSEC-12, Jeju-Korea, pp 29-30, 2001

[5] Bernard Loriferne, *Analog-digital and digital-analog conversion*, Heyden and Sons, Besacon, France, 1982.

[6] Carlos A. F. de Lima, Joäo Batista Vieira Júnior, Luiz Carlos de Freitas, *A dc-ac converter with low harmonic distortion and without losses of commutation*, IEEE, pp. 558-563, 1995.

[7] David Leggate, Russel J. Kerkman, *Pulse based dead time compensator for PWM voltage inverters*, IEEE, pp. 474-481, 1995.

[8] Harrish C. Rai, *Power electronics: devices, circuits, systems and application*, Galgotia Publications pvt. Ltd, New delhi, Indian, 1999.

[9] Harry R. Chesley, Mitchell Waite, *Supercharging C with assembly language*, Addison-Wesley Pusblishing Company, 1987.

[10] Harsono Hadi, Shinobu Tokuda, Slamet Rahardjo, *Evaluation of performance of photovoltaic system with maximum power point (MPP),* Solar energy materials & solar cells, Elsevier, pp. 673-678, 2003.

[11] Hussein M. Mashaly, Adel M. Sharaf, Mohamed Mansour, Ahmed A. El-Sattar, *A photovoltaic maximum power tracking using neural networks*, IEEE, pp. 167-172, 1994.

[12] John Bates, Malik E. Elbuluk, Donald S. Zinger, *Neural network control of a chopper-fed dc motor*, IEEE, pp. 9-15, 1996.

[13] Kamiel Z., M. Tayel, M. Elbanna, A. Nasser *Effect of shunt resistance and reverse saturation current on the performance of solar cell*, proceeding of the thirteen national, radio science conference, march 19-21, 1996, Cairo, Egypt.

[14] Koenig D., Ebest G., *Novel external field source by localization of electrons for improving field effect solar cells*, Technical digest of the international PVSEC-12, Jeju-Korea, pp 285-286, 2001

[15] Korner P.K., *A review on the diversity of photovoltaic water pumping systems*, Reric International Energy Journal, Volume 15. No. 2, pp 89-110, December 1993.

[16] Lasnier France, Ang Tony Gan, *Photovoltaic engineering handbook*, Adam Hilger, New York 1990.

[17] Lawrance W, Wichert B., Langridge D., *Simulation and performance of a photovoltaic pumping system*, IEEE (513-518), 1995.

[18] Muhammad Harunur Rashid, *Power electronics: circuits, devices and applications*, Prentice-Hall international, Inc., New Jersey, 1998.

[19] Parrott J.E., *Thermodynamics of solar cell efficiency*, Solar Materials and Solar Cells 25, pp. 73-85, 1992.

[20] Putta Swamy C.L., Singh B., Singh B.P., *Dynamic performance of a permanent magnet brushless dc motor powered by a PV array for water pumping*, Solar Energy Materials and Solar Cells 36, pp. 187-200, 1995.

[21] Raymond S., Guoliang Xie, Barry W. Hendreson, Johan H. de Groot, *A PWM inverter algorithm for adjustable speed ac drives using a nonconstant voltage source*, IEEE, pp. 673-677, 1986.

[22] Schumacher-Gröhn , *Interactive simulation of renewable electrical energy supply systems (INSEL)*, version 4.70, Renewable Energy Group, Department of Physics, University of Oldenburg, Germany, 1992.

[23] Shinohara H., Kimoto K., Itami H., Ambo T., Okado C., Nakajima K., Hojo S., Ioka S., Kuniyoshi M., *Development of residential use, utility interractive PV inverter with high-frequency isolation*, Solar Energy Materials and Solar cells 35, pp. 429-436, 1994.

[24] Shireen W., Misir D., Malki H., Arefeen M.S., *A soft switching scheme for a PWM inverter using a fuzzy logic controller*, IEEE, pp. 428-433, 1996.

[25] Siswa Trihadi, *Eastern Indonesia hybrid energy project: design and implementation*, Technical digest of the international PVSEC-12, Jeju-Korea, pp 331-333, 2001

[26] Stuart R. Wenham, Martin A. Green, muriel E. Watt, *Applied photovoltaics, Centre for photovoltaic devices and systems*, Australian, 1994.

[27] Sze S.M., *Semiconductor Devices*, second edition, John Wiley and Sons, 1985.

[28] Tony K.P. Wong, Philip C.H. Chan, *An equivalent circuit approach to solar cell modeling*, IEEE (222-225), 1955.

[29] Toshie Kunii, Junichi Kitao, Norimitsu Yoshida, Shuichi Nonomura, *Temperature dependence of absorption coefficient spectra for mc-Si films by resonant photothermal bending spectroscopy*, Technical digest of the international PVSEC-12, Jeju-Korea, pp 29-30, 2001

[30] Wagdy R. Anis, *Stepped sine wave DC/AC inverter*, Solar Materials and Solar Cells 28, pp. 123-130, 1992.

[31] Wagdy R. Anis, *An alternative design of a novel battery voltage regulator for PV systems*, Solar Materials and Solar Cells 28, pp. 143-150, 1992.

[32] Yoshihiro Hamakawa, Solar PV energy conversion and 21st century's civilization, Technical digest of the international PVSEC-12, Jeju-Korea, pp 15-18, 2001

[33] Ziyad Salameh, Arun K. Mulpur, Fouad Dagher, *Two-stage electrical array reconfiguration controller for PV powered water pump*, Solar Energy, Volume 44 No.1 pp. 51-56, 1990.

[34] Ziyad Salameh, Daniel Taylor, *Step-up maximum power point tracker for photovoltaic arrays*, Solar energy volume 41, No. 1 pp 57-61, 1990.